Kent Academic Repository

Birgul, Olcay (1968) *Radiochemical studies of neutron induced fission in heavy nuclides*. Doctor of Philosophy (PhD) thesis, University of Kent.

Downloaded from
https://kar.kent.ac.uk/94212/ The University of Kent's Academic Repository KAR

The version of record is available from
https://doi.org/10.22024/UniKent/01.02.94212

This document version
UNSPECIFIED

DOI for this version

Licence for this version
CC BY-NC-ND (Attribution-NonCommercial-NoDerivatives)

Additional information
This thesis has been digitised by EThOS, the British Library digitisation service, for purposes of preservation and dissemination. It was uploaded to KAR on 25 April 2022 in order to hold its content and record within University of Kent systems. It is available Open Access using a Creative Commons Attribution, Non-commercial, No Derivatives (https://creativecommons.org/licenses/by-nc-nd/4.0/) licence so that the thesis and its author, can benefit from opportunities for increased readership and citation. This was done in line with University of Kent policies (https://www.kent.ac.uk/is/strategy/docs/Kent%20Open%20Access%20policy.pdf). If you ...

Versions of research works

Versions of Record
If this version is the version of record, it is the same as the published version available on the publisher's web site. Cite as the published version.

Author Accepted Manuscripts
If this document is identified as the Author Accepted Manuscript it is the version after peer review but before type setting, copy editing or publisher branding. Cite as Surname, Initial. (Year) 'Title of article'. To be published in ***Title of Journal*** , Volume and issue numbers [peer-reviewed accepted version]. Available at: DOI or URL (Accessed: date).

Enquiries
If you have questions about this document contact ResearchSupport@kent.ac.uk. Please include the URL of the record in KAR. If you believe that your, or a third party's rights have been compromised through this document please see our Take Down policy (available from https://www.kent.ac.uk/guides/kar-the-kent-academic-repository#policies).

"Radiochemical Studies of Neutron Induced Fission in Heavy Nuclides"

THESIS

presented in candidature for the degree

of

DOCTOR OF PHILOSOPHY

in the

UNIVERSITY OF KENT AT CANTERBURY

by

OLCAY BİRGÜL, B.Sc.(Ankara).

ACKNOWLEDGEMENTS

I am grateful to Dr. S.J. Lyle for his advice, assistance and interest through the course of this work.

I wish to thank Mr. R.J. Oliver, Mr. W.T. Povey and Mrs. I.T. Salvadori for technical assistance and for operating the neutron generator.

Thanks are due to Mrs. J.M. Teverson and Miss L.J. Hurst for helping to prepare the manuscript.

I am indebted to the Scientific and Technical Research Council of Turkey for the award of a Research Studentship.

MEMORANDUM

The work described in this thesis was carried out at the Radiochemical Laboratory, University of Kent at Canterbury between October 1965 and October 1968, under the supervision of Dr. S.J. Lyle, Lecturer in Radiochemistry.

This thesis contains the results of some original research by the author; no part of the material offered has previously been submitted by the candidate for a degree in this or other university. Where use has been made of the results and conclusions of other authors in relevant studies, care has always been taken to ensure that the source of information is clearly indicated, unless it is of such a general nature that indication is impracticable.

ABSTRACT

The presence of tin-129 isomers has been confirmed among fission products. Their half-lives were measured and found to be 7.5 ± 0.1 min and 2 min. No evidence was found for a longer-lived isomer previously reported. 0.17 ± 0.01 and 0.39 ± 0.03% were obtained for the cumulative yields of 7.5 min tin-129 and antimony-129 respectively in the thermal neutron induced fission of uranium-235.

The cumulative yields of 10 fission products (bromine-83, and -84, strontium-91, zirconium-97, molybdenum-99, ruthenium-105, silver-113, antimony-129, cerium-143 and praseodymium-145) from the fission of protactinium-231 induced by 3 MeV neutrons have been measured radiochemically using a recoil method. The mass-yield distribution was found to be highly asymmetric with a peak to trough ratio of about 100 and a peak width at half-height of 14 mass units. The maxima were observed at masses 91 and 138 with yields around 7.2%.

Previously a correlation between the relative width ratio for symmetric fission and neutron re-emission and a term depending on the relative energies available for the two processes was derived and tested for 14 MeV neutron induced fission of heavy nuclides. In the present

work this was tested for fission induced by 3 MeV neutrons. The fission cross-section of protactinium-231 for 14.8 MeV neutrons was measured by a radiochemical method and found to be 1.43 ± 0.12 barns. This result was used in a discussion of the correlation mentioned above.

In a search for irregularities in yields in the mass region 131-135 for 14.8 MeV neutron induced fission of protactinium-231, the independent yield of xenon-135 and the cumulative yields of iodine-131, -133 and -134 and xenon-133 and -135 were measured radiochemically. Fine structure was observed at mass-134. A comparison of the results with those obtained in 14 MeV neutron induced fission of thorium-232 and uranium-238 suggests that the prominence of the fine structure increases with decreasing atomic number.

In all measurements zirconium-97 or molybdenum-99 and where possible both of them were used as reference masses. Counting was carried out using an end-window gas-flow β-proportional counter for solid, and a gas Geiger-counter for gaseous samples.

CONTENTS

Page

CHAPTER 1

Introduction.

1.1. Nuclear Fission. 1

1.2. The Probability of Fission. 3

1.3. Mass Distribution in Fission. 6

1.4. Purpose of the Present Work. 12

References. 14

CHAPTER 2

General Experimental Method and Apparatus.

2.1. Introduction. 18

2.2. Sample Preparation. 18

2.3. The Neutron Generator. 20

2.4. Counting Equipment.

(a) Proportional Counter. 22

(b) Gas Geiger-Counter. 24

2.5. Reference Mass. 25

2.6. Preparation of Solid Samples for Counting Purposes. 26

References. 27

CHAPTER 3

General Method of Calculations.

3.1. Introduction. 28
3.2. Calculation of Relative Yields. 28
3.3. Estimation of Independent Yields. 33
References. 36

CHAPTER 4

An Investigation of the Mass-129 Decay Chain in Fission.

4.1. Introduction. 37
4.2. Experimental - Separation Procedures. 37
(a) 7 min Tin-129. 37
(b) 2 min Tin-129. 39
(c) Long-lived Tin-129. 40
(d) Antimony-129. 42
4.3. Counter Calibration and Evaluation of Results. 43
4.4. Results and Discussion. 46
References. 50

CHAPTER 5

Mass Distribution in the Fission of Protactinium-231 Induced by 3 MeV Neutrons.

5.1. Introduction. 51
5.2. Experimental. 52
5.3. Treatment of Experimental Data and Evaluation of Results. 54
(a) Bromine-83. 55
(b) Bromine-84. 56
(c) Strontium-91. 56
(d) Zirconium-97. 57
(e) Molybdenum-99. 58
(f) Ruthenium-105. 58
(g) Silver-113. 60
(h) Antimony-129. 60
(i) Cerium-143. 61
(j) Praseodymium-145. 61
(k) Fission Cross-Section of Protactinium-231 for 14.8 MeV Neutrons. 62
(l) Evaluation of Γ_s/Γ_n for 3 MeV Neutrons. 63
5.4. Results and Discussion. 64
References. 69

Page

CHAPTER 6

Fission Induced in Protactinium-231 by 14 MeV Neutrons: Fine Structure in the Mass Region 131-135.

6.1. Introduction. 71

6.2. Separation Procedures. 71

(a) Iodine. 71

(b) Xenon. 71

(c) Calibration of the Gas Geiger-Counter. 74

6.3. Treatment of Experimental Data and Evaluation of Results. 75

(a) Iodine-131. 75

(b) Iodine-133. 78

(c) Iodine-134. 79

(d) Xenon-133. 79

(e) Xenon-135. 80

6.4. Results and Discussion. 82

References. 87

CHAPTER 7

General Discussion and Further Suggestions. 89

References. 95

Page

APPENDIX I

Chemical Procedures.

1. Bromine. 96
2. Strontium. 97
3. Zirconium. 98
4. Molybdenum. 101
5. Ruthenium. 103
6. Silver. 104
7. Antimony. 106
8. Cerium. 108
9. Praseodymium. 110
10. Iodine. 115
References. 117

APPENDIX II

Derivation of the Ratio of the Partial Width for Symmetric Fission to that for Neutron Re-emission (Γ_s/Γ_n). 118
References. 123

CHAPTER 1

Introduction

1.1 Nuclear Fission

Fission is a process in which a nucleus usually divides into two main fragments of comparable mass. It was first discovered by Hahn and Strassmann[1] in 1939 and in the same year an extensive treatment of the theory of the liquid drop model of fission was given by Bohr and Wheeler[2].

According to this model the nucleus is described as a uniformly charged, incompressible droplet of constant density possessing a well-defined surface. It is assumed that the energy changes occurring during the fission process very much resemble the energy changes due to surface tension effects in a drop of liquid which is changing its shape. The total potential energy of an idealized liquid drop is made up of two terms, the electrostatic energy, tending to pull the drop apart and the surface energy, tending to hold it together. For a stable nucleus the sum of the surface and Coulomb energy changes must be positive for any small distortion from equilibrium. However, it can be shown that for certain distortions of a drop the (negative) Coulomb term overtakes the surface term if the distortion is increased beyond a certain amount and the drop undergoes fission.

So far the theory has been worked out fairly completely only for the lighter fissionable elements, below about radium.

Another theory developed by Fong[3,4] takes into account the shell structure of the nucleus which can be related to asymmetric fission and fine structure on the heavy mass peak (see later).

Fission is normally induced by giving a certain amount of energy to the nucleus, but a nucleus in its ground state can occasionally undergo fission which is called spontaneous fission, first observed by Petrzhak and Flerov[5] in uranium. Although the break-up of any heavy nucleus ($A \geqslant 100$) into two nuclei of approximately equal size is exoergic, spontaneous fission has been observed only for nuclei with $A \geqslant 230$. The separation of a heavy nucleus into two positively charged fragments is hindered by a Coulomb barrier and fission can thus be treated as a barrier penetration problem. The barrier height increases more slowly with increasing nuclear size than does the decay energy for fission. Because of this steep dependence of barrier penetrability on the ratio of available energy to barrier height, spontaneous fission is observed only among the very heavy elements.

In the case of even-even nuclides spontaneous fission half-lives decrease rapidly with increasing atomic number, whereas nuclides with an odd number of nucleons decay at a much slower rate[6,7].

Bohr and Wheeler[4] defined a fissionability parameter which is equal to the dimensionless ratio of the Coulomb to the surface energies. It can also be written as $\frac{Z^2/A}{(Z^2/A)\text{crit}}$ where $(Z^2/A)\text{crit} = 48.4$. According to this definition all nuclei of $Z > \sim 120$ will be characterised by the absence of a classical barrier toward spontaneous fission.

In the discussion which follows, attention is mainly given to fission induced by neutrons.

1.2 The Probability of Fission

In the fission process, at low and moderate excitation energies the first step usually involves the formation of a compound nucleus excited to an energy which is the sum of the kinetic energy of the bombarding particle and its binding energy in the newly formed nucleus. This excitation energy is assumed to be rapidly distributed back and forth over all the possible degrees of freedom of the compound nucleus and is eventually disposed of by ejection of particles of light mass, by nuclear fission or by gamma-ray emission. The cross-section for any of these reactions, σ_i, may be related to the compound nucleus formation cross-section, σ_c, by the relation

$$\sigma_i = \sigma_c \frac{\Gamma_i}{\Gamma_t}$$

where Γ_i is the probability of decay of the compound nucleus by any of the reactions mentioned above, and Γ_t is the total probability of decay of the compound nucleus.

A comparison of the change of the fission cross-sections with neutron energy[8-17] for a number of nuclei having $Z > 90$ shows that for most of the nuclei, fission has a threshold except for uranium-233, uranium-235 and plutonium-239. The very high thermal fission cross-section and the absence of a threshold for these three nuclei can be explained as a result of their possessing odd numbers of neutrons. In such cases the compound nucleus is excited to a greater extent because of the energy released in the pairing of neutrons when the incoming neutron is absorbed. The question of whether or not a nucleus is fissionable through the agency of slow neutrons depends on whether or not the binding energy of the last neutron exceeds the height of the fission barrier, and if these two quantities are of similar magnitude the pairing effects are critical in determining the sign of the difference. Fission by slow neutrons is not observed for nuclei having $Z < 90$ since the fission barrier is significantly greater than the neutron binding energy for both odd and even number of neutrons.

The cross-sections of nuclei like protactinium-231, uranium-234, uranium-236, uranium-238, neptunium-237, plutonium-240 and americium-241 which have thresholds to fission induced by neutrons above thermal energies, first increase with increasing neutron energy and then stay constant over a range of several MeV until a new rise occurs at about 5 to 7 MeV. This second rise is due to the fact that the excitation energy is high enough to permit evaporation of one neutron from the compound nucleus without reducing the excitation energy of the residual nucleus below the fission threshold. In such cases the nucleus has a second chance of undergoing fission. If the energy of the incident particle is further increased a third step is observed at about 12 or 13 MeV corresponding to the emission of two neutrons followed by fission. In the case of uranium-238, three such steps have been observed with evidence for a fourth near 19 MeV[18].

Charged particle induced fission always has a threshold and the fission cross-sections rise rapidly with the bombarding particle energy[19-24].

1.3 Mass Distribution in Fission

In nuclear fission many fission products are produced; nearly 400 ranging in mass from 72 to 161 and in atomic number from 30 to 65 have been identified, and several hundred more probably remain undiscovered. The nuclear species which are formed from the simple division of the compound nucleus before emission of particles and loss of energy are called primary fission fragments. Part of the excitation energy of these fragments is expended in the evaporation of neutrons - the so-called prompt neutrons - and the rest of it is emitted as gamma-rays, leaving the products in their ground states. Prompt neutron emission takes place in times less than 4 x 10^{-14} seconds[25] after scission and the average number of neutrons released per fission is between two and five[26]. The primary fission products which are formed after prompt neutron emission still have too many neutrons for stability which is eventually achieved by successive β-decay. Each product thus starts a short isobaric radioactive series. These series are called fission decay chains. In the β-decay stage of a few chains there is a small probability for the emission of a 'delayed' neutron.

The fission yield for a particular nuclide is a measure of the probability of that nuclide being formed in the process. It may be expressed as the ratio of the number of nuclei of a given mass number to the total number of fission events. If it is due entirely to its direct formation as a primary product it is called an 'independent fission-yield'. However, in most cases this is difficult to measure, because the half-lives of the primary products are so short that by the time the necessary experimental manipulations are carried out, the primary products have been completely converted into different elements and the measured yield is the sum of all independent yields up to that point on the chain. Such yields are called 'cumulative yields'. An exception occurs in decay chains which possess a shielded nuclide, that is one which has a stable isobar as its precursor in the chain so that it is not formed as a daughter product in β-decay. Then the measured fission yield of the shielded nuclide is the 'independent yield'.

For fission induced by neutrons of < 14 MeV energy total chain yields can be calculated from cumulative yields by using the so-called 'equal charge displacement' hypothesis[27]. According to this hypothesis the most probable charges for each of a pair of complementary fragments lie an equal number of units away from β-stability. Further, the charge distribution about the most probable charge is a symmetrical function with the same form for all mass divisions in all fissile nuclides[28]. Since for a given mass number the charge distribution is narrow and is centred several charge units below a stable isobar, the cumulative yield of the stable isobar, or of a radioactive isobar near the stable end of the chain is very close to the total chain yield.

Charge distribution at high excitation energies[29] can be described by the 'unchanged charge displacement' hypothesis,[27] according to which the neutron-to-proton ratios of the light and heavy fragments are identical with that of the fissioning nucleus.

Neither of these postulates have been satisfactory for charged-particle induced fission at moderate bombarding energies[30,31].

The mass distribution of fission products is normally presented in the form of a fission yield curve in which the cumulative mass-yields of the different products are plotted against their mass numbers. Mass-yield curves can be discussed in terms of two fundamentally different types of fission associated with, essentially, asymmetric and symmetric modes of nuclear division. The fissioning nuclei are roughly divided into three main categories according to the mass distributions they give in fission induced at different excitation energies[32]. Thorium and heavier elements (sometimes called highly fissile elements) show a double-peaked mass-yield curve at low excitation energies[33,34,35]. The position of the heavy peak is essentially constant, probably because of the preferential formation of 50-proton and 82-neutron shells in the primary fission act, while the light peak adjusts itself accordingly moving towards higher mass numbers with increasing mass of the fissioning nucleus[36]. The degree of asymmetry is often expressed in terms of a peak-to-trough ratio. This is the ratio of the fission yields at the maxima corresponding to asymmetric division of the excited nucleus, to the fission yield occurring in the region of half the mass of the nucleus undergoing fission. This ratio is greatest for spontaneous fission and decreases with increasing excitation energy since symmetric fission is an increasing function of nuclear excitation energy. At higher excitation energies (> 40 MeV) the fission yield curve shows one broad maximum[37,38] in which symmetric division of the nucleus contributes most to the yield.

As the mass and atomic number of fissioning nuclide decrease below those of uranium isotopes the probability of fission at small excitation energies decreases sharply, and, at the higher excitation energies necessary for fission, symmetric mass division becomes more probable than asymmetric division. Elements like radium give a three-humped mass-yield curve[39] at excitation energies near the threshold, which shows the equal probability of symmetric and asymmetric fission. At higher energies the mass-yield curve turns into an overall broad symmetric distribution[40]. In the fission of elements like lead and bismuth the mass distribution is always symmetric[41] with an increase of the width of the mass division as the excitation energy increases.

Mass-yield curves show some fine structure on the peaks. This was first observed by Thode and co-workers[42,43,44]. They found a value for the yield of xenon-134, 35 percent higher than had been expected in uranium-235 fission. And also the fission yield of iodine-136 showed a departure from the smooth curve[45]. Since these isotopes lie close to the shell of 82-neutrons the deviations were explained as a result of shell structure. The nuclides with 82 neutrons are expected to have an increased independent yield due to structural preference in the primary fission act[46]. If this is so, any irregularity in the yield of these species must appear symmetrically in the complementary fragments. In the fission of both plutonium-239 and uranium-233 induced by thermal neutrons there are maxima at mass-100, but in neither case is the yield of the complementary fragment to mass-134 abnormally high[47]. Therefore, it was suggested by Farrar and Tomlinson[47] and independently by Terrell[48] that some effects occurring after scission rather than in the primary fission act must cause the observed deviations. According to this view, fine structure is a result of slow variation with mass of the neutron emission probability from the prompt fission fragments.

The division of the fissioning nucleus into three fragments (ternary fission) has also been observed. The best established type of ternary fission is the emission of alpha particles in coincidence with two heavy fragments of the conventional type[49]. The probability of this kind of fission is about one for every 400 giving rise to the more usual binary fission event[50]. Examples of the other types are the emission of a triton[51] in coincidence with two heavy fragments with a yield of 1 or 2 tritons for every 10,000 fission events, and the splitting of the nucleus into three or four fragments of roughly equal size with a probability of (6.7 ± 3.0) in 10^6 normal binary events[52] in low energy fission of uranium-235.

1.4 Purpose of the Present Work

The work on which this thesis is based is set out below:

(1) an investigation of the mass-129 decay-chain in fission,

(2) mass distribution in the fission of protactinium-231 by essentially 3 MeV neutrons, and

(3) studies of fine structure on the heavy mass-yield peak in the fission of protactinium-231.

Antimony is a suitable isotope on which to base cumulative mass-yield measurements for the 129 mass chain. However, when this work was undertaken, there were some contradictions in the literature concerning the half-lives of the antimony precursors. Since a reliable measurement of the fission yield of a fission product requires a knowledge of the half-life of its precursor it was considered prudent to establish the half-lives of the tin-129 isomers before carrying out any yield measurements for this mass chain. The cumulative yield of antimony-129 could then be measured with greater confidence in the work done to obtain points on a mass-yield curve for protactinium-231 in fission induced by 3 MeV neutrons.

Experiments carried out by Iyer and his co-workers[53] showed that the mass distribution for protactinium-231 in fission induced by fission spectrum neutrons results in a normal two humped curve. On the other hand, Brown, Lyle and Martin[54] obtained a substantially different type of yield distribution for fission induced by 14 MeV neutrons. In the last mentioned work a less direct method of measurement was employed. It was therefore considered useful to use this method to obtain yields under (as near as possible with available facilities) the conditions of fission employed by Iyer et al. Yields were measured at masses chosen either because they facilitated comparison with previously published values or provided additional results which assisted in the drawing of a more complete mass-yield curve.

The results from several investigations suggest that irregularities in the cumulative mass-yield curve in the mass region 130 to 136 are greater for uranium and heavier elements than for the lighter elements. The work done by Sellars[55] of this laboratory on thorium-232 and uranium-238 supports this apparent trend. The last-mentioned work has been extended to protactinium-231 since it was thought to be interesting to investigate fine structure in this fissioning nucleus as it is intermediate in nuclear charge between uranium and thorium.

References

1. O. Hahn and F. Strassmann, Naturwiss, 27, 11 (1939).
2. N. Bohr and J.A. Wheeler, Phys. Rev., 56, 426 (1939).
3. P. Fong, Phys. Rev., 102, 434 (1956).
4. P. Fong, Bull. Amer. Phys. Soc. Ser. II, 1, 303 (1956).
5. K.A. Petrzhak and G.N. Flerov, Compt. Rend. U.S.S.R., 28, 500 (1940), J. Phys. U.S.S.R., 3, 275 (1940).
6. W.J. Whitehouse and W. Galbraith, Nature, 169, 494 (1952).
7. G.T. Seaborg, Phys. Rev., 85, 157 (1952).
8. R.L. Henkel, L. Cranberg, R.B. Day, W.K.Hawkins, G.A. Jarvis, A. Lazar, R.A. Nobles, J.E. Perry, R.K. Smith and K.D.Walt, Report LA-1495 (1952).
9. R.A. Nobles, R.L. Henkel and R.K. Smith, Phys. Rev., 99, 616(A), (1955).
10. R.K. Smith, R.L. Henkel and R.A. Nobles, Bull. Am. Phys. Soc., 2, 196 (1957).
11. D.J. Hughes and J.A. Harvey, Report BNL-325 (1955).
12. R.L. Henkel, Report LA-2122 (1957).
13. W.D. Allen and A.T.G. Ferguson, Reports NP/R 1667 and NP/R 1720 (1955).
14. R.W. Lamphere, Phys. Rev., 104, 1654 (1956).
15. B.C. Diven, Phys. Rev., 105, 1350 (1957).
16. D. Szteinsznaider, V. Naggiar and F. Netter, Proceedings of the International Conference on the Peaceful Uses of Atomic Energy, 4, P/355,(1956).
17. W.D. Allen and R.L. Henkel, Progr. in Nuclear Energy, Ser. I, 2, 2 (1958).
18. A. Hemmendinger, Proceedings of the Second United Nations International Conference on the Peaceful Uses of Atomic Energy, 15, P/663 (1958).

19. J. Jungerman, Phys. Rev., 79, 632 (1950).

20. G.H. McCormick and B.L. Cohen, Phys. Rev., 96, 722 (1954).

21. J.R. Huizenga, R. Vandenbosch and H. Warhanek, Phys. Rev., 124, 1964 (1961).

22. J.R. Huizenga, R. Chaudhry and R. Vandenbosch, Phys. Rev., 126, 210 (1962).

23. G.L. Bate, R. Chaudhry and J.R. Huizenga, Phys. Rev., 131, 722 (1963).

24. G.R. Choppin, J.R. Meriwether and J.D. Fox, Phys. Rev., 131, 2149 (1963).

25. J.S. Fraser, Phys. Rev., 88, 536 (1952).

26. R.B. Leachman, Proceedings of the Second United Nations International Conference on the Peaceful Uses of Atomic Energy, 15, P/2467 (1958).

27. L.E. Glendenin, C.D. Coryell and R.R. Edwards, "Radiochemical Studies: The Fission Products", N.N.E.S., Div. IV, Vol. 9, P/52 (McGraw-Hill Co., New York, 1951).

28. C.D. Coryell, M. Kaplan and R.D. Fink, Can. J. Chem., 39, 646 (1961).

29. R.H. Goeckermann and I. Perlman, Phys. Rev., 76, 628 (1949).

30. W.M. Gibson, Report UCRL-3493 (1956).

31. Y.Y. Chu, Report UCRL-8926 (1959).

32. E.K. Hyde, "The Nuclear Properties of the Heavy Elements", Vol. III (Prentice-Hall, 1964).

33. S. Katcoff, Nucleonics, 18 (No. 11), 201 (1960).

34. E.K. Bonyushkin, Yu. S. Zamyatin, V.V. Spektor, V.V. Rachev, V.R. Negina and V.N. Zamyatnina, At. Energ., (USSR), 10 (1), 13 (1961).

35. R.N. Keller, E.P. Steinberg and L.E. Glendenin, Phys. Rev., 94, 969 (1954).

36. A.C. Wahl, "Physics and Chemistry of Fission", IAEA, Vol. I, 317 (1965).

37. R. Vandenbosch, T.D. Thomas, S.E. Vandenbosch, R.A. Glass and G.T. Seaborg, Phys. Rev., 111, 1358 (1958).

38. R.A. Glass, R.J. Carr, J.W. Cobble and G.T. Seaborg, Phys. Rev., 104, 434 (1956).

39. R.C. Jensen and A.W. Fairhall, Phys. Rev., 109, 942 (1958).

40. A.W. Fairhall, R.C. Jensen and E.F. Neuzil, Proceedings of the Second United Nations International Conference on the Peaceful Uses of Atomic Energy, 15, P/677 (1958).

41. A.W. Fairhall, Phys. Rev., 102, 1335 (1956).

42. H.G. Thode and R.L. Graham, Can. J. Research, 25A, 1 (1947).

43. J. Macnamara, C.B. Collins and H.G. Thode, Phys. Rev., 78, 129 (1950).

44. R.K. Wanless and H.G. Thode, Can. J. Phys., 33, 541 (1955).

45. C.W. Stanley and S. Katcoff, J. Chem. Phys., 17, 653 (1949).

46. D.R. Wiles, B.W. Smith, R. Horsley and H.G. Thode, Can. J. Phys., 31, 419 (1953).

47. H. Farrar and R.H. Tomlinson, Can. J. Phys., 40, 943 (1962).

48. J. Terrell, Phys. Rev., 127, 880 (1962).

49. L.W. Alvarez - reported by G. Farwell, E. Segre and C. Wiegand, Phys. Rev., 71, 327 (1947).

50. R.A. Nobles, Phys. Rev., 126, 1508 (1962).

51. E.L. Albenesius, Phys. Rev. Letters, 3, 274 (1959).

52. L. Rosen and A.M. Hudson, Phys. Rev., 78, 533 (1950).

53. R.S. Iyer, H.C. Jain, M.N. Namboodiri, M. Rajagopalan Rajkishore, M.V. Ramaniah, C.L. Rao, N. Ravindran and H.D. Sharma, "Physics and Chemistry of Fission", IAEA, Vol. I, 434 (1965).

54. M.G. Brown, S.J. Lyle and G.R. Martin, Radiochim.Acta, 6, 16 (1966).

55. J. Sellars, Ph.D. Thesis (Durham University, 1967).

CHAPTER 2

General Experimental Method and Apparatus

2.1 Introduction

In this chapter an outline of the general method of sample preparation is given together with an account of the neutron generator and the counting equipment used.

2.2 Sample Preparation

Protactinium deposits prepared previously[1] were used in the present work. The procedure by which they were obtained consisted of the successive application of a mixture of protactinium(V)chloride in absolute alcohol (5 mg/ml), acetone and a 3% solution of selulose nitrate in amyl acetate in the proportion of 1 : 1½ : 1½ to both sides of 24 platinum discs 2 cm in diameter and 0.005 cm thick.

On drying, each successive layer of deposit was ignited, polished and finally, when the total thickness was sufficient, covered with a layer of evaporated gold 0.5 mg cm^{-2} in thickness. The total weight of protactinium deposit on the discs was about 147 mg (126 mg protactinium, assuming the protactinium is present as protactinium(V)oxide). For irradiations, these discs were interleaved with catcher foils in a cylindrical polythene container which was then sealed into an inner and an outer polythene bag before it was taken from the glove box in which the protactinium was stored because of its high alpha activity. Finally, it was surrounded by a third bag and fixed to the target block of the accelerator.

Polystyrene (13 mg cm^{-2}), copper (44 mg cm^{-2}) and aluminium (7 mg cm^{-2}) were tried as catcher substances in the earlier work[1] and aluminium was found more suitable than the others. Aluminium foils were therefore used in the present work except in the xenon determinations (Chapter 6), in which it was necessary to avoid the production of much gas or vapour which can result from acid dissolution of metals. The foils used to retain xenon were melted in the presence of xenon carrier as a first step in the separation of xenon from fission products. Its lower melting point and the very low vapour pressure of the liquid,made tin (m.p. 231.8) preferable to aluminium (m.p. 659.7) as catcher material in a glass apparatus. In all measurements isotopic exchange was ensured by refluxing the solution of catcher foils for 30 minutes with a mixture of hydrochloric and nitric acids or sodium hydroxide and sodium hypochlorite as suggested by Jensen and Fairhall[2].

When the target element was uranium, metal of natural isotopic composition was used for thermal and uranyl nitrate depleted in uranium-235 for fast neutron irradiations. Because of the large amount of uranyl nitrate used the sample was irradiated in the form of a compressed pellet to increase the neutron flux through the sample.

2.3 The Neutron Generator

Fast neutrons were produced using the Van-de-Graaff type Electrostatic Rotary Generator at the University of Kent at Canterbury (supplied by the Societe Anonyme de Machines Electrostatiques, Grenoble, France) by the following reactions:

$$^{2}_{1}H + ^{2}_{1}H \longrightarrow ^{3}_{2}He + ^{1}_{0}n \qquad Q = 3.27 \text{ MeV}$$

$$^{2}_{1}H + ^{3}_{1}H \longrightarrow ^{4}_{2}He + ^{1}_{0}n \qquad Q = 17.6 \text{ MeV}$$

The cross-section of the first reaction is an increasing function of deuteron energy; but it is still quite low (70 millibarns[3]) at 400 keV which is the maximum deuteron energy obtainable from the linear accelerator used. The reaction is anisotropic[4], neutrons are preferentially emitted in the forward and backward direction.

Fluxes of 10^8 to 10^9 neutrons per second were obtained from new deuterium targets. It remained fairly constant throughout the irradiation. The energy of neutrons produced under the irradiation conditions has been estimated to be 3.0 ± 0.4 MeV[5].

The excitation function of the second reaction[6] which gives 14 MeV neutrons has a resonance at about 5 barns for deuterons of 110 keV incident energy striking the tritium target. The neutron energy is slowly varying function of the angle of emission relative to the incident deuteron beam; the variation was estimated to be less than 3% under the irradiation conditions.

The neutron fluxes obtained from new tritium targets were 10^{10} to 10^{11} neutrons per second with an incident deuteron beam of 200 keV. The flux fell continuously during the irradiation probably due to the loss of tritium and deposition of pump oil on the target[7]. There is also some accummulation of deuterium in the target during the operation which makes D + D reaction possible producing lower energy neutrons. After about 8000 μ amp-hours the tritium targets were not used because of the appreciable amount of deuterium deposited. The energy of neutrons produced under the irradiation conditions has been estimated to be 14.8 ± 0.4 MeV.

The tritium and deuterium targets were obtained from the Radiochemical Centre at Amersham. They are copper discs 2.5 cm in diameter and 1 mm in thickness coated with a thin layer of titanium metal (about 1 mg/cm²) in which tritium or deuterium is absorbed. For convenience each disc was divided into four segments and they were bombarded separately. The target segments were soldered on to water-cooled metal blocks which were fixed at the end of the accelerator drift-tube. The target assemblies are illustrated in Fig. 2.1.

During irradiations the neutron flux was monitored using a proton-recoil plastic scintillator placed in a fixed position relative to the source. Corrections applied to take account of the variation in neutron flux through the target sample are discussed in Chapter 3.

2.4 Counting Equipment

2.4(a) Proportional Counter

An end-window gas-flow β-proportional counter was used for counting of all solid sources. The counter body which acted as the cathode was constructed from a cylinder of polished brass (internal diameter 2.6 cm, height 5 cm). The anode loop (about 10 mm in diameter) was made of constantan wire (0.025 mm in diameter) soldered into a nickel tube (external diameter about 1 mm), passing through a teflon insulator inserted in the top of the counter body. The distance between the bottom of the loop and the counter window was 9.5 mm. 'Melinex' film

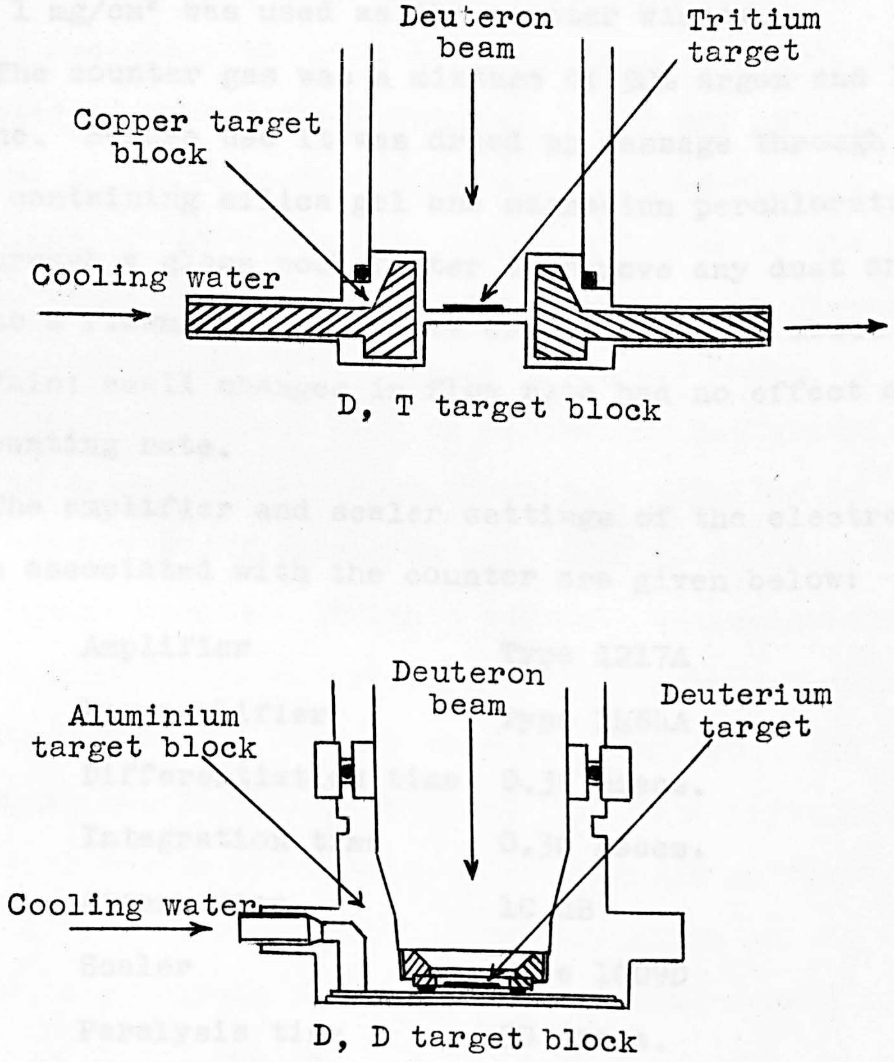
Deuteron beam
Tritium target
Copper target block
Cooling water
D, T target block
Deuteron beam
Deuterium target
Aluminium target block
Cooling water
D, D target block

Fig. 2.1. Target assemblies for S.A.M.E.S. machine.

aluminised on both sides giving a final thickness of about 1 mg/cm^2 was used as the counter window.

The counter gas was a mixture of 90% argon and 10% methane. Before use it was dried by passage through tubes containing silica gel and magnesium perchlorate, and through a glass wool filter to remove any dust and then to a flowmeter. The rate of gas flow was about 40 ml/min; small changes in flow rate had no effect on the counting rate.

The amplifier and scaler settings of the electronic system associated with the counter are given below:

Amplifier	Type 1217A
Pre-amplifier	Type 1484A
Differentiation time	0.32 μsecs.
Integration time	0.32 μsecs.
Attenuation	10 dB
Scaler	Type 1009D
Paralysis time	50 μsecs. 560 μsecs.(for the anti-coincidence system)
Discriminator level	15 volts.

Under these conditions the counter gave a plateau about 150 volts long with the optimum operating voltage at about 1.8 kV and a background of 8 to 10 counts per minute in a lead castle having walls 3.2 cm thick.

The very low activity obtained from the irradiation of protactinium-231 with 3 MeV neutrons made it necessary to use a low background counter. This consisted of an end-window counter which was essentially the same as the type described above. However, the connection to the anode wire was on the side of the counter and a miniature amplifier was attached directly to the counter body to accommodate the lot under the anticoincidence shield used to reduce the background. Eighteen Geiger-Müller tubes (Type G24) supplied by Twentieth Century Electronics were used to surround the proportional counter. Using a suitable anticoincidence circuit pulses from the proportional counter coincident with those from the Geigers were not recorded. The background counting rate obtained from this arrangement was 2 to 3 counts per minute. To eliminate multiple pulses arising from possible α-contamination in the sources, a paralysis time of 560 μsecs was imposed upon the proportional counter.

The block diagram of the electronic system is shown in Fig. 2.2.

2.4(b) Gas Geiger-Counter

The gas Geiger-counters constructed previously[8] by modifying a commercial Geiger-counter (Type G24 from Twentieth Century Electronics) by the

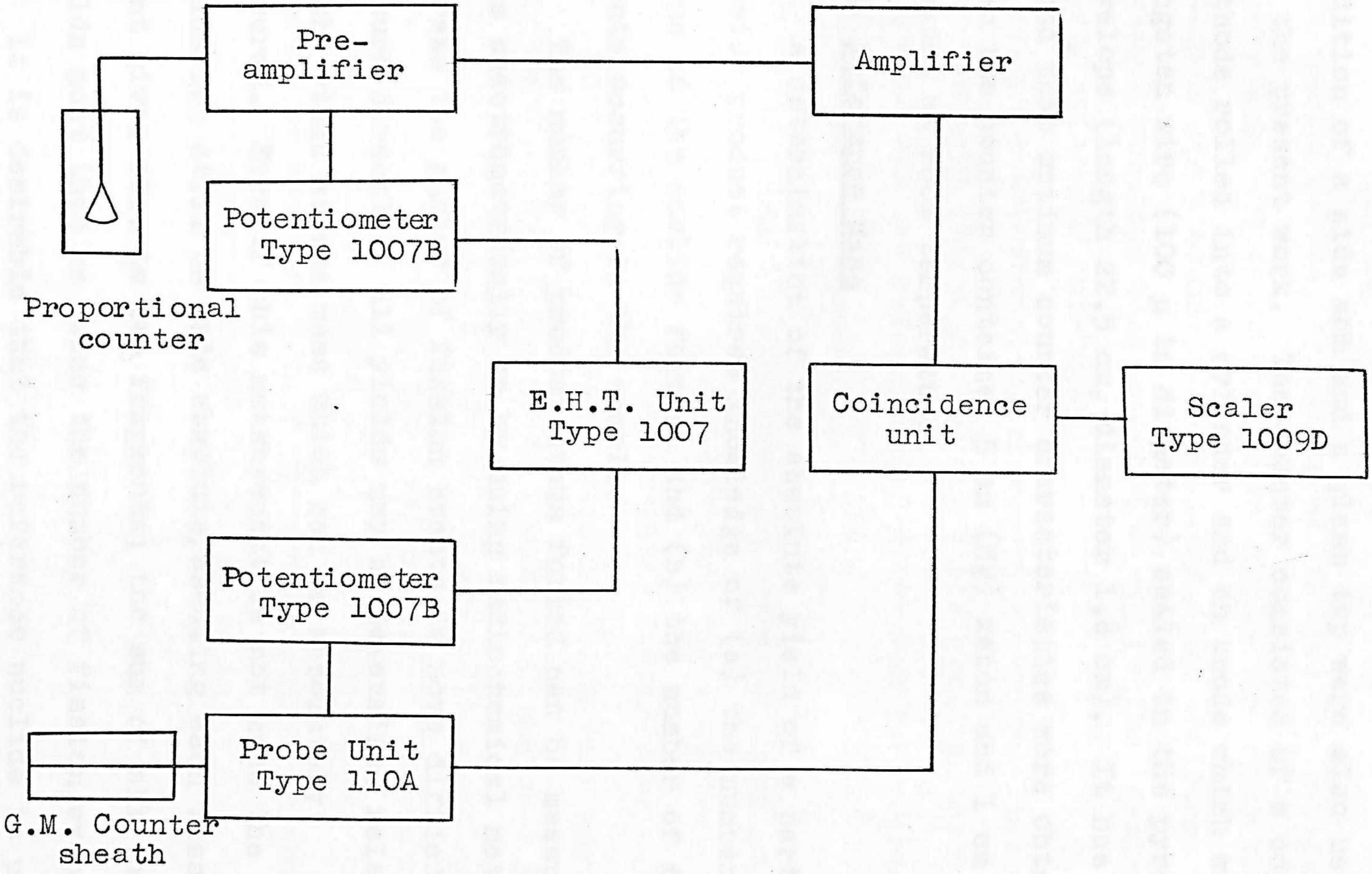
Pre-
amplifier
Potentiometer
Type 1007B
Proportional
counter
Amplifier
E.H.T. Unit
Type 1007
Coincidence
unit
Scaler
Type 1009D
Potentiometer
Type 1007B
Probe Unit
Type 110A
G.M. Counter
sheath

Fig. 2.2. Electronic system associated with proportional counter.

addition of a side arm and a glass tap were also used in the present work. The counter consisted of a copper cathode rolled into a cylinder and an anode which was a tungsten wire (100 μ in diameter) sealed in the pyrex envelope (length 22.5 cm, diameter 1.8 cm). It has been found[8] that optimum counter characteristics were obtained when the counter contained 5 cm (Hg) xenon and 1 cm (Hg) ethanol at room temperature.

2.5 Reference Mass

A determination of the absolute yield of a particular fission product requires knowledge of (a) the number of atoms of the nuclide formed, and (b) the number of fission events occurring in the sample.

The number of product atoms formed can be measured mass spectrometrically or by using radiochemical methods; whereas the number of fission events is more difficult to measure directly. All yields may be determined relative to the yield at one mass which can be absolutely measured. Even if this measurement is not made the yields can still be made absolute, assuming each fission event gives rise to two fragments; the sum of all the mass yields must then be twice the number of fission events.

It is desirable that the reference nuclide is produced with a high yield in fission and readily separated from irradiated material and other fission products. Its half-life should be long enough to allow time for a careful separation, but short enough to enable the decay to be followed for a number of half-lives. In addition isotopic exchange between carrier and active species should be easily obtained.

In the present study zirconium-97 ($t_{\frac{1}{2}}$ = 17hr) or molybdenum-99 ($t_{\frac{1}{2}}$ = 66.7hr) and where possible both of them were used as reference radionuclides for yields at their respective masses.

2.6 Preparation of Solid Samples for Counting Purposes

A slurry of the source material was filtered through a weighed glass-fibre (Whatman GF/A) filter disc which was supported on a sintered polythene disc in a demountable (Hahn type) filter stick (internal diameter 2.5 cm). After washing it was placed on an aluminium planchet, dried in a vacuum desiccator and weighed on a Stanton semi-micro balance (Model MCIA). The balance was accurate to at least ± 0.05 mg and the source weights were usually between 5 and 50 mg.

References

1. M.G. Brown, S.J. Lyle and G.R. Martin, Nucl. Instru. Methods, 35, 353 (1965).
2. R.C. Jensen and A.W. Fairhall, Phys. Rev., 109, 942 (1958).
3. J.L. Tuck, Nuclear Fusion, 1, 201 (1961).
4. G. Preston, P.F.D. Shaw and S.A. Young, Proc. Roy. Soc., 226A, 206 (1954).
5. Md. M. Rahman, Ph.D. Thesis (Durham University 1965).
6. J.P. Conner, T.W. Bonner and J.R. Smith, Phys. Rev., 88, 468 (1952).
7. E.J. Wilson and C. Evans, Atomics, 9, 238 (1958).
8. J. Sellars, Ph.D. Thesis (Durham University 1967).

CHAPTER 3

General Method of Calculations

3.1. Introduction

In this chapter the general equations used in the fission yield calculations are discussed. An account of the charge distribution in fission is also given in connection with the estimation of the independent yields.

3.2. Calculation of Relative Yields

The general method of calculating relative yields is based on a comparison of the number of atoms of the nuclide of interest with that of the reference mass at a time t. Three cases depending on the half-lives of the precursors in the decay chain may be distinguished in the calculation of the number of atoms of the nuclide isolated.

(a) The precursors are short-lived.

(b) The isolated nuclide has one long-lived precursor.

(c) It has two long-lived precursors.

If the half-lives of the precursors of the nuclide in question are very short compared with that of the daughter and the separation time, the decay chain may be considered to begin at the separated nuclide. Consequently the number of nuclei isolated is not dependent on the half-life of the precursors.

At time t after the beginning of the irradiation the number of nuclei produced in the time interval dt is given by

$$dN = B.Y.\phi(t).dt$$

where B is a constant which contains the number of target nuclei and the fission cross-section, Y is the cumulative fission yield of the nuclide and $\phi(t)$ is the neutron flux at time t.

If η is the efficiency of the instrument with which the neutron flux is monitored and I(t) is the monitor reading,

$$\phi(t) = I(t)/\eta$$

and

$$dN = \frac{B}{\eta}.Y.I(t)\ dt$$

or

$$dN = K.Y.I(t)\ dt$$

The number of nuclei at the end of the irradiation is

$$dN = K.Y.I(t)\ e^{-\lambda(T-t)}dt$$

where T is the time of the irradiation.

The total number of nuclei remaining at the end of the irradiation

$$N = \int_{t=o}^{t=T} K.Y.I(t)\ e^{-\lambda(T-t)}dt$$

at the time t' after the end of the irradiation

$$N(t') = K.Y\, e^{-\lambda t'} \int_{t=o}^{t=T} I(t)\, e^{-\lambda(T-t)} dt$$

For a constant neutron flux the solutions of these equations are

$$N = K.Y.I. \frac{(1-e^{-\lambda T})}{\lambda} \qquad (1)$$

and

$$N(t') = K.Y.I. \frac{(1-e^{-\lambda T})}{\lambda}\, e^{-\lambda t'} \qquad (2)$$

respectively.

If the neutron flux is varying, the irradiation may be divided into time intervals δt during each of which the flux is considered to be approximately steady. In the event that the time intervals are short compared to the half-life of the nuclide in question, the integral may be replaced by the summation

$$S = \sum_{t=o}^{t=T} I(t)\, e^{-\lambda(T-t)} \delta t$$

and the number of atoms at the end of the irradiation

$$N = K.Y.S \qquad (3)$$

at the time t'

$$N(t') = K.Y.S.\, e^{-\lambda t'} \qquad (4)$$

If the half-life of one of the precursors of the separated nuclide is long compared with that of its daughter, the number of nuclei isolated is dependent on the half-life of the precursor and this must be taken into account in the yield calculations.

At time t' after the end of the irradiation the number of nuclei which are formed only from the immediate precursor is given[1] by

$$N_2(t') = K.I.Y_2.F.\frac{\lambda_1}{\lambda_2-\lambda_1}\left[\frac{(1-e^{-\lambda_1 T})}{\lambda_1}e^{-\lambda_1 t'} - \frac{(1-e^{-\lambda_2 T})}{\lambda_2}e^{-\lambda_2 t'}\right] \quad (5)$$

for a constant flux, and

$$N_2(t') = K.Y_2.F\frac{\lambda_1}{\lambda_2-\lambda_1}\left(S_1\, e^{-\lambda_1 t'} - S_2\, e^{-\lambda_2 t'}\right) \quad (6)$$

for a varying flux,

where subscripts 1 and 2 refer to the long-lived precursor and the isolated nuclide respectively, and F is the fraction of the cumulative yield of nuclide 2 formed from nuclide 1.

If the isolated nuclide has two precursors with relatively long half-lives, the number of nuclei at time t' formed from the precursors is given[1] by

$$N_3(t') = K.I.Y_3.F\left[C_1\frac{(1-e^{-\lambda_1 T})}{\lambda_1}e^{-\lambda_1 t'} + C_2\frac{(1-e^{-\lambda_2 T})}{\lambda_2}e^{-\lambda_2 t'} + C_3\frac{(1-e^{-\lambda_3 T})}{\lambda_3}e^{-\lambda_3 t'}\right] \quad (7)$$

for a constant flux, and

If the half-life of one of the precursors of the separated nuclide is long compared with that of its daughter, the number of nuclei isolated is dependent on the half-life of the precursor and this must be taken into account in the yield calculations.

At time t' after the end of the irradiation the number of nuclei which are formed only from the immediate precursor is given[1] by

$$N_2(t') = K.I.Y_2.F.\frac{\lambda_1}{\lambda_2-\lambda_1}\left[\frac{(1-e^{-\lambda_1 T})}{\lambda_1}e^{-\lambda_1 t'} - \frac{(1-e^{-\lambda_2 T})}{\lambda_2}e^{-\lambda_2 t'}\right] \qquad (5)$$

for a constant flux, and

$$N_2(t') = K.Y_2.F\frac{\lambda_1}{\lambda_2-\lambda_1}\left(S_1\,e^{-\lambda_1 t'} - S_2\,e^{-\lambda_2 t'}\right) \qquad (6)$$

for a varying flux,
where subscripts 1 and 2 refer to the long-lived precursor and the isolated nuclide respectively, and F is the fraction of the cumulative yield of nuclide 2 formed from nuclide 1.

If the isolated nuclide has two precursors with relatively long half-lives, the number of nuclei at time t' formed from the precursors is given[1] by

$$N_3(t') = K.I.Y_3.F\left[C_1\frac{(1-e^{-\lambda_1 T})}{\lambda_1}e^{-\lambda_1 t'} + C_2\frac{(1-e^{-\lambda_2 T})}{\lambda_2}e^{-\lambda_2 t'} + C_3\frac{(1-e^{-\lambda_3 T})}{\lambda_3}e^{-\lambda_3 t'}\right] \qquad (7)$$

for a constant flux, and

$$N_3(t') = K.Y_3.F(C_1.S_1\ e^{-\lambda_1 t'} + C_2S_2\ e^{-\lambda_2 t'} + C_3S_3\ e^{-\lambda_3 t'}) \quad (8)$$

for a varying flux.

Subscripts 1, 2 and 3 refer to the long-lived precursors and the isolated nuclide as shown below

$$1 \xrightarrow{\lambda_1} 2 \xrightarrow{\lambda_2} 3 \xrightarrow{\lambda_3}$$

F is the fraction of the cumulative yield of nuclide 3 formed from 1 via 2; C_1, C_2 and C_3 are given by

$$C_1 = \frac{\lambda_1 \lambda_2}{(\lambda_2-\lambda_1)(\lambda_3-\lambda_1)}$$

$$C_2 = \frac{\lambda_1 \lambda_2}{(\lambda_1-\lambda_2)(\lambda_3-\lambda_2)}$$

$$C_3 = \frac{\lambda_1 \lambda_2}{(\lambda_1-\lambda_3)(\lambda_2-\lambda_3)}$$

If the nuclide is formed by more than one of the ways discussed above, then the number of nuclide at the time t' will be the sum of the numbers of nuclide formed by each separate route.

N or N(t') is obtained from the observed activity after having made corrections for counter efficiency, chemical recovery and the presence of any daughter activity.

Similarly if a reference nuclide is isolated at the time t", the relative yield is calculated from the relation obtained by taking the ratio of the numbers of atoms of the nuclide in question and the reference nuclide.

For example, the relative yield of a nuclide which is formed only from its long-lived precursor is

$$\frac{Y_2}{Y_R} = \frac{N_2(t')}{N_R(t'')} \; \frac{\dfrac{(1-e^{-\lambda_R T})}{\lambda_R}\, e^{-\lambda_R t''}}{\dfrac{\lambda_1}{\lambda_2-\lambda_1}\left[\dfrac{(1-e^{-\lambda_1 T})}{\lambda_1}\, e^{-\lambda_1 t'} - \dfrac{(1-e^{-\lambda_2 T})}{\lambda_2}\, e^{-\lambda_2 t'}\right]} \qquad (9)$$

for a constant flux, and

$$\frac{Y_2}{Y_R} = \frac{N_2(t')}{N_R(t'')} \quad \frac{S_R\, e^{-\lambda_R t''}}{\dfrac{\lambda_1}{\lambda_2-\lambda_1}\,(S_1\, e^{-\lambda_1 t'} - S_2\, e^{-\lambda_2 t'})} \qquad (10)$$

for a varying flux.

3.3. Estimation of Independent Yields

In the course of the present work independent yields were required in order to calculate the cumulative yields of some fission products and to obtain the total chain yields from the measured cumulative yields.

For excitation energies below about 20 MeV, the most plausible and widely used procedure by means of which independent yields are calculated is the 'equal charge displacement' hypothesis which has been mentioned very briefly in Chapter 1.

It may be expressed in the form

$$(Z_A - Z_P)_L = (Z_A - Z_P)_H$$

where Z_P is the most probable charge of the initial primary fragment (before prompt neutron emission as suggested by Pappas[2]), Z_A is the most stable charge for the particular mass number and L and H refer to the light and heavy fragments respectively. In the original postulate[3] the fragments were considered to be those remaining after prompt neutron emission.

According to the definition given above

$$(Zp)_L + (Zp)_H = Z_f$$

and

$$A_L + A_H = A_f$$

where subscript f refers to the fissioning nucleus. The most probable charge is then given by

$$Zp = Z_A - \tfrac{1}{2}(Z_A + Z_{(A_f - A)} - Z_f)$$

In the various interpretations of the postulate essentially the same charge-distribution curve is used; the differences are in the methods of obtaining Zp.

Glendenin, Coryell and Edwards[3] used a continuous Z_A function evaluated from the Bohr-Wheeler[4] mass equation and they therefore obtained a continuous Z_P function.

Pappas[2] modified the method of estimating Z_A by taking shell-effects into account and he based his calculations of Z_A on the treatment of beta stability by Coryell, Brightsen and Pappas[5,6]. In this treatment use is made of empirical Z_A curves which are essentially straight lines for nuclides whose nucleon numbers lie within a given shell, but separate Z_A lines are used in different shell regions. Z_A and Z_P functions evaluated this way are discontinuous.

Steinberg and Glendenin[7] used this same discontinuous Z_A function but took average values in the regions of shell edges and obtained a Z_P function with smaller discontinuities.

Because of the uncertainties about the most appropriate method of calculating the Z_P function, Wahl[8] determined it empirically using independent yield data for the thermal fission of uranium-235. He assumed that the same charge distribution curve was appropriate for all fission chains and obtained an empirical Z_P value from each independent yield value which had been determined. In the regions where the Z_A functions are discontinuous due to crossing of the shell edges, the Z_P curve made a smooth continuous transition.

In the present work Z_P was calculated according to the method given by Pappas[2]. The fractional independent yields were assumed to be given by the Gaussian function

$$f(Z) = \frac{1}{\sqrt{\pi C}} \, e^{-\frac{(Z-Z_P)^2}{C}}$$

where f(Z) is the fractional chain yield of an isobar of charge Z and C is a constant for a given chain. The C values used in calculations are given in the appropriate chapters.

References

1. W. Rubinson, J. Chem. Phys., 17, 542 (1949).
2. A.C. Pappas, Proceedings of the United Nations International Conference on the Peaceful Uses of Atomic Energy, 7, P/881 (1956).
3. L.E. Glendenin, C.D. Coryell and R.R. Edwards, 'Radiochemical Studies: The Fission Products', N.N.E.S., Div. IV, Vol. 9, P/52 (McGraw-Hill Co., New York, 1951).
4. N. Bohr and J.A. Wheeler, Phys. Rev., 56, 426 (1939).
5. C.D. Coryell, R.A. Brightsen and A.C. Pappas, Phys. Rev., 85, 732 (1952).
6. C.D. Coryell, Ann. Rev. Nucl. Sci., 2, 305 (1953).
7. E.P. Steinberg and L.E. Glendenin, Proceedings of the United Nations International Conference on the Peaceful Uses of Atomic Energy, 7, P/614 (1956).
8. A.C. Wahl, J. Inorg. Nucl. Chem., 6, 263 (1958).

CHAPTER 4

An Investigation of the Mass-129 Decay Chain in Fission

4.1 Introduction

Considerable disagreement exists in the literature with regard to the half-lives of tin-129 isomers. 8.8 ± 0.6 min and 1.0 ± 0.1 hr have been reported by Hagebø, Kjelberg and Pappas[1], whereas shortly afterwards Dropesky and Orth[2] were unable to observe a tin isotope of half-life other than 6.2 ± 1.2 min in the 6 to 120 min range. Recently Chu and Marinsky[3] found no evidence for 1 hr tin-129, instead observed a half-life of about 2 min with 7 min isomer.

In the present investigation a further search has been made for tin-129 isomers and the cumulative yields in fission induced in uranium-235 by thermal neutrons have been measured for 7 min tin-129 and for 4.4 hr antimony-129 for which yields ranging from 0.2 to 1.12 are reported in the literature[4].

4.2 Experimental - Separation Procedures

4.2(a) 7 min Tin-129

50 mg of natural uranium metal were irradiated in the thermal column of B.E.P.O., A.E.R.E., Harwell for 20 minutes. (The thermal neutron flux was estimated at 1.2×10^{12} n cm^{-2}sec^{-1} with a fast component of 10^{11} n cm^{-2}sec^{-1}.)

The methods described by Chu and Marinsky[3] and Hagebø et al.[1] were used for milkings and purification of antimony respectively.

1. The sample was dissolved in a few drops of concentrated hydrochloric acid and 1 drop of concentrated nitric acid. Standardised zirconium (50 mg) and tin(IV) (1 mg) carriers were added and tin was precipitated as sulphide which was washed with water.
2. The sulphide precipitate was dissolved in a few drops of concentrated sulphuric acid; the solution was made 2.5 M in each of sodium iodide and perchloric acid (total volume, 10 ml) and the tin extracted into benzene (30 ml) by shaking for 1 minute. The benzene phase was washed twice with 10 ml portions of solution 2.5 M in sodium iodide and 2.5 M in perchloric acid. The starting time for growth of antimony from tin was taken as the end of the second acid scrub.
3. Antimony was removed from the benzene phase with the 2.5 M sodium iodide and 2.5 M perchloric acid mixture containing 10 mg of Sb(III) carrier at 10 minute intervals and the benzene phase was washed with sodium iodide-perchloric acid solution after each milking. The final separation of the phases was taken as the 'milking' time.

4. Antimony was precipitated by passing hydrogen sulphide and purified as described in Appendix I. The final precipitation of antimony as the sulphide was carried out by saturating the solution with hydrogen sulphide.

The tin in the organic phase was determined spectrophotometrically using phenylfluorone[5].

The separation of tin was completed some 25 minutes after the end of the irradiation and 4 milkings for antimony were carried out in each run.

The zirconium was isolated (from the residual solution remaining after the initial precipitation of the tin) by a well-established procedure[6] as described in Appendix I. It was counted as the tetramandelate under the end-window proportional counter.

4.2(b) 2 min Tin-129

10 g of uranyl nitrate were irradiated in a flux of 14.8 ± 0.4 MeV neutrons produced by the D + T nuclear reaction using the electrostatic accelerator.

The irradiated sample was dissolved in a freshly prepared aqueous slurry (20 ml) of tin(IV) sulphide (about 1.5 mg) which was subsequently separated and dissolved in a few drops of concentrated sulphuric acid. The procedure then followed was the same as in the study of 7 min tin-129 except that the milkings were carried out either at 2 or at 3 minute intervals and the washings between milkings were omitted. About 6 minutes were required for the tin separation from target material and fission products. Between 8 and 10 milkings were performed in each experiment.

4.2(c) Long-lived Tin-129

Irradiations were carried out on uranium-238 and uranium-235 by 14.8 MeV and thermal neutrons respectively. The tin separation was performed by the method of Seiler[7] - except when the iodide-benzene extraction was used for tin-antimony separation - 90 minutes after the irradiation so that the contributions from 7 min tin-129 were insignificant. Milkings were carried out at 1 hour intervals. Apart from the iodide-benzene method, the thiocyanate-ether[1] and an ion-exchange method were tried for the tin-antimony separation.

1. The irradiated sample (uranyl nitrate or natural uranium metal) was dissolved in the presence of 10 mg tin(IV) carrier, tin was precipitated as sulphide, centrifuged and washed with 1 M hydrochloric acid.
2. The precipitate was dissolved in 1 ml of concentrated hydrochloric acid and the excess hydrogen sulphide removed by boiling the solution. 10 ml of saturated oxalic acid and a few mg of each of antimony(III), tellurium(VI), indium and cadmium carriers were added

and the mixture warmed to about 80°C. The metal sulphides were then precipitated by hydrogen sulphide.

3. The liquid remaining from step (2) was neutralised, 3 ml of concentrated ammonia were added in excess and the solution again treated with hydrogen sulphide.

4. Nitric acid was carefully added to the solution from step (3) until it was acid; tin(II) sulphide was then precipitated by passing hydrogen sulphide into it. The precipitate was centrifuged and washed with water.

5. The precipitate was dissolved in 2 ml of 6 N hydrochloric acid and 0.1 N ceric sulphate solution was added until the yellow colour persisted. The solution was diluted to 25 ml by the addition of 7 M aqueous potassium thiocyanate. It was then transferred to a separatory funnel containing 25 ml ethylether into which the tin was extracted by shaking for one minute. The organic phase was washed twice with 10 ml of 7 M potassium thiocyanate 0.5 N in hydrochloric acid and containing 10 mg of antimony(III) carrier.

The end of the last shaking period was taken as the time of commencement of growth of antimony from tin.

6. Antimony was removed from the organic phase with a solution of 7 M potassium thiocyanate 0.5 N in hydrochloric acid containing 10 mg of antimony(III) carrier by shaking the phases together in the separatory funnel for one minute. The aqueous extract contained the active antimony which was purified as described above for 7 min tin-129. When the ion-exchange method was used for tin-antimony separation, tin(IV)chloride was adsorbed on a column of anion-exchanger (De-acidite FF) after having been purified; antimony(V) was eluted with 2.5 M hydrochloric acid containing a little bromine.

4.2(d) Antimony-129

2 mg of uranium metal of natural isotopic composition were irradiated with thermal neutrons for 10 minutes followed by a cooling period of 90 minutes. After having dissolved the metal as described in the search for the 7 min tin-129, standardised antimony, zirconium and molybdenum carriers (10 mg of each element) were added. Isotopic exchange was ensured by the addition of bromine and fluoride. Molybdenum was first isolated by precipitating with α-benzoin oxime followed by the antimony as sulphide and then zirconium as hydroxide.

Antimony was purified according to the procedure given in Appendix I.

Molybdenum[8] and zirconium[6] were isolated in solid form by conventional methods as described in Appendix I. The antimony content obtained from the precipitate weight was checked spectrophotometrically using rhodamine-B[9] in all the experiments.

4.3 Counter Calibration and Evaluation of Results

Calibration of the proportional counter was based on the method suggested by Bayhurst and Prestwood[10]. This method makes use of an experimentally determined relationship between counter efficiency and the average energy of the β-particles. The procedure is to calculate average β-energies for each of several chosen nuclides and then plot the values against counter efficiency obtained from self-absorption curves for a range of precipitate weights. To obtain the unknown counter efficiency for a β-emitter, the average β-energy is calculated and the efficiency is read from the graph for the appropriate precipitate weight.

The counter efficiency of nuclides with complex β-groups can be calculated by weighting the efficiency of each group by its abundance.

Experiments on the samples irradiated with thermal neutrons were carried out at the Rutherford High Energy Laboratory, Chilton, Didcot, and the efficiency curves prepared previously by the members of this laboratory[11] were used to obtain the counter efficiencies for the fission products measured, except that for antimony-129.

Because of the lack of precise data for β-decay energetics of antimony-129, the counter was calibrated directly for the antimony-129 - tellurium-129 equilibrium. For this purpose antimony was separated from irradiated uranium by using 1 mg of carrier. The specific activity of the purified antimony solution was measured by counting a weighed amount in a 4π β-proportional counter and this solution was used to prepare a series of antimony(III)-sulphide sources of known specific activity in the required thickness range.

The efficiency of the counter for the antimony-129 - tellurium-129 mixture is given by

$$\eta_{total} = \frac{A_{Sb}\eta_{Sb} + A_{Te}\eta_{Te}}{A_{Sb} + A_{Te}} \qquad (1)$$

where A and η refer to the absolute activity and counter efficiency respectively. Since antimony-129 and tellurium-129 are in transient equilibrium

$$\frac{A_{Te}}{A_{Sb}} = \frac{\lambda_{Te}}{\lambda_{Te}-\lambda_{Sb}} \; \frac{85}{100} \qquad (2)$$

85% of the antimony-129 was assumed to go to the 69 min. tellurium-129 state[12].

From equations (1) and (2)

$$\eta_{Sb} = \eta_{total}\left(1 + \frac{\lambda_{Te}}{\lambda_{Te}-\lambda_{Sb}}\,0.85\right) - \frac{\lambda_{Te}}{\lambda_{Te}-\lambda_{Sb}}\,0.85\,\eta_{Te} \qquad (3)$$

η_{Te} was calculated from its known β-decay energetics and counter efficiency curves prepared as described above and η_{Sb} was obtained by using equation (3). The experimental counter efficiency curve for the antimony-129 - tellurium-129 equilibrium and the calculated counter efficiency for tellurium-129 are shown in Fig. 4.1.

The fission yield of tin is given by

$$\frac{Y_{Sn}}{Y_R} = \frac{N_{Sn}}{N_R} \qquad (4)$$

where Y_R is the fission yield for the reference nuclide, N is the number of atoms produced in the irradiation. N_{Sn} is evaluated using the following expression

$$N_{Sn} = \frac{A_{Sb}}{\lambda_{Sb}}\,\frac{\lambda_{Sb}-\lambda_{Sn}}{\lambda_{Sn}}\,\frac{1}{e^{-\lambda_{Sn}t_1} - e^{-\lambda_{Sb}t_1}}\,\frac{\lambda_{Sn}t}{1-e^{-\lambda_{Sn}t}}\,e^{\lambda_{Sn}T} \qquad (5)$$

where A_{Sb} = absolute activity of antimony-129 at the time of 'milking'. λ_{Sb} and λ_{Sn} are the decay constants for antimony-129 and 7.5 min. tin-129. t_1 = growing in time between 'milkings'. t = time of irradiation. T = time between the end of the irradiation and the beginning of the growing in time of the appropriate 'milking'.

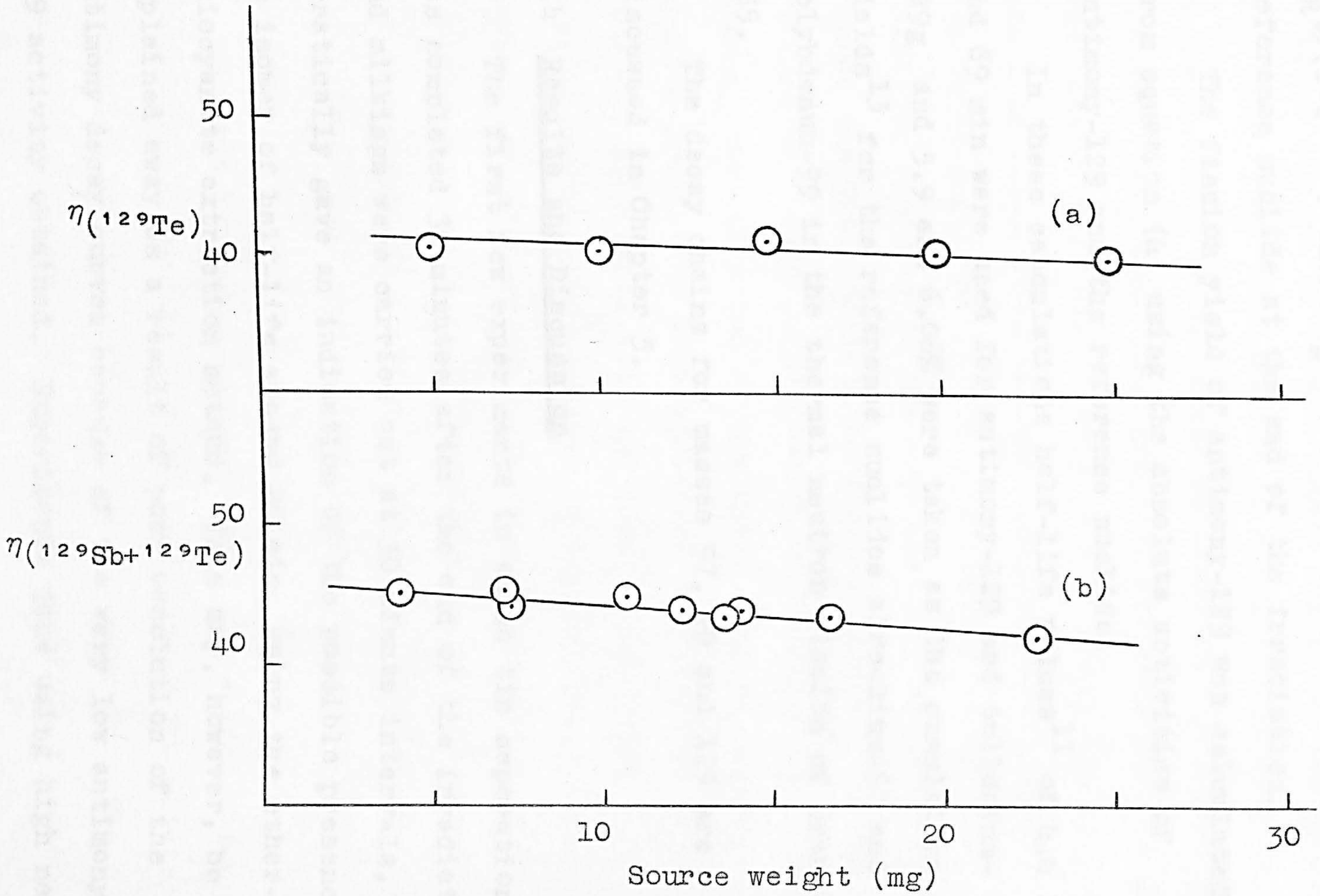

Fig. 4.1. (a) Calculated counter efficiency curve for tellurium-129.
(b) Experimental counter efficiency curve for antimony-129 - tellurium-129.

The number of atoms of reference nuclide, N_R, is $A_R t/(1-e^{-\lambda_R t})$ where A_R is the absolute activity of the reference nuclide at the end of the irradiation.

The fission yield of antimony-129 was calculated from equation (4) using the absolute activities of antimony-129 and the reference nuclide.

In these calculations half-life values[11] of 4.4 hr and 69 min were used for antimony-129 and tellurium-129g and 5.9 and 6.06% were taken as the cumulative yields[13] for the reference nuclides zirconium-97 and molybdenum-99 in the thermal neutron fission of uranium-235.

The decay chains for masses 97, 99 and 129 are discussed in Chapter 5.

4.4 Results and Discussion

The first few experiments in which tin separation was completed 30 minutes after the end of the irradiation and milkings were carried out at 30 minute intervals, erratically gave an indication of the possible presence of an isomer of half-life around 20 min using the ether-thiocyanate extraction method. This may, however, be explained away as a result of poor resolution of the antimony decay curves because of the very low antimony-129 activity obtained. Experiments done using high neutron fluxes and hence giving larger yields of fission products did not provide evidence for a tin isotope of this half-life. The absence of antimony-129 activity in the antimony decay curves obtained in the search for 1 hr tin (see above) also provides evidence for the non-existence of a 20 min as well as a 1 hr tin-129 isomer. When 1 hr tin-129 was being sought, irradiations of uranium were carried out to give fission at various excitation energies in the hope that one or other might enhance the yield of this particular isomer. But no evidence was found for an isomer of half-life of 1 hr; however, the other two of the three tin-129 isomers reported previously were confirmed. Half-lives of 7.5 ± 0.1 min (Table 4.1) and about 2 min were obtained for the tin isomers. A typical decay curve showing the existence of both isomers and obtained by the milking experiments is given in Fig. 4.2. The results from an experiment leading to the establishment of the half-life of the longer-lived isomer are contained in Fig. 4.3.

Chu and Marinsky[3] consider that the evidence found by Hagebø et al.[1] for the 1 hr tin-129 isomer was obtained as a result of incomplete removal of antimony from the organic phase in the ether-thiocyanate milking procedure.

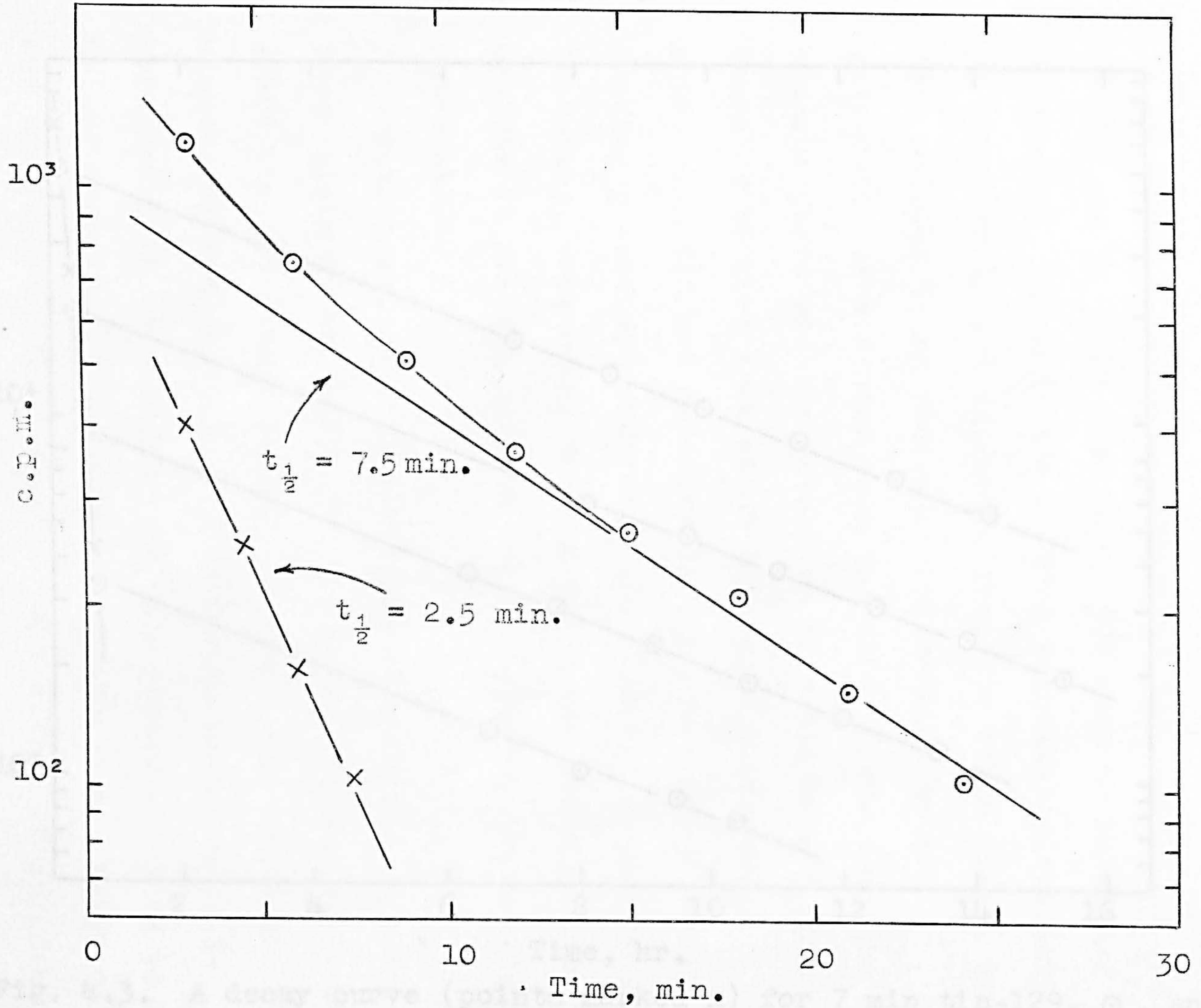

Fig. 4.2. A tin-129 decay curve. (A half life of 7.5 min is assumed for the longer lived tin-129 isotope because of the uncertainty in the lower experimental points.)

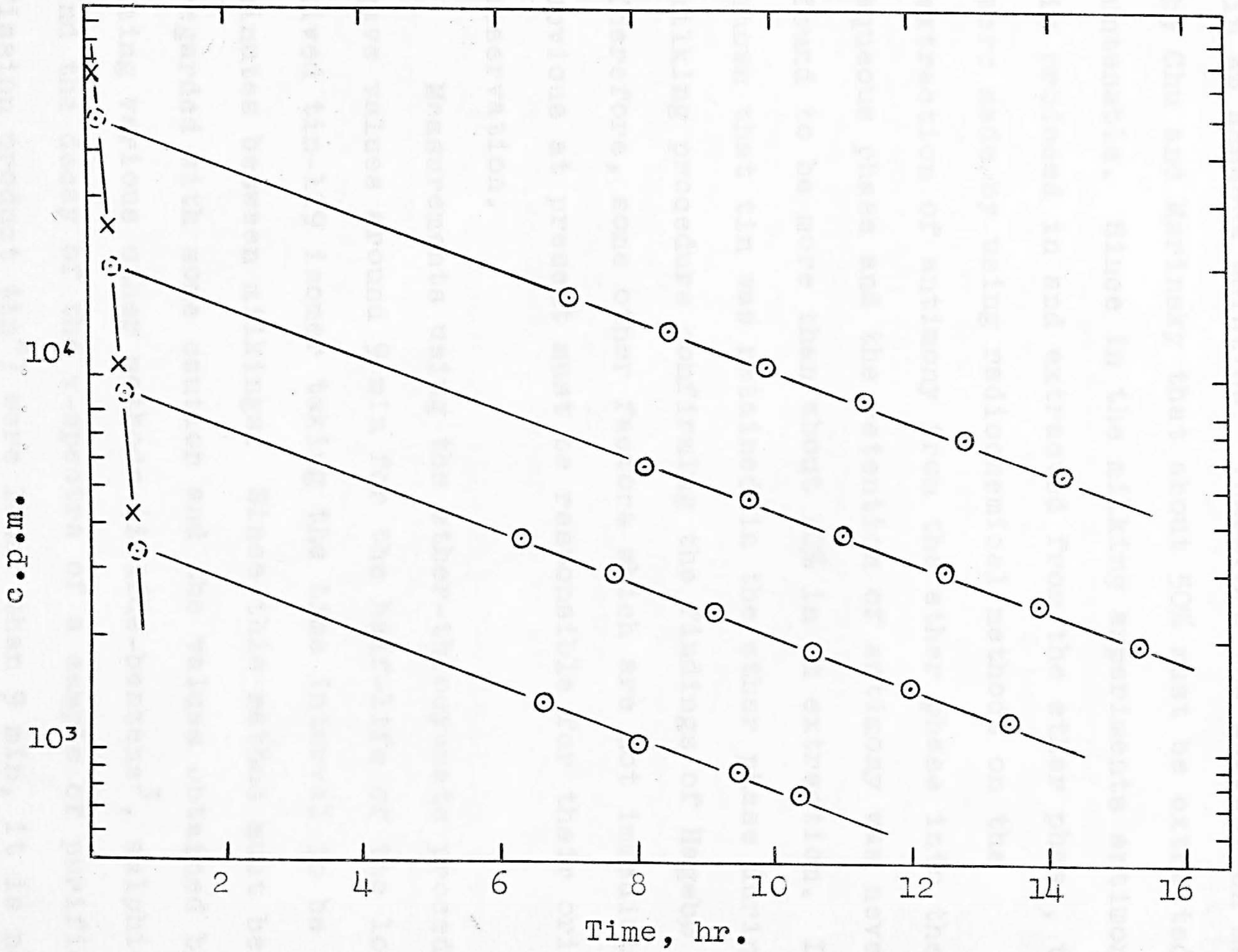

Fig. 4.3. A decay curve (points marked x) for 7 min tin-129. ⊙ , antimony-129 counting rates. ⊙ , antimony-129 counting rates extrapolated to the appropriate times of 'milking'. × , extrapolated values corrected for chemical yield. (The counting rates for antimony-129 have been corrected for contributions due to other antimony isotopes).

Control experiments in the present work using this method confirmed the original observation of Bock[14] that this system only extracts 2 or 3% of the antimony present in an aqueous solution. Therefore the suggestion made by Chu and Marinsky that about 50% must be extracted is untenable. Since in the milking experiments antimony-129 is produced in and extracted from the ether phase, tests were made by using radiochemical methods on the extraction of antimony from the ether phase into the aqueous phase and the retention of antimony was never found to be more than about 10% in an extraction. It was shown that tin was retained in the ether phase during the milking procedure confirming the findings of Hagebø et al.[1] Therefore, some other factors which are not immediately obvious at present must be responsible for their original observation.

Measurements using the ether-thiocyanate procedure gave values around 9 min for the half-life of the longer-lived tin-129 isomer taking the time interval to be 10 minutes between milkings. Since this method must be regarded with some caution and the values obtained by using various other methods (iodide-benzene[3], sulphide[2] and the decay of the γ-spectra of a sample of purified fission product tin[2]) were lower than 9 min, it is not unreasonable to consider 7.5 min nearer the correct one.

Because of the limitation placed on obtaining experimental points on the decay curve (Fig. 4.2) by the experimental method used it has not been possible to deduce whether or not one isomer level is 'feeding' the other.

The results of the yield measurements are summarised in Tables 4.1 and 4.2. A mean value of 0.17% was obtained for the cumulative yield of the 7.5 min tin-129 nuclide; this compares with 0.39% for antimony-129. The antimony-129 value is in better agreement with that found earlier by Pappas[15] (0.4%) than with either the value of 0.2% attributed to Grummit[16] or 1.12% found by Hagebø[4]. A value of 0.46% is obtained for the yield of antimony-129 if 64%[12] rather than 85% of this nuclide is assumed to decay to 69 min tellurium-129. Even making a generous allowance for absolute errors in the measurement it does not seem possible to reconcile the value obtained here with a 1.12% yield.

Table 4.1

Half-lives and cumulative fission yields for 7.5 min tin-129 in the thermal neutron induced fission of Uranium-235

Run	Half-life of long-lived ^{129}Sn (min)	A(^{129}Sb + ^{129}Te) at the time of milking	T (min)	A(^{97}Zr + ^{97}Nb) at the end of irradiation	Chemical recovery (%)			Counter efficiency (%)		Relative yield of 7.5min ^{129}Sn	Mean
					Sb	Sn	Zr	^{129}Sb	^{97}Zr		
1	7.4	$5.08\ 10^{4}$	23	$1.23\ 10^{6}$	86.68	52.36	6.013	47.9	36.2	0.19	0.20
		$2.25\ 10^{4}$	33		82.67			47.9		0.22	
		$7.70\ 10^{3}$	43		79.01			48.3		0.21	
		$3.09\ 10^{3}$	53		83.44			47.9		0.19	
2	7.7	$6.08\ 10^{4}$	23	$1.77\ 10^{6}$	85.03	66.18	9.04	47.9	35.4	0.17	0.16
		$1.94\ 10^{4}$	33		79.72			48.1		0.15	
		$8.05\ 10^{3}$	43		85.03			47.9		0.14	
		$3.93\ 10^{3}$	53		89.28			47.7		0.17	
3	7.4	$8.29\ 10^{4}$	20	$1.48\ 10^{6}$	85.85	80.38	7.56	47.9	36.7	0.15	0.15
		$3.39\ 10^{4}$	30		85.85			47.9		0.16	
		$1.15\ 10^{4}$	40		75.67			48.3		0.15	
		$5.32\ 10^{3}$	50		89.29			47.7		0.15	
4	7.7	$1.71\ 10^{4}$	22	$1.60\ 10^{6}$	86.68	16.86	8.97	47.9	36.4	0.18	0.18
		$6.50\ 10^{3}$	32		93.46			47.5		0.16	
		$2.95\ 10^{3}$	42		92.59			47.5		0.19	
		$1.22\ 10^{3}$	52		96.15			47.5		0.19	
5	7.7	$2.56\ 10^{4}$	25	$1.07\ 10^{6}$	91.74	33.14	7.79	47.5	36.6	0.19	0.17
		$9.00\ 10^{4}$	35		83.44			47.9		0.17	
		$3.81\ 10^{3}$	45		90.91			47.7		0.16	
		$1.14\ 10^{3}$	55		67.64			48.7		0.15	
6	7.4										
7	7.4										
Mean	7.5 ± 0.1									Mean 0.17 ± 0.01	

Table 4.2

Cumulative fission yields for antimony-129 in the thermal neutron induced fission of uranium-235

Run	Activity at the end of irradiation 129	97	99	Chemical recovery (%) Sb	Zr	Mo	Counter efficiency (%) ^{129}Sb	^{97}Zr	^{99}Mo	Relative yield of ^{129}Sb ^{97}Zr as ref.	^{99}Mo as ref.
1	$3.26\ 10^4$	$1.52\ 10^5$	-	33.56	58.99	-	50.7	35.0	-	0.39	-
2	$6.30\ 10^4$	$1.87\ 10^5$	$9.25\ 10^3$	43.77	46.10	18.09	50.0	36.0	35.4	0.39	0.41
3	$6.48\ 10^4$	$1.84\ 10^5$	$3.40\ 10^4$	53.15	46.32	76.28	49.2	35.7	31.2	0.34	0.35
4	$9.80\ 10^4$	$2.68\ 10^5$	$5.2\ 10^4$	53.79	48.08	77.46	49.2	35.7	31.2	0.35	0.35
									Mean	0.39 ± 0.03	0.39 ± 0.03

References

1. E. Hagebø, A. Kjelberg and A.C. Pappas, J. Inorg. Nucl. Chem., 24, 117 (1962).
2. B.J. Dropesky and C.J. Orth, J. Inorg. Nucl. Chem., 24, 1301 (1962).
3. P. Chu and J.A. Marinsky, J. Inorg. Nucl. Chem., 28, 1339 (1966).
4. E. Hagebø, J. Inorg. Nucl. Chem., 25, 615 (1963).
5. G. Charlot, 'Colorimetric Determination of Elements', New York, Elsevier Pub. Co., (1964).
6. R.B. Hahn and R.F. Skomieczmy, Nucleonics, 14 (No. 4), 56 (1956).
7. J.A. Seiler, 'Radiochemical Studies: The Fission Products', N.N.E.S., Div. IV, Vol. 9, Paper 269 (p. 1586).
8. E.M. Scadden, Nucleonics, 15 (No. 4), 102 (1957).
9. R.E. Van Aman, F.D. Hollibaugh and J.H. Kanzelmeyer, Anal. Chem., 31 (No. 11), 1783 (1959).
10. B.P. Bayhurst and R.J. Prestwood, Nucleonics, 17 (No. 3), 82 (1959).
11. J.G. Cuninghame, G.P. Kitt, M.P. Edwards, J.A.B. Goodall, C.B. Webster and H.H. Willis, Report AERE-R 4727 (1964).
12. G. Herrmann, Radiochim. Acta, 3, 174 (1964).
13. S. Katcoff, Nucleonics, 18 (No. 11), 201 (1960).
14. R. Bock, Z. Anal. Chem., 113, 110 (1951).
15. A.C. Pappas, Report AECU-2806, MIT-LNS-63 (1953).
16. W.E. Grummit, Personal communication to A.C. Pappas (quoted in ref. 4).

CHAPTER 5

Mass Distribution in the Fission of Protactinium-231 Induced by 3 MeV Neutrons

5.1 Introduction

Very little work has been done concerning neutron induced fission of protactinium-231. Iyer and his coworkers[1] determined the relative cumulative yields for some 18 masses produced by fission spectrum neutrons; they obtained a highly asymmetric mass-yield curve having a peak to trough ratio around 100. On the other hand, Brown, Lyle and Martin[2] observed a third peak in measured cumulative yields in fission induced by 14.7 MeV neutrons in the region of symmetric fission. Yields at the maximum were about one third of those on either asymmetric peak.

In the experiments at lower bombarding energy fission products were separated directly from irradiated protactinium-231 while in those at higher energy a recoil method employing catcher foils was used for collection of fission products. In the present investigation yields for 3 MeV neutron induced fission were measured using the recoil method.

Previously[3], an expression relating the ratio of the probabilities of symmetric fission (Γ_s) and neutron re-emission (Γ_n) from the compound nucleus to a term depending on the relative energies available for the two processes was derived and tested for a range of heavy nuclides in which fission was induced by 14 MeV neutrons. This relation has been used to test available data for fission induced in heavy nuclides including protactinium-231 by essentially 3 MeV neutrons. Protactinium-231 was not included in the earlier comparison because of the lack of essential cross-section data. The cross-section for 14.8 MeV neutron induced fission has been estimated in the course of the present work. It is used in an attempt to compare the behaviour of protactinium-231 with that of other nuclides undergoing fission induced by 3 and 14 MeV neutrons.

5.2 Experimental

Preparation of protactinium sample for the irradiation, the neutron generator and the proportional counter have been discussed in detail in Chapter 2. A description of the chemical procedures and of the preparation and standardisation of the carrier solutions are given in Appendix I.

Irradiations lasted about two hours except in experiments leading to the isolation of bromine-84 when 30 minutes sufficed. Because of the very low activity obtained with 3 MeV neutrons, irradiations were carried out on aluminium catcher foils in the absence of the protactinium-231 to test for fission products coming from impurities in the metal; none were detected.

In the estimation of fission cross-section a set of uranium-238 (oxide) discs, prepared to correspond as closely as possible to those of protactinium-231 were used as a reference. Uranium-238 and protactinium-231 discs were stacked in an alternate manner for irradiation. Each disc had its own pair of aluminium catcher foils, one above and the other below it, in the stack. The target assembly thus constructed was irradiated for 4 hours in a 3 MeV or 1 to 2 hours in a 14.8 MeV neutron flux. The catcher foils were then carefully segregated into two groups and molybdenum-99 separated from each set and counted. The stack was so arranged in successive experiments that uranium-238 and protactinium-231 each appeared an equal number of times in the position slightly nearer the neutron source.

5.3 Treatment of Experimental Data and Evaluation of Results

Following the separation of the fission products they were counted until enough data were collected to enable the curves to be resolved, giving the decay of the nuclide of interest. The analyses of the decay curves were carried out both by graphical method and with the aid of an Elliott 803B computer at the University of Kent at Canterbury, employing programmes prepared by Sellars[4] and Wellum[5].

The efficiency curves prepared previously by members[4] of this laboratory were used to obtain the counter efficiencies for the fission products measured except that for antimony-129. For the reason discussed in Chapter 4 the counter was calibrated for this nuclide.

The decay chains for masses in question and the half-lives were taken from the paper by Herrmann[6] and the data given in Nuclear Data Sheets[7] were used to calculate the corrections for the presence of conversion electrons where necessary.

Total chain yields were obtained from the measured cumulative yields according to the 'equal charge displacement' hypothesis which has been discussed in Chapter 3.

5.3(a) Bromine-83

The decay chain for mass-83 is set out below

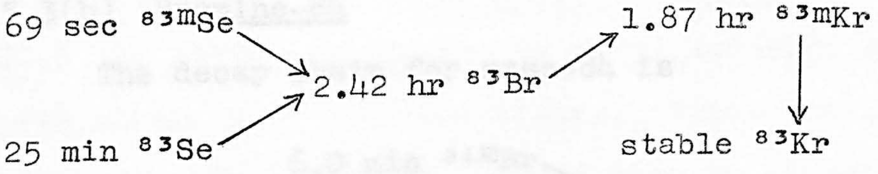

The separation of bromine was started about 4 hours after the irradiation to allow time for the decay of 25 min selenium-83. The decay curves showed only the presence of bromine-83 activity since the time interval between the end of the irradiation and the beginning of the counting was always long enough for the complete decay of bromine-84 (see 5.3(b)).

For the purpose of the calculations, the ratio of the cumulative yields of the bromine-83 precursors was assumed to be the same[8] as it is in the thermal neutron induced fission of uranium-235. It was shown by calculation that this can be done without loss of accuracy. Using 0.64 for the ratio of selenium-83 to selenium-83m, 39% was found for the fraction of bromine-83 formed from 25 min selenium-83 and 61% for the apparent independent yield of bromine-83. (The last mentioned includes the fraction formed from 69 sec selenium-83). The independent yield of bromine-83 was calculated to be only 1% of the total chain yield.

The necessary equations required for the calculation of the cumulative yield of bromine-83 are given in Chapter 3.

5.3(b) Bromine-84

The decay chain for mass-84 is

$$\begin{tikzcd}
 & 6.0\text{ min } {}^{84m}\mathrm{Br} \arrow[dr] & \\
 & & \text{stable } {}^{84}\mathrm{Kr} \\
3.3\text{ min } {}^{84}\mathrm{Se} \arrow[r] & 31.7\text{ min } {}^{84}\mathrm{Br} \arrow[ur] &
\end{tikzcd}$$

The separation of bromine was performed after a cooling time of about 30 minutes. The decay curves showed the presence of 2.42 hr bromine with a very small contribution from a long-lived component.

Because of the short irradiation time the activity obtained for molybdenum-99 was too low for reliable measurements. Therefore, zirconium was separated as reference. It was shown by calculation that the half-life of selenium-84 is short enough to assume that the chain starts at 31.7 min bromine-84.

5.3(c) Strontium-91

The decay chain for mass-91 is

$$\begin{tikzcd}
 & & & 50.5\text{min } {}^{91m}\mathrm{Y} \arrow[dd] & \\
8.4\text{sec } {}^{91}\mathrm{Kr} \arrow[r] & 71\text{sec } {}^{91}\mathrm{Rb} \arrow[r] & 9.67\text{hr } {}^{91}\mathrm{Sr} \arrow[ur, ".59"] \arrow[dr] & & \text{stable } {}^{91}\mathrm{Zr} \\
 & & & 58.9\text{day } {}^{91}\mathrm{Y} \arrow[ur] &
\end{tikzcd}$$

The samples were cooled for about 24 hours before starting the separation so that strontium-92 ($t_{\frac{1}{2}}$ = 2.68 hr) and its daughter yttrium-92 ($t_{\frac{1}{2}}$ = 3.52 hr) were not observed in the decay curves.

50.5 min yttrium-91 decays by γ-ray emission having 0.551 MeV energy with 4.4% conversion. Since these conversion electrons will be counted with an efficiency of 0.9% a correction was applied by dividing the observed counting rate by 1.031.

5.3(d) Zirconium-97

The decay chain for mass-83 is given below.

$$\begin{tikzcd}
 & 60\text{ sec }^{97m}\text{Nb} \arrow[dd] & \\
17\text{ hr }^{97}\text{Zr} \arrow[ur] \arrow[dr, ".06"'] & & \text{stable }^{97}\text{Mo} \\
 & 74\text{ min }^{97}\text{Nb} \arrow[ur] &
\end{tikzcd}$$

Enough time was given for the transient equilibrium between zirconium-97 and 74 min niobium-97 to be established before starting the counting of the samples. Samples decayed with the expected 17 hr half-life. Any long-lived background was very small. The observed activity was corrected for the presence of 74 min niobium-97 by dividing by 2.078.

5.3(e) Molybdenum-99

The decay chain for mass-99 is set out below.

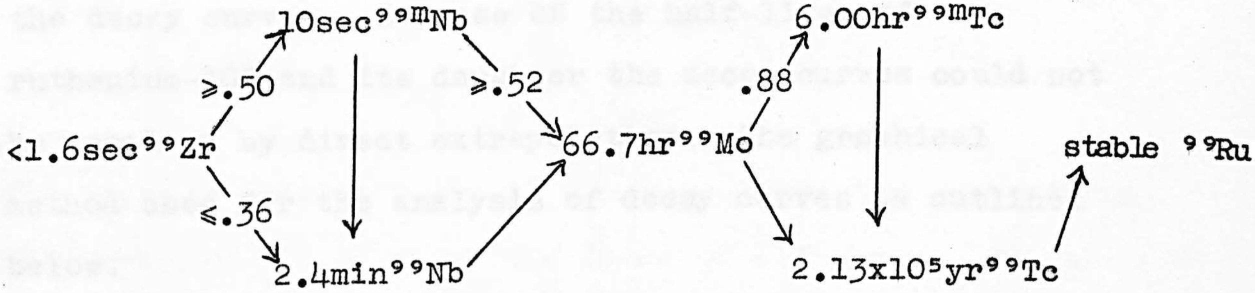
10sec ⁹⁹ᵐNb
≥.50
≥.52
6.00hr ⁹⁹ᵐTc
.88
<1.6sec ⁹⁹Zr
66.7hr ⁹⁹Mo
stable ⁹⁹Ru
≤.36
2.4min ⁹⁹Nb
2.13x10⁵yr ⁹⁹Tc

Since the other radioactive molybdenum isotopes produced during the irradiation have short half-lives compared with that of molybdenum-99, they were not observed in the decay curves. Counting was always delayed to allow 6.0 hr technetium-99 to reach equilibrium with the parent.

The observed activity was corrected for the presence of conversion electrons given by the 0.140 MeV γ-rays from the decay of 6.0 hr technetium. The counter efficiency for the conversion electrons was 1.1% having a conversion coefficient of about 0.095. The correction factor was then calculated to be 1.036.

5.3(f) Ruthenium-105

The decay chain for mass-105 is

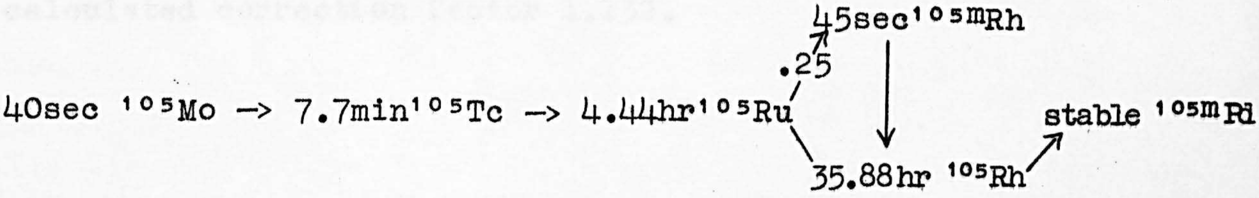
45sec ¹⁰⁵ᵐRh
.25
40sec ¹⁰⁵Mo -> 7.7min ¹⁰⁵Tc -> 4.44hr ¹⁰⁵Ru
stable ¹⁰⁵ᵐRd
35.88hr ¹⁰⁵Rh

Enough time was given for the complete decay of 7.7 min technetium before starting the separation. Ruthenium-105 and 35.88 hr rhodium-105 were observed in the decay curves. Because of the half-lives of ruthenium-105 and its daughter the decay curves could not be resolved by direct extrapolation. The graphical method used for the analysis of decay curves is outlined below.

The total activity at the time t is represented by the following equation

$$A(t) = A^{o}_{Ru} \left[e^{-\lambda_{Ru} t} + \frac{\eta_{Rh}}{\eta_{Ru}} \left(\frac{\lambda_{Rh}}{\lambda_{Rh} - \lambda_{Ru}} \right) \left(e^{-\lambda_{Ru} t} - e^{-\lambda_{Rh} t} \right) \right]$$

where A^{o}_{Ru} is the activity at the time of separation of ruthenium and η is the counter efficiency. A straight line of slope A^{o}_{Ru} should be obtained when A(t) is plotted against

$$\left[e^{-\lambda_{Ru} t} + \frac{\eta_{Rh}}{\eta_{Ru}} \left(\frac{\lambda_{Rh}}{\lambda_{Rh} - \lambda_{Ru}} \right) \left(e^{-\lambda_{Ru} t} - e^{-\lambda_{Rh} t} \right) \right]$$

45 sec rhodium-105 decays giving a 0.129 MeV γ-ray which has a conversion coefficient of 1.57. The counter efficiency for conversion electrons is 4.4% and the calculated correction factor 1.132.

5.3(g) Silver-113

The decay chain for mass-113 is given below.

$$\begin{tikzcd}
 & \text{1.2 min } {}^{113m}\text{Ag} \arrow[dd, ".90"] \arrow[dr] & \\
\text{1.5 min } {}^{113}\text{Pd} \arrow[ur] & & \text{stable } {}^{113}\text{Cd} \\
 & \text{5.3 hr } {}^{113}\text{Ag} \arrow[ur] &
\end{tikzcd}$$

The samples were left for 15 minutes before the separations were carried out to allow the decay of 1.5 min palladium-113 and 1.2 min silver-113. 5.3 hr silver was the only activity observed in the decay curves.

5.3(h) Antimony-129

The decay chain for mass-129 is

$$\begin{tikzcd}
 & & \text{33.6day } {}^{129m}\text{Te} \arrow[dr, ".32"] & & \\
\left.\begin{array}{c}\text{2 min}\\ \text{and}\\ \text{7.5 min}\end{array}\right\} {}^{129}\text{Sn} \arrow[r] & \text{4.4hr } {}^{129}\text{Sb} \arrow[ur, ".15"] \arrow[dr, ".85"] & & 1.6\text{x}10^{7}\text{yr } {}^{129}\text{I} \arrow[r] & \text{stable } {}^{129}\text{Xe} \\
 & & \text{68.8min } {}^{129}\text{Te} \arrow[ur] & &
\end{tikzcd}$$

The half-lives of tin-129 isomers are discussed in Chapter 4. The samples were cooled 75 min before the separation, and counting was started 5 hours after the preparation of the source to allow 68.8 min tellurium-129 to come to equilibrium with the parent. The observed activity was corrected for the contribution of shorter-lived tellurium-129.

As mentioned above the counter was calibrated for antimony-129. This has been discussed in detail in Chapter 4. The experimental counter efficiency curve for the antimony-129 - tellurium-129 equilibrium and the calculated counter efficiency curve for tellurium-129 are shown in Fig. 5.1.

5.3(i) Cerium-143

The decay chain for mass-143 is

0.96sec ^{143}Xe -> 2.0sec ^{143}Cs -> 12sec ^{143}Ba -> 14.0min ^{143}La
->33.4 hr ^{143}Ce -> 13.59day ^{143}Pr -> stable ^{143}Nd

Enough time was given for the complete decay of 14 min lanthanum-143 before starting the separation. The decay curves showed only the presence of 33.4 hr cerium-143 with a small contribution of longer-lived daughter.

The analysis of the decay curves were carried out as described for that of ruthenium-105. For cumulative yield calculations it was assumed that the chain started at cerium-143.

5.3(j) Praseodymium-145

The decay chain for mass-145 is given below.

3.0min ^{145}Ce -> 5.96hr ^{145}Pr -> stable ^{145}Nd

The separation of praseodymium was started after a 30 minute cooling period. The decay curves were easily

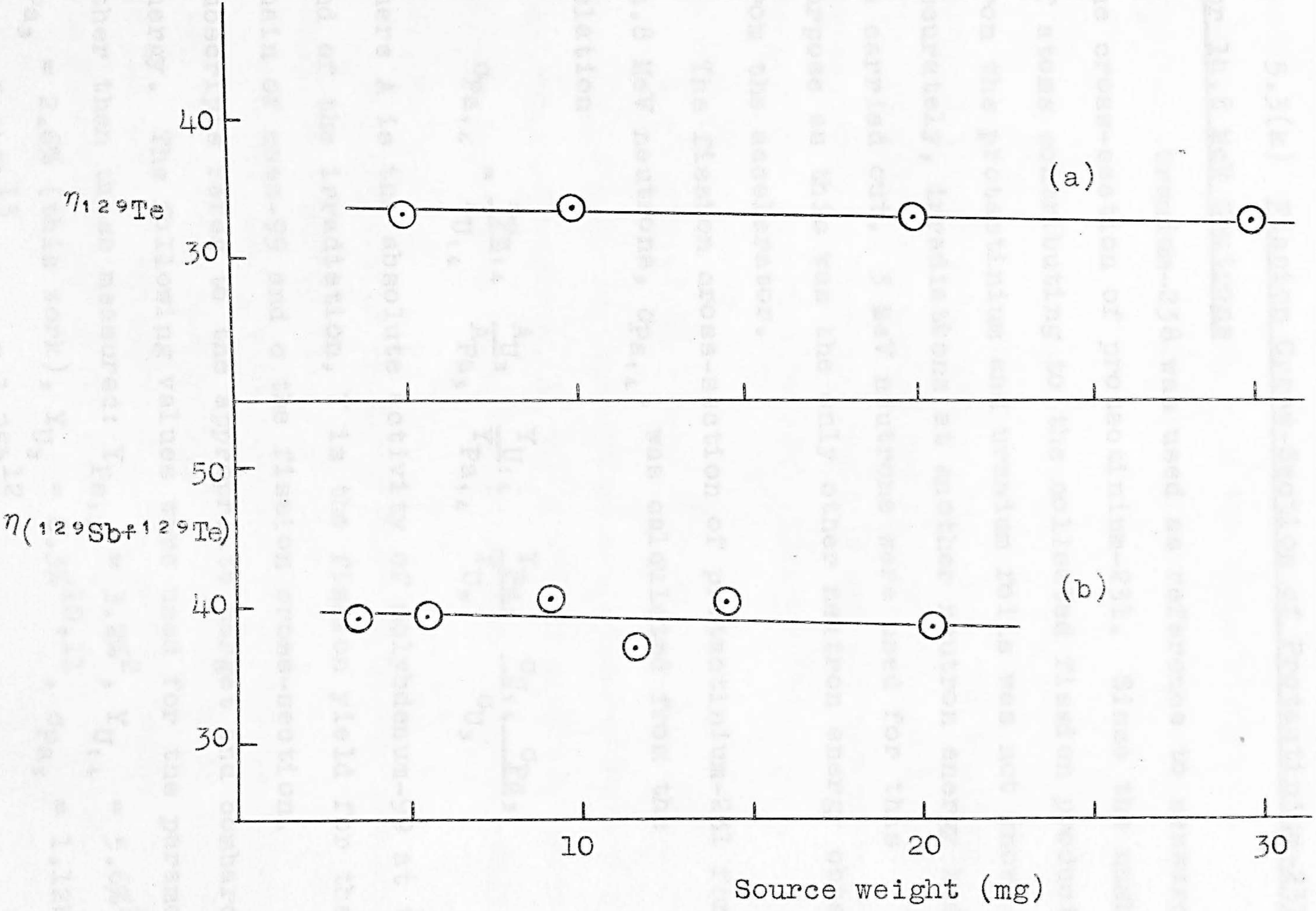

Fig. 5.1. (a) Calculated counter efficiency curve for tellurium-129.
(b) Experimental counter efficiency curve for antimony-129 - tellurium-129.

resolved as they only contained praseodymium-145 and a very small contribution of a long-lived component.

5.3(k) Fission Cross-Section of Protactinium-231 for 14.8 MeV Neutrons

Uranium-238 was used as reference to measure the cross-section of protactinium-231. Since the number of atoms contributing to the collected fission products from the protactinium and uranium foils was not known accurately, irradiations at another neutron energy had to be carried out. 3 MeV neutrons were used for this purpose as this was the only other neutron energy obtained from the accelerator.

The fission cross-section of protactinium-231 for 14.8 MeV neutrons, $\sigma_{Pa_{14}}$, was calculated from the relation

$$\sigma_{Pa_{14}} = \frac{A_{Pa_{14}}}{A_{U_{14}}} \frac{A_{U_3}}{A_{Pa_3}} \frac{Y_{U_{14}}}{Y_{Pa_{14}}} \frac{Y_{Pa_3}}{Y_{U_3}} \frac{\sigma_{U_{14}}\sigma_{Pa_3}}{\sigma_{U_3}}$$

where A is the absolute activity of molybdenum-99 at the end of the irradiation, Y is the fission yield for the chain of mass-99 and σ the fission cross-section. Subscripts refer to the appropriate target and bombarding energy. The following values were used for the parameters other than those measured: $Y_{Pa_{14}}$ = 3.2%[2], $Y_{U_{14}}$ = 5.6%[9], Y_{Pa_3} = 2.6% (this work), Y_{U_3} = 6.3%[10,11], σ_{Pa_3} = 1.12b[12], σ_{U_3} = 0.540b[13], $\sigma_{U_{14}}$ = 1.25b[12].

5.3(1) Evaluation of Γ_s/Γ_n for 3 MeV Neutrons

The expression derived previously[3] for the ratio of the probabilities of symmetric fission (the fission cross-section, σ_f x the symmetric fission yield Y_s) and neutron re-emission from the compound nucleus is

$$\ln\left(\frac{\Gamma_s}{\Gamma_n}\right) = \text{constant} + (8a_f T)^{\frac{1}{2}} - 2(a_r E_n)^{\frac{1}{2}}$$

where T is the total energy available for excitation of fission fragments and a_f and a_r are the level density parameters for fission fragments and for the neutron evaporation residual nucleus, respectively.

T is given by

$$T = 0.096\, Z_0^2/A_0^{\frac{1}{3}} - 3.41\, A_0^{\frac{2}{3}} + 22.6 + E_n + B_n$$

where Z_0 and A_0 are the charge and mass respectively of the compound nucleus, E_n the incident neutron energy and B_n the separation energy of a neutron from the nuclide (Z_0, A_0).

The derivation of these expressions are discussed in detail in Appendix II.

Values for Y_s were obtained from various sources (see Table 5.13) and $\sigma_f/\sigma_{n,n'}$ was taken to be the inverse of the partial width ratio Γ_n/Γ_f calculated by Vandenbosch and Huizenga[14] for 3 MeV neutron induced fission.

5.4 Results and Discussion

The measured relative cumulative yields in the 3 MeV neutron induced fission of protactinium-231 are recorded in Tables 5.1 - 5.9 and the absolute yields are given in Table 5.10. They are also plotted in Fig. 5.2 with the yields determined by Iyer et al.[1] for comparison, after they were normalised. Normalisation was based on the assumption that the total area under the curve should be 200%. The necessary initial adjustment between the values obtained in the present and the earlier work was made through the relative yields for mass-99. In the measurements where only zirconium-97 was separated as reference, relative yields were converted using the measured mass-99/mass-97 ratio. Mirror points were considered to fit the curve best if a value of 3.5 was taken for the average number of neutrons, $\bar{\nu}$, emitted per fission event. (The quantity $\bar{\nu}$ has not been reported in the literature.)

It is seen from the Fig. 5.2 that the agreement between the two sets of measurements is good and it may be taken as an indication of the reliability of the recoil method under the experimental conditions employed in the present and the earlier[2] measurements on protactinium-231. The yield curve is highly asymmetric with a peak to trough ratio of 100 and a peak width at half height of 14 mass

Table 5.1

Cumulative fission yields for bromine-83

Run	A(t') (^{83}Br)	t'(hr)	A(^{99}Mo)	Chemical recovery(%)		Counter efficiency(%)		S x 10^6		Relative yield
				Br	Mo	^{83}Br	^{99}Mo	^{83}Br	^{99}Mo	
1	36.97	6	13.90	52.43	78.22	32.4	30.4	0.972	1.282	0.953
2	35.68	6	15.00	41.41	85.21	32.4	30.1	1.120	1.453	1.136
3	20.55	6	12.00	43.49	86.30	32.4	30.0	1.054	1.396	0.807
4	22.11	6	7.55	52.68	87.64	32.4	30.0	6.307	8.094	1.123

Mean 1.00 ± 0.08

Table 5.2

Cumulative fission yields for bromine-84

Run	$A_{(^{84}Br)}$	$A_{(^{97}Zr + ^{97}Nb)}$	Chemical recovery(%)		Counter efficiency(%)		S x 10^5		Relative yield
			Br	Zr	^{84}Br	^{97}Zr	^{84}Br	^{97}Zr	
1	77.10	42.20	7.83	49.46	34.0	31.9	3.564	4.726	0.927
2	60.34	40.71	6.98	60.62	34.1	31.5	3.431	4.567	1.024
3	131.47	57.59	13.91	77.85	33.9	31.0	2.946	4.059	1.036
								Mean	0.99 ± 0.03

Table 5.3

Cumulative fission yields for strontium-91

Run	$A_{(^{91}Sr)}$	$A_{(^{97}Zr\ +\ ^{97}Nb)}$	$A_{(^{99}Mo)}$	Chemical recovery (%)			Counter efficiency(%)			S x 10^6			Relative yield	
				Sr	Zr	Mo	^{91}Sr	^{97}Zr	^{99}Mo	^{91}Sr	^{97}Zr	^{99}Mo	^{97}Zr as ref.	^{99}Mo as ref.
1	200	106.7	-	71.37	66.65	-	31.4	31.4	-	1.855	1.911	-	2.069	-
2	415	267	29.07	77.41	74.89	80.38	31.2	31.0	30.3	2.565	2.653	2.744	1.779	2.318
3	265	-	21.24	73.80	-	88.76	31.4	-	30.0	2.350	-	2.507	-	2.231
4	332	208	25.28	75.55	57.49	90.43	31.4	31.6	29.9	2.046	2.113	2.183	1.448	2.326
											Mean		1.76 ± 0.02	2.29 ± 0.03

Table 5.4

Cumulative fission yields for zirconium-97

Run	A(^{97}Zr + ^{97}Nb)	A(^{99}Mo)	Chemical recovery (%)		Counter efficiency (%)		S x 10^6		Relative yield
			Zr	Mo	^{97}Zr	^{99}Mo	^{97}Zr	^{99}Mo	
1	118	17.79	53.72	92.94	31.8	29.9	1.647	1.697	1.410
2	149	17.18	60.03	89.97	31.6	29.9	1.548	1.594	1.601
3	156	17.68	60.82	92.96	31.6	29.8	1.677	1.727	1.653
4	128	12.88	58.84	84.90	31.6	30.2	2.073	2.136	1.764
5	85.8	9.10	66.34	82.72	31.4	30.2	1.516	1.562	1.479
6	123	10.40	81.40	77.47	30.8	30.4	1.397	1.440	1.458
7	222	25.45	58.50	85.86	31.6	30.1	2.546	2.627	1.592
8	267	29.07	74.89	80.38	31.0	30.3	2.653	2.744	1.303
9	208	25.28	57.49	90.43	31.6	29.9	2.113	2.183	1.606

Mean 1.54 ± 0.05

Table 5.5

Cumulative fission yields for ruthenium-105

Run	A(^{105}Ru)	A(^{97}Zr + ^{97}Nb)	A(^{99}Mo)	Chemical recovery (%)			Counter efficiency (%)			S x 10^6			Relative yield	
				Ru	Zr	Mo	^{105}Ru	^{97}Zr	^{99}Mo	^{105}Ru	^{97}Zr	^{99}Mo	^{97}Zr as ref.	^{99}Mo as ref.
1	6.26	128	12.88	23.12	58.84	84.90	33.3	31.6	30.2	1.854	2.073	2.136	0.064	0.112
2	9.52	85.84	9.10	53.44	66.34	82.72	33.6	31.4	30.2	1.356	1.516	1.562	0.069	0.102
3	6.68	123	10.40	45.00	81.40	77.47	33.7	30.8	30.4	1.248	1.397	1.440	0.048	0.070
4	14.53	222	25.45	33.49	58.50	85.86	33.7	31.6	30.1	2.268	2.546	2.627	0.058	0.092
												Mean	0.059 ± 0.005	0.094 ± 0.009

Table 5.6

Cumulative yields for silver-113

Run	A(^{113}Ag)	A(^{97}Zr + ^{97}Nb)	A(^{99}Mo)	Chemical recovery (%)			Counter efficiency(%)			S x 10^6			Relative yield	
				Ag	Zr	Mo	^{113}Ag	^{97}Zr	^{99}Mo	^{113}Ag	^{97}Zr	^{99}Mo	^{97}Zr as ref.	^{99}Mo as ref.
1	1.97	118	17.79	35.02	53.72	92.94	34.1	31.8	29.9	1.511	1.647	1.697	0.0169	0.0237
2	3.76	149	17.18	61.23	60.03	89.97	34.0	31.6	29.9	1.420	1.548	1.594	0.0163	0.0261
3	4.79	156	17.68	59.89	60.82	92.96	34.0	31.6	29.8	1.539	1.677	1.727	0.0206	0.0341
4	4.03	126	-	48.91	51.82	-	34.0	31.8	-	1.314	1.444	-	0.0226	-
5	3.24	130	-	46.27	57.27	-	34.0	31.6	-	1.695	1.852	-	0.0203	-
												Mean	0.019 ± 0.001	0.028 ± 0.003

Table 5.7

Cumulative yields for antimony-129

Run	$A(^{129}Sb + ^{129}Te)$	$A(^{97}Zr + ^{97}Nb)$	Chemical recovery(%)		Counter efficiency(%)		S x 10^6		Relative yield
			Sb	Zr	^{129}Sb	^{97}Zr	^{129}Sb	^{97}Zr	
1	61.69	93.16	29.83	39.47	47.9	32.2	1.363	1.528	0.197
2	47.90	210	21.17	68.67	48.6	31.3	1.757	1.963	0.161
3	74.23	113	34.27	50.43	47.8	31.9	1.195	1.343	0.215
4	100.2	116	39.82	40.46	47.6	32.2	1.802	2.017	0.198
								Mean	0.19 ± 0.01

Table 5.8

Cumulative yields for cerium-143

Run	A(^{143}Ce)	A(^{99}Mo)	Chemical recovery (%)		Counter efficiency (%)		S x 10^{6}		Relative yield
			Ce	Mo	^{143}Ce	^{99}Mo	^{143}Ce	^{99}Mo	
1	73.36	35.88	47.02	78.12	31.2	30.4	3.371	3.414	2.044
2	5.64	24.29	5.93	84.40	31.8	30.1	3.127	3.162	1.925
3	21.06	24.65	20.33	84.88	31.6	30.1	1.722	1.737	1.955

Mean 1.97 ± 0.04

Table 5.9

Cumulative yields for praseodymium-145

Run	$A_{(^{145}Pr)}$	$A_{(^{99}Mo)}$	Chemical recovery (%)		Counter efficiency (%)		S x 10^6		Relative yield
			Pr	Mo	^{145}Pr	^{99}Mo	^{145}Pr	^{99}Mo	
1	200	35.88	32.09	78.12	34.0	30.4	3.008	3.414	1.272
2	82.50	20.84	25.45	81.19	34.0	30.4	2.204	2.578	1.242
3	84.56	24.29	21.85	84.40	34.0	30.1	2.822	3.162	1.249
								Mean	1.25 ± 0.01

Table 5.10

Yield data for 3.0 ± 0.4 MeV neutron induced fission of protactinium-231

Mass	Measured yield relative to mass-99	% chain*	Total chain yield	Absolute chain yield (%)
83	1.00 ± 0.08	99.99	1.00 ± 0.08	2.58 ± 0.24
84	1.52 ± 0.05	99.94	1.52 ± 0.05	3.91 ± 0.14
91	2.29 ± 0.03	99.89	2.29 ± 0.03	5.89 ± 0.08
97	1.54 ± 0.05	99.75	1.54 ± 0.05	3.96 ± 0.12
99	1.00	100	1.00	2.57
105	0.094 ± 0.009	100	0.094 ± 0.009	0.24 ± 0.02
113	0.028 ± 0.003	100	0.028 ± 0.003	0.072 ± 0.01
129	0.29 ± 0.02	93.18	0.32 ± 0.02	0.81 ± 0.05
143	1.97 ± 0.04	97.58	2.02 ± 0.04	5.19 ± 0.09
145	1.25 ± 0.01	99.99	1.25 ± 0.01	3.22 ± 0.02

*C = 0.9 was used in the independent yield calculations.

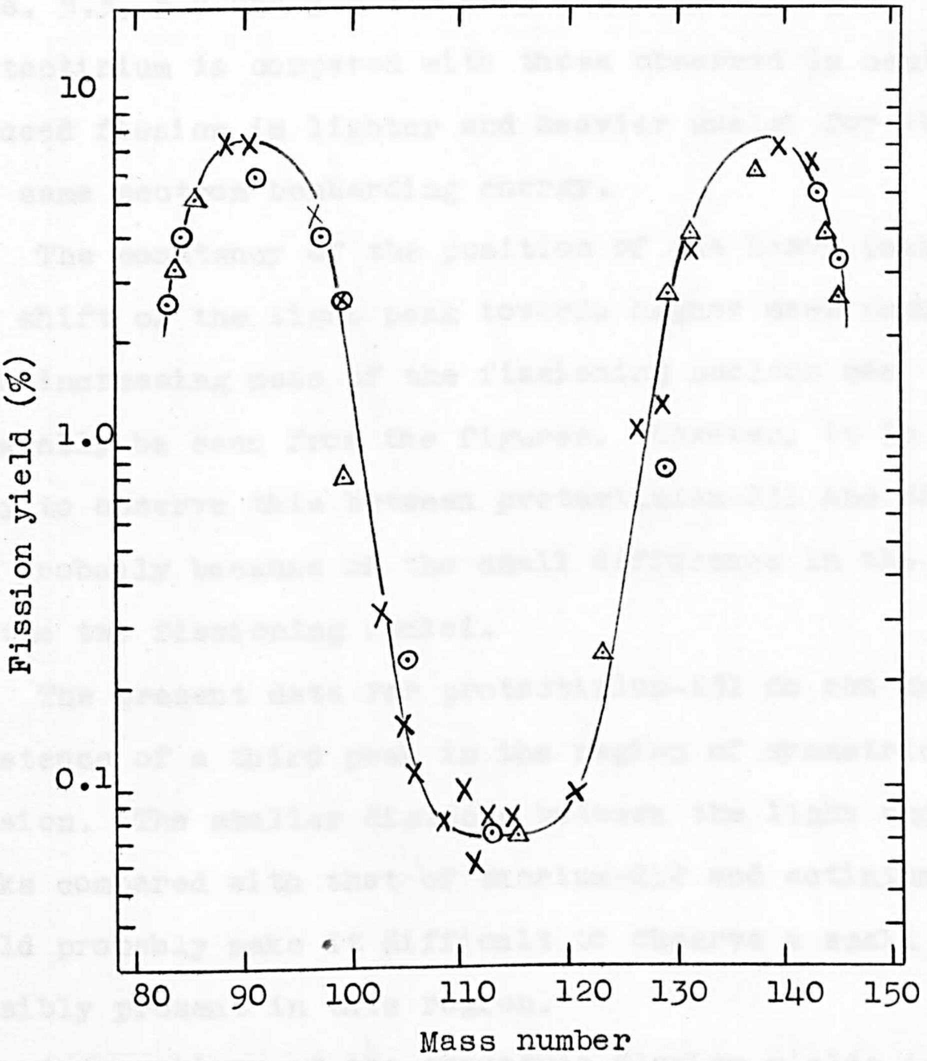

Fig. 5.2. Cumulative mass-yield curve for 3 MeV neutron induced fission of protactinium-231. ⊙, △, represent measured and mirror points respectively from the present work and × values derived from the data of Iyer et al.[1]

units. The maxima of the light and heavy peaks fall at masses 91 and 138 with peak yields around 7.2%. In Figs. 5.3, 5.4 and 5.5 the mass distribution from protactinium is compared with those observed in neutron induced fission in lighter and heavier nuclei for about the same neutron bombarding energy.

The constancy of the position of the heavy peak and the shift of the light peak towards higher mass numbers with increasing mass of the fissioning nucleus can generally be seen from the figures. However, it is not easy to observe this between protactinium-231 and thorium-232 probably because of the small difference in the masses of the two fissioning nuclei.

The present data for protactinium-231 do not show the existence of a third peak in the region of symmetric fission. The smaller distance between the light and heavy peaks compared with that of thorium-232 and actinium-227 would probably make it difficult to observe a small peak possibly present in this region.

A comparison of the symmetric fission yields in fission induced by 3 and 14.8 MeV neutrons for a number of fissioning systems (Table 5.11) shows that the increase in the symmetric fission probability is higher for protactinium-231 than it is for the others. The probability of symmetric fission is a rapidly increasing

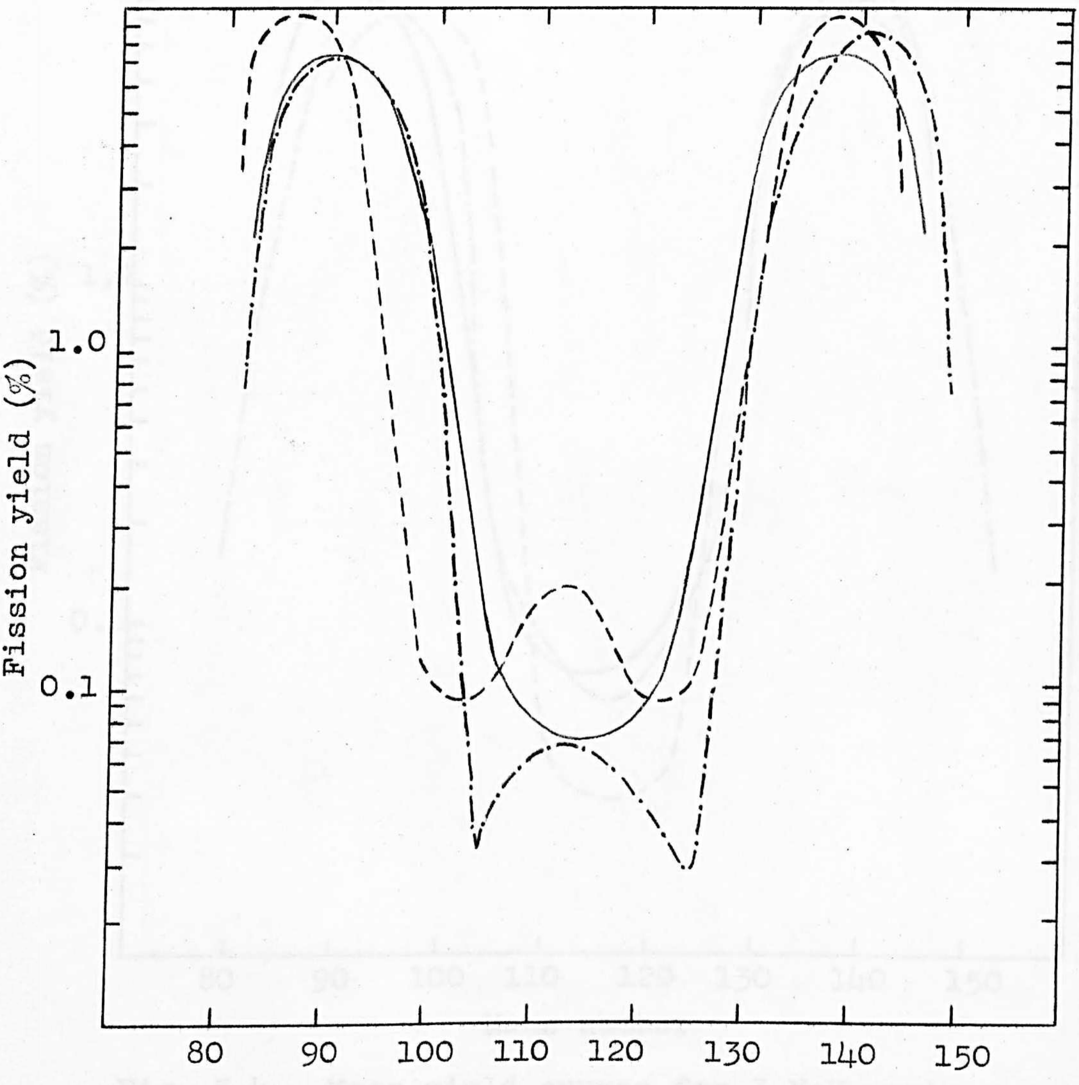

Fig. 5.3. Mass-yield curves for 3 MeV neutron induced fission of protactinium-231, actinium-227 and thorium-232.

——^{231}Pa, ----^{227}Ac (ref. 1),

-·-·-^{232}Th (ref. 15).

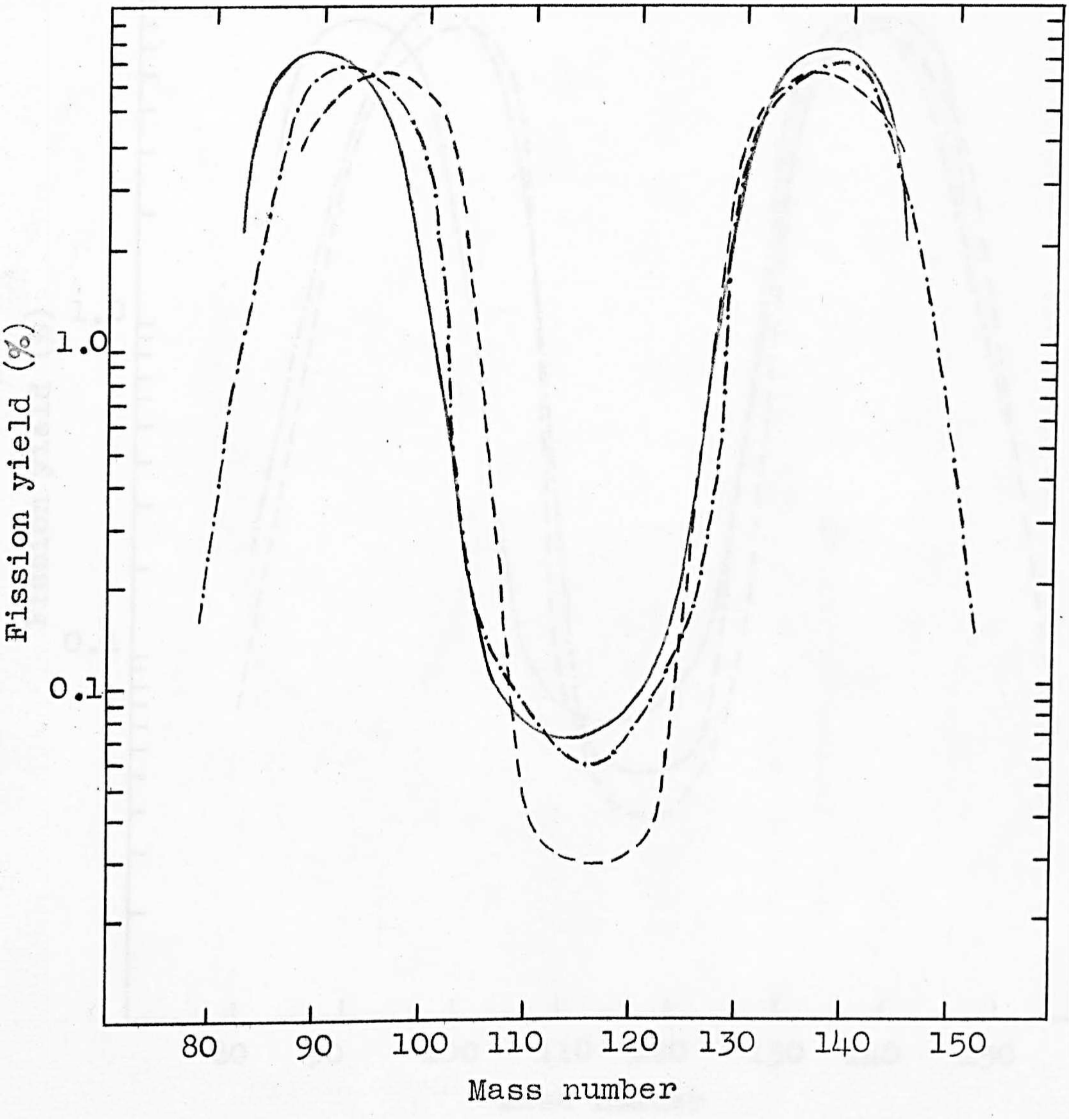

Fig. 5.4. Mass yield curves for 3 MeV neutron induced fission of protactinium-231, uranium-233 and uranium-235.
——^{231}Pa, -·-·-^{233}U (ref. 16),
----^{235}U (ref. 17).

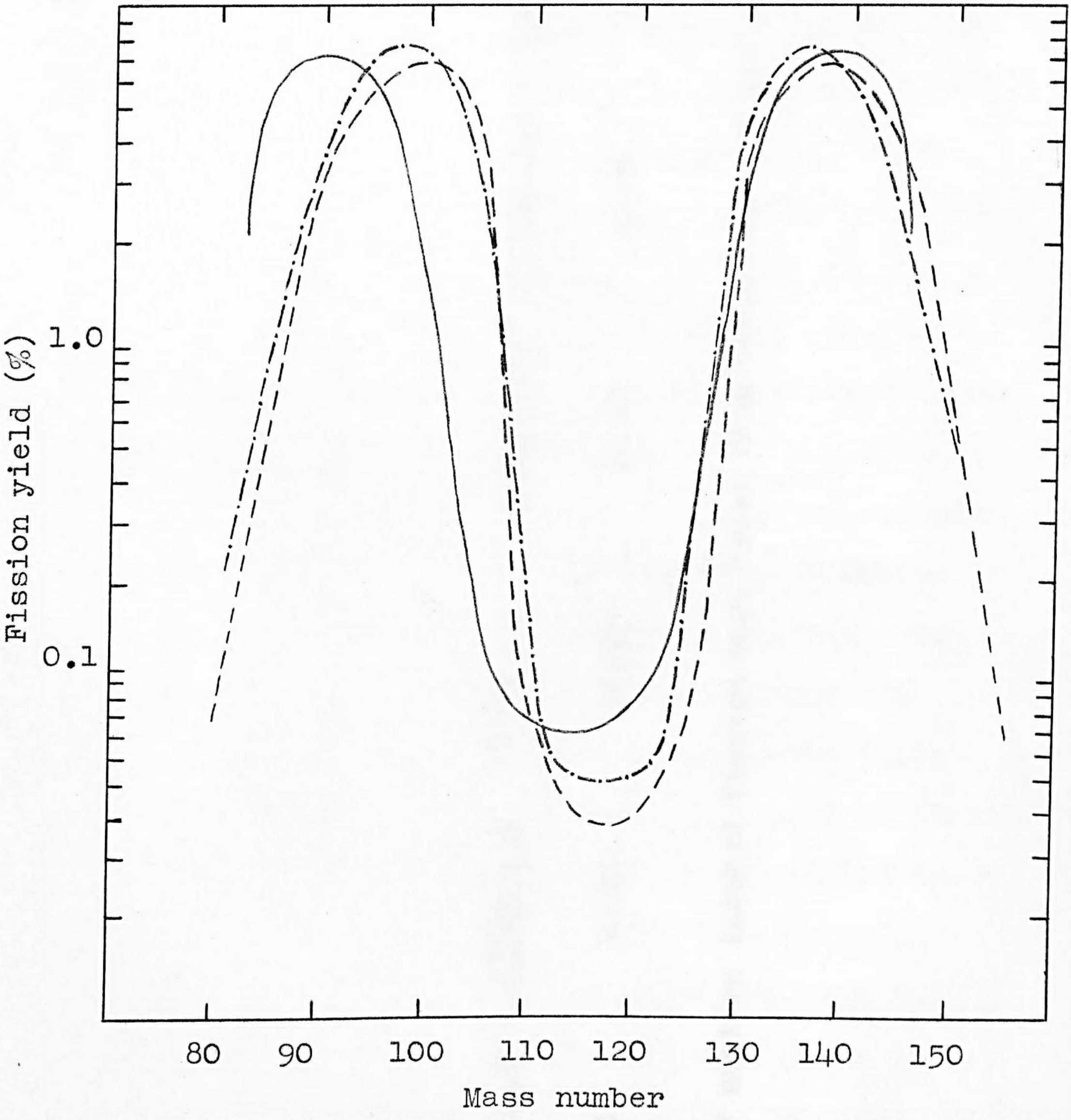

Fig. 5.5. Mass-yield curves for 3 MeV neutron induced fission of protactinium-231, neptunium-237 and uranium-238.
——^{231}Pa, -·-·-^{237}Np (ref. 1),
----^{238}U (ref. 11, 17).

Table 5.11

Comparison of symmetric fission yields at 3 and 14.8 MeV neutron energies for various fissioning systems.

Fissioning system	$^{232}Th + n$	$^{231}Pa + n$	$^{235}U + n$	$^{238}U + n$	$^{237}Np + n$	$^{239}Pu + n$
$(Y_s)_{14}/(Y_s)_3$	19.23	34.42	22.97	18.68	24.90	19.52

Data for 3 and 14 MeV neutron induced fission were taken from Table 5.12 and ref. 3 respectively.

function of the nuclear excitation energy which would be expected to be high at an energy just below that at which additional neutron emission becomes probable. It is then possible that where a high symmetric fission probability is observed fission is taking place at such an excitation energy. The energies at which the emission of one, two or more neutrons becomes probable are known from a study of the variation of fission cross-section with energy. For protactinium-231 no cross-section measurements have been made for neutron energies above 3 MeV. In the present study the fission cross-section of protactinium-231 for 14.8 MeV neutrons was measured and a value of 1.43b was found. Since the previously measured value for 3 MeV neutrons is 1.12b additional neutron emission over the range of 3 to 15 MeV does not seem probable, resulting in a high excitation energy.

The measured fission cross-sections for 14.8 MeV neutron bombardment of protactinium-231 are given in Table 5.12.

Table 5.12 - The fission cross-section, $\sigma_{Pa_{14}}$, of protactinium-231 for 14.8 MeV neutrons

Exp.	1	2	3	4
σ_f	1.75	1.19	1.47	1.33

σ_f(mean) 1.43 ± 0.12

In experiments 1 and 3 the Pa, and in 2 and 4 the U discs were stacked nearest the neutron source. Although the distance between neighbouring protactinium-231 and uranium-238 discs in the composite stack is unlikely to exceed 100 microns there is evidence from the results in the table that $\sigma_{Pa_{14}}$ reflects to some extent which type of disc is placed nearest the neutron source. However, variations thus produced in the calculated cross-section are likely to be adequately accounted for by taking the arithmetic mean of the separately determined values. The calculated standard error, ± 0.12, is likely to be overshadowed by the potentially larger absolute error arising from insufficiently accurate yield data particularly for $Y_{Pa_{14}}$, Y_{Pa_3} and Y_{U_3}. The mean value, 1.43, obtained may thereby be in error by 20 or 30% which makes it comparable with the value reported recently by Drake and Nichols[18] obtained by assuming that the fission cross-section of protactinium-231 varies with neutron energy in the same way as similar nuclides.

In Fig. 5.6 log Γ_s/Γ_n is plotted as a function of $(A_0T/2)^{\frac{1}{2}}$ for nuclides undergoing fission induced by essentially 3 MeV neutrons. The data giving rise to those used in Fig. 5.6 are given in Table 5.13. To enable a comparison to be made, the results obtained previously[3] for

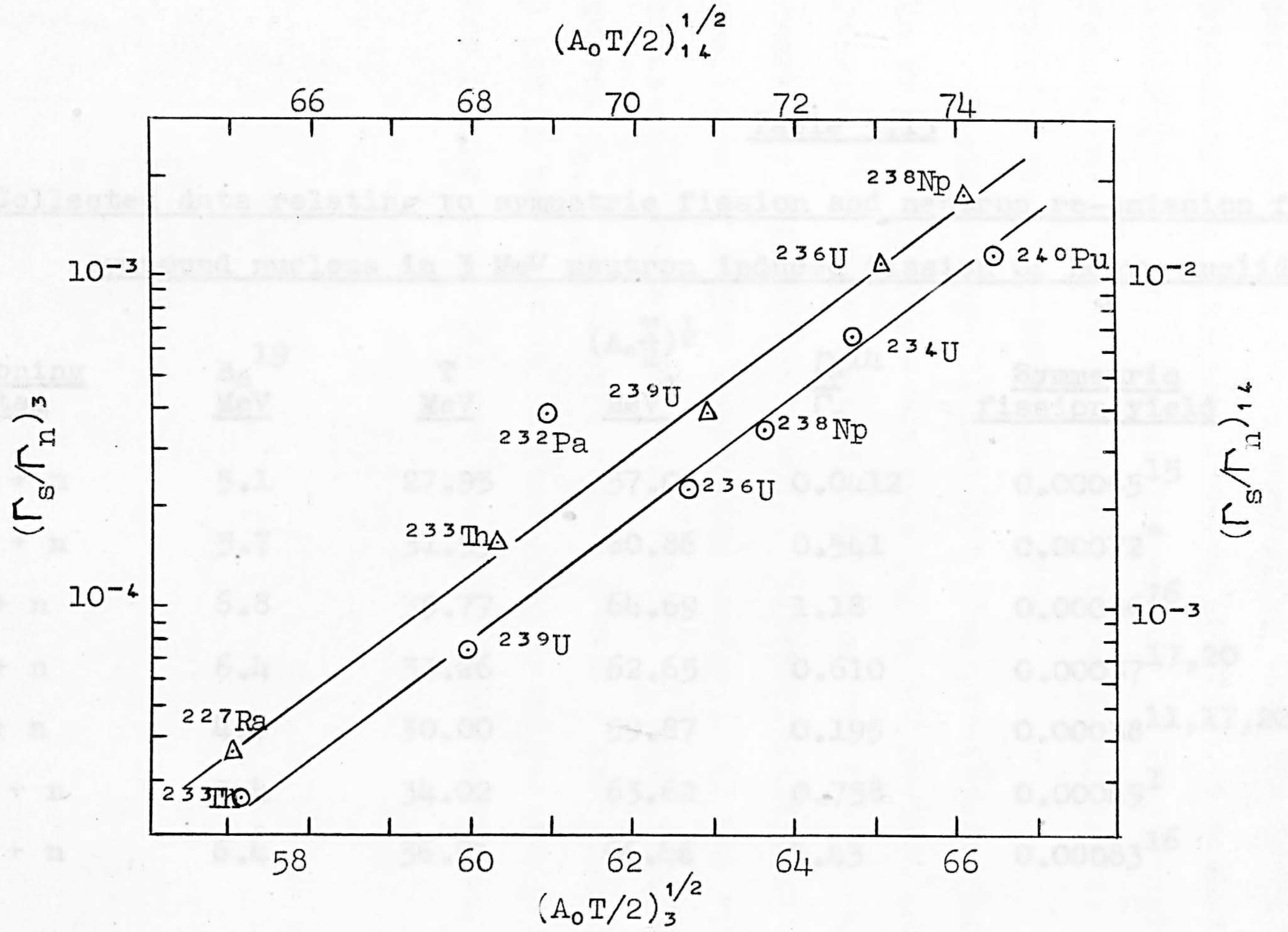

Fig. 5.6. Γ_s/Γ_n, plotted against $(A_oT/2)^{1/2}$

⊙, △ represent data for 3 MeV and 14 MeV neutron induced fission respectively. Subscripts 3 and 14 refer to the neutron bombarding energy.

Table 5.13

Collected data relating to symmetric fission and neutron re-emission from the compound nucleus in 3 MeV neutron induced fission of heavy nuclides

Fissioning system	B_n [19] MeV	T MeV	$(A_0 \frac{T}{2})^{\frac{1}{2}}$ $\mathrm{MeV}^{\frac{1}{2}}$	$\frac{\Gamma_f}{\Gamma_n}$ [14]	Symmetric fission yield	Γ_s/Γ_n
^{232}Th + n	5.1	27.95	57.06	0.0412	0.00065[15]	2.68×10^{-5}
^{231}Pa + n	5.7	31.93	60.86	0.541	0.00072*	3.89×10^{-4}
^{233}U + n	6.8	35.77	64.69	1.18	0.00056[16]	6.59×10^{-4}
^{235}U + n	6.4	33.26	62.65	0.610	0.00037[17,20]	2.26×10^{-4}
^{238}U + n	4.8	30.00	59.87	0.195	0.00038[11,17,20]	7.44×10^{-5}
^{237}Np + n	5.4	34.02	63.62	0.758	0.00049[1]	3.71×10^{-4}
^{239}Pu + n	6.4	36.81	66.46	1.43	0.00083[16]	1.19×10^{-3}

*This work.

14 MeV neutron induced fission are also plotted in Fig. 5.6. It is seen that both sets fall on or near parallel straight lines suggesting that the level density parameter for symmetric fission products is essentially independent of the bombarding energy in this range; a result perhaps not unexpected if the parameter is proportional to the nuclidic mass.

Protactinium-231 does not give parameters fitting on or near the curve representing 3 MeV neutron induced fission; the only exception found so far for which the necessary data are available. (Insufficient data are available at higher bombarding energy.) If the fission cross-sections are accepted and Γ_s / Γ_n read from the curves $\sigma_{n,n'}$ would have values around 7 and 11.5b for 3 and 14 MeV neutron induced fission respectively which are larger than that for the other heavy nuclides.

References

1. R.S. Iyer, H.C. Jain, M.N. Namboodri, M. Rajagopalan Rajkishore, M.V. Ramaniah, C.L. Rao, N. Ravindran and H.D. Sharma, 'Physics and Chemistry of Fission', IAEA, Vienna, 1965, Vol. I., p.439.

2. M.G. Brown, S.J. Lyle and G.R. Martin, Radiochim. Acta, 6, 16 (1966).

3. S.J. Lyle, G.R. Martin and J.E. Whitley, Radiochim. Acta, 3, 80 (1964).

4. J. Sellars, Ph.D. Thesis (Durham University , 1967).

5. R. Wellum, Ph.D. Thesis (Durham University), to be submitted.

6. G. Herrmann, Radiochim. Acta, 3, 174 (1964).

7. Nuclear Data Sheets, Nuclear Data Group, National Academy of Sciences - National Research Council, Washington D.C.

8. I.F. Croall and H.H. Willis, J. Inorg. Nucl. Chem., 24, 221 (1962).

9. R. Ganapathy and H. Ihochi, J. Inorg. Nucl. Chem., 28, 3071 (1966).

10. J. Terrell, W.E. Scott, J.S. Gilmore and C.O. Minkkinen, Phys. Rev., 92, 1091 (1953).

11. R.N. Keller, E.P. Steinberg and L.E. Glendenin, Phys. Rev., 94, 969 (1954).

12. D.J. Hughes and R.B. Schwartz, Brookhaven National Laboratory Compilation, BNL-325 (1958).

13. W.G. Davey, Nucl. Sci. Eng., 26, 149 (1966).

14. R. Vandenbosch and J.R. Huizenga, Proceedings of the Second United Nations International Conference on the Peaceful Uses of Atomic Energy, 15, P/688 (1958).

15. R.H. Iyer, C.K. Mathews, N. Ravindran, K. Rengan, D.V. Singh, M.V. Ramaniah and H.D. Sharma, J. Inorg. Nucl. Chem., 25, 465 (1963).

16. E.K. Bonyushkin, Yu. S. Zamyatnin, V.V. Spector, V.V. Rachev, V.R. Negina and V.N. Zamyatnina, At. Energ. (USSR), 10(1), 13 (1961).

17. E.K. Bonyushkin, Yu. S. Zamyatnin, I.S. Kirin, N.P. Martynov, E.A. Skuortsov and V.N. Ushatskii, Report AEC-tr-4682 (1960).

18. M.K. Drake and P.F. Nichols, Report GA-7462 (1967).

19. F. Everling, L.A. Konig, J.H.E. Mattauch and A.H. Wapstra, Nucl. Phys., 18, 529 (1960).

20. M.P. Grechushkina, Moscow Atomizdat (1964), (Nucl. Sci. Abs., 18, 38180).

CHAPTER 6

Fission Induced in Protactinium-231 by 14 MeV Neutrons: Fine Structure in the Mass Region 131-135

6.1 Introduction

Irregularities in the 131-135 mass region have been studied in fission of protactinium-231 induced by 14.8 MeV neutrons. For this purpose the independent yield of xenon in the mass-135 decay chain and cumulative yields at various masses were determined; the latter were based on iodine-131, -133 and -134 and xenon-133 and -135 measured radiochemically.

6.2 Separation Procedure

6.2(a) Iodine

The method for the separation and purification of iodine is given in Appendix I.

6.2(b) Xenon

The method first described by James, Martin and Silvester[1] and subsequently modified by Lyle and Sellars[2] was used in the separation and purification of xenon. The vacuum system employed for this purpose is shown in Fig. 6.1.

For the reasons discussed in Chapter 2, tin foils were used to collect the fission products during the

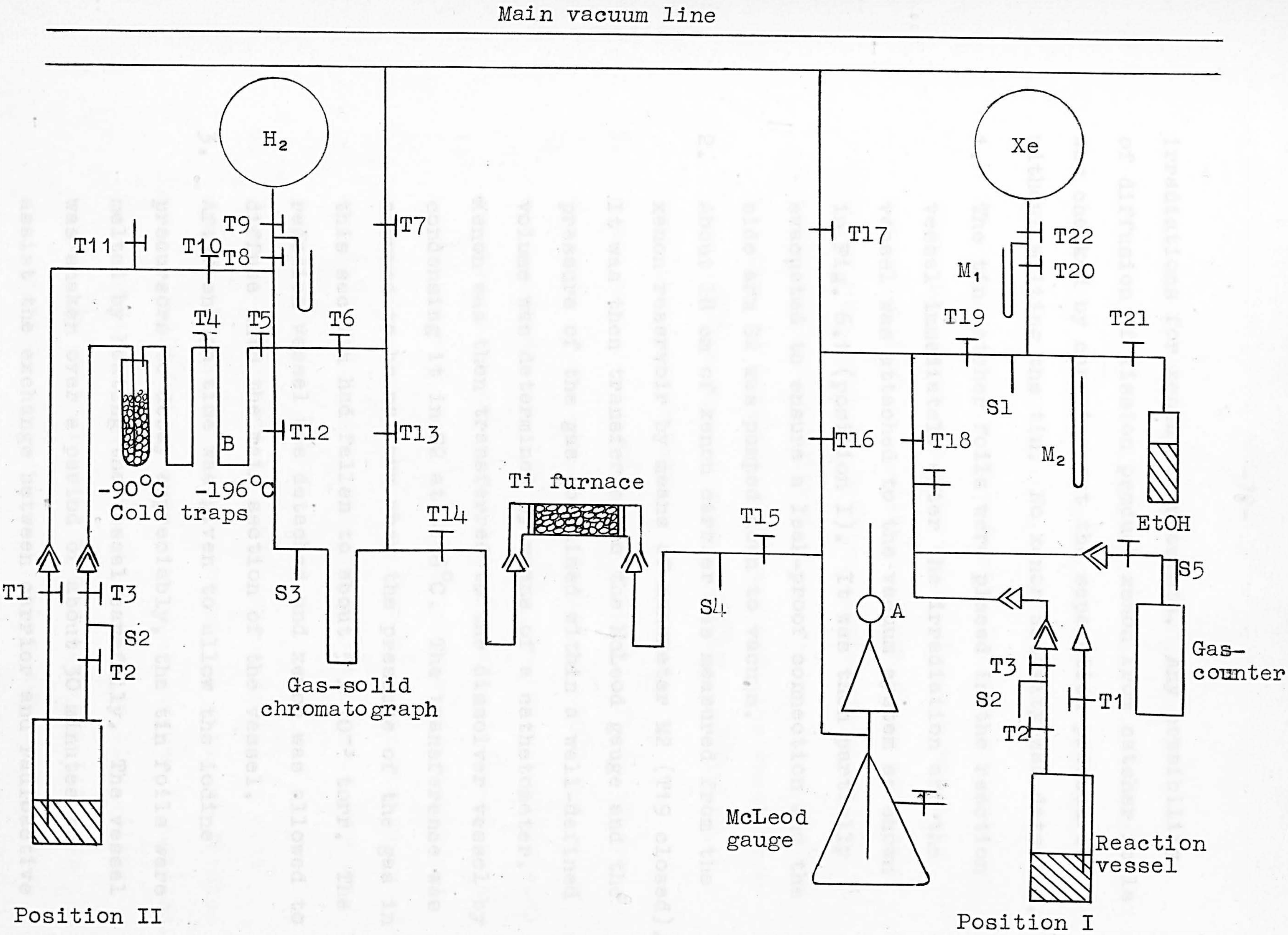
Main vacuum line
H₂
Xe
T11
T10
T9
T8
T7
T17
T22
T20
M₁
T4
T5
T6
T19
T21
S1
T12
T13
T16
T18
M₂
B
-90°C
-196°C
Cold traps
Ti furnace
T14
T15
EtOH
S5
T1
T3
S2
T2
S3
S4
A
Gas-solid chromatograph
Gas-counter
T3
S2
T2
T1
McLeod gauge
Reaction vessel
Position II
Position I

Fig. 6.1. Vacuum system used for separation of Xenon.

irradiations for xenon measurements. Any possibility of diffusion of fission product xenon from catcher foils was checked by carrying out the separation procedure without melting the tin. No xenon activity was detected.

1. The tin catcher foils were placed in the reaction vessel immediately after the irradiation and the vessel was attached to the vacuum system as shown in Fig. 6.1 (position I). It was then partially evacuated to ensure a leak-proof connection and the side arm S2 was pumped down to vacuum.
2. About 18 cm of xenon carrier was measured from the xenon reservoir by means of manometer M2 (T19 closed). It was then transferred to the McLeod gauge and the pressure of the gas contained within a well-defined volume was determined by means of a cathetometer. Xenon was then transferred to the dissolver vessel by condensing it in S2 at -196°C. The transference was assumed to be maximum when the pressure of the gas in this section had fallen to about 5×10^{-3} torr. The reaction vessel was detached and xenon was allowed to diffuse into the main section of the vessel.
3. After enough time was given to allow the iodine precursors to decay appreciably, the tin foils were melted by heating the vessel carefully. The vessel was shaken over a period of about 30 minutes to assist the exchange between carrier and radioactive xenon.

4. The vessel was connected to the vacuum system as shown in Fig. 6.1 (position II) and the system was partially evacuated above the taps T1 and T3. About 20 cc of air at NTP were allowed between T1 and T10 by opening T11 to atmosphere. The air was used to flush the gases from the vessel through the cold traps. Iodine was retained in the first two traps which were held at -90°C and xenon was condensed in the third trap at -196°C.
   The time of flushing the gases from the vessel was taken as the time of separation of xenon isotopes from their precursors.
5. B was pumped at -196°C after closing T4 to remove the bulk of the air, then warmed to -90°C and xenon was condensed at -196°C in S3. In the chromatography section which contained 1 g of charcoal (60-80 mesh) activated with zinc chloride and was previously out-gassed for about 6 hours at 300°C, xenon was adsorbed at -20°C and krypton removed by a stream of hydrogen (about 50 cc at NTP).
6. Xenon was desorbed at 200°C and condensed in side arm S4 at -196°C passing through the titanium furnace at about 900°C to remove remaining gaseous impurities.
   The titanium furnace consisted of a shallow silica U-tube (15 cm in length) packed with the titanium granules held in position by plugs of copper gauze.

7. Xenon was transferred to the McLeod gauge to be measured and then condensed in S5 at -196°C. Inactive xenon and ethanol were admitted in quantities such that their partial pressures within the counter were 5 cm and 1 cm (Hg) respectively at room temperature. (Ethanol was degassed by repeated freezing at -195°C and pumping.)

Tin in the vessel was dissolved in concentrated hydrochloric acid-nitric acid mixture in the presence of 20 mg of molybdenum carrier and molybdenum was separated as described in Appendix I.

6.2(c) Calibration of the gas Geiger-Counter

Previously[3] calibrated gas counters were used for cumulative yield measurements of xenon-133 and xenon-135. Since they eventually deteriorated, new gas counters were calibrated and used.

For this purpose about 20 mg of U_3O_8 were irradiated for 15 minutes in a flux of thermal neutrons in B.E.P.O., Harwell, England. The sample was contained in a silica tube (about 15 mm long, 3 mm in internal diameter) sealed at both ends by copper foil bonded to the silica with 'Araldite'.

The irradiated sample was placed in the dissolver vessel as shown in Fig. 6.2. After carrier gas was allowed into the system the sample was dissolved by

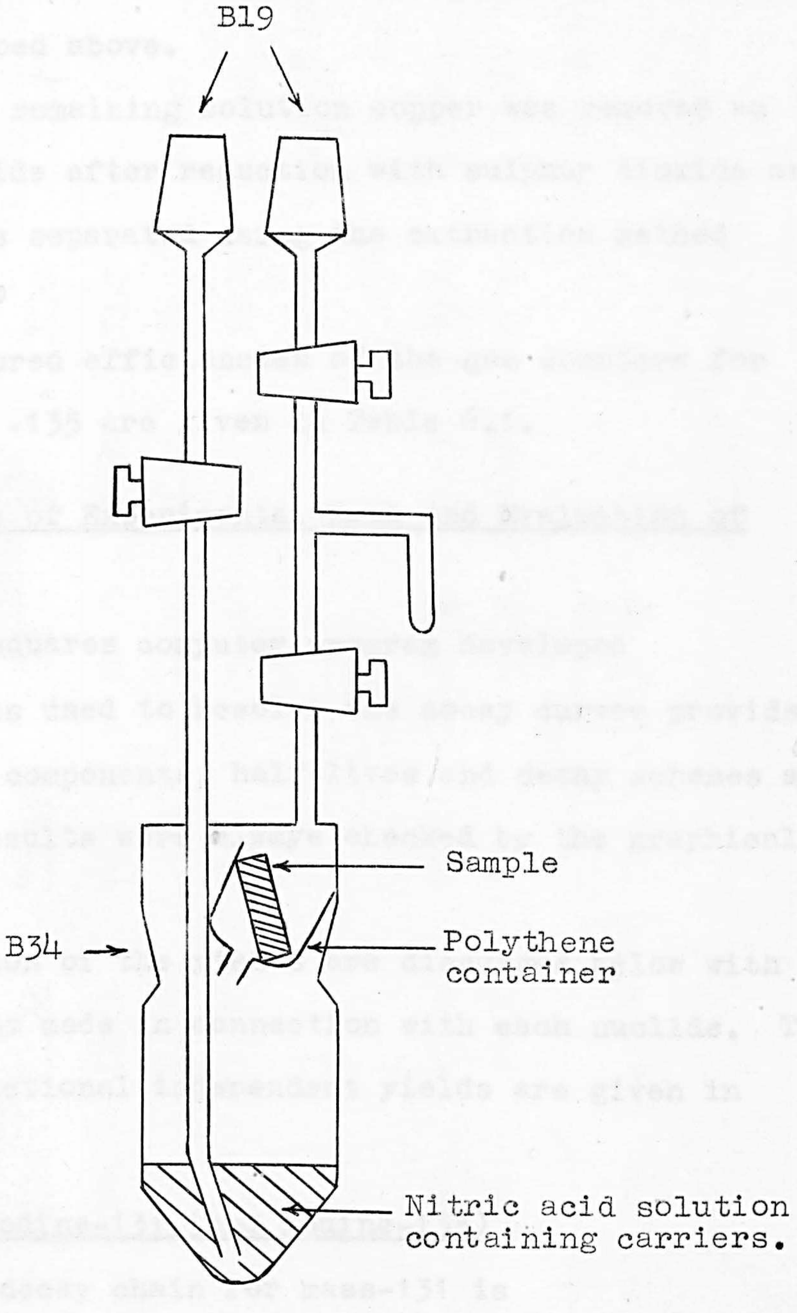
B19
Sample
B34
Polythene container
Nitric acid solution containing carriers.

Fig. 6.2. The reaction vessel.

tilting the vessel. The separation of xenon was carried out as described above.

From the remaining solution copper was removed as copper(I) iodide after reduction with sulphur dioxide and molybdenum was separated using the extraction method (Appendix I).

The measured efficiencies of the gas counters for xenon-133 and -135 are given in Table 6.1.

6.3 Treatment of Experimental Data and Evaluation of Results

A least squares computer program developed previously[3] was used to resolve the decay curves provided the number of components, half-lives and decay schemes are known. The results were always checked by the graphical method.

Calculation of the yields are discussed below with the assumptions made in connection with each nuclide. The calculated fractional independent yields are given in Table 6.2.

6.3(a) Iodine-131 (and iodine-133)

The decay chain for mass-131 is

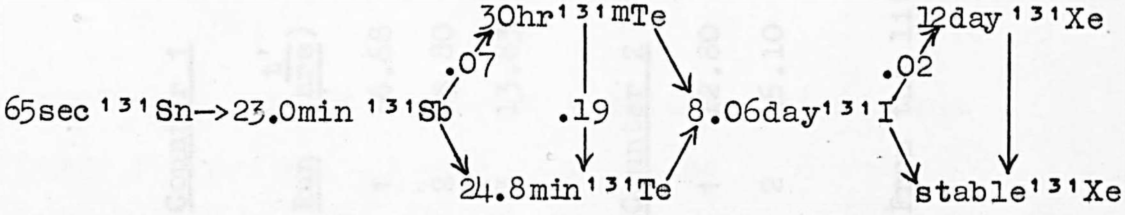

Table 6.1

Calibration of the gas counters

Run	t' (hrs)	A(t')		$A_{^{99}Mo}$	Chemical recovery (%)		Counter efficiency (%)		
		^{133}Xe	^{135}Xe		Xe	Mo	^{99}Mo	^{133}Xe	^{135}Xe
Counter 1									
1	36.68	4460	12540	8120	56.75	42.43	33.5	40.52	36.44
2	15.80	2030	24100	11750	18.90	29.11	34.1	42.58	37.66
3	13.83	1196	17690	20400	16.18	72.77	31.8	43.13	41.46
							Mean	42.1±0.8	38.5±1.5
Counter 2									
1	12.80	1238	20010	9300	25.76	45.43	33.4	42.76	41.81
2	16.10	2364	29870	12200	45.89	70.08	32.0	43.80	42.14
								43.3±0.5	42.0±0.2

From the literature: $Y_{99} = 6.25$[4], $Y_{133} = 6.62$[5] and $Y_{135} = 6.45$[5].

Table 6.2

Calculated fractional independent yields in fission of protactinium-231 induced by 14 MeV neutrons

Mass A	Charge Z	The most probable charge Zp	Fractional independent yield
131	49	51.34	2.6
	50		16.3
	51		37.7
	52		32.1
	53		10.1
	54		1.2
132	49	51.71	1.1
	50		9.2
	51		31.0
	52		38.3
	53		17.4
	54		2.9
133	50	52.08	4.6
	51		22.3
	52		39.8
	53		26.1
	54		6.3
134	51	53.15	3.9
	52		20.6
	53		39.4
	54		27.8
	55		7.2
135	51	53.52	1.7
	52		12.6
	53		34.8
	54		35.6
	55		13.4
	56		1.8

The constant C and the number of neutrons emitted from the heavy fragments (ν_H) were taken to be 2 in these calculations.

Since a decay curve contained all of the iodine isotopes was considered to be difficult to resolve, the samples were cooled for 3 days before starting the separation to allow time for the decay of iodine-134 and -135.

The decay curves were then easily analysed for iodine-131, -132 and -133 assuming that the contributions from xenon-131m and -133m were negligible. The graphical analysis of the decay curves is outlined below.

About 24 hours after the separation of iodine the decay curves contained only iodine-131 and -133 since at the end of this period the contribution of iodine-132 ($t_{\frac{1}{2}} = 2.28$ hr) was negligible. The observed activity at the time t is then given by

$$A(t) = A^{o}_{I^{131}}\, e^{-\lambda_{I^{131}} t} + A^{o}_{I^{133}} \left[e^{-\lambda_{I^{133}} t} + \frac{\lambda_{Xe^{133}}}{\lambda_{Xe^{133}} - \lambda_{I^{133}}} \cdot \frac{\eta_{Xe^{133}}}{\eta_{I^{133}}} \left(e^{-\lambda_{I^{133}} t} - e^{-\lambda_{Xe^{133}} t} \right) \right]$$

where A^{o} is the activity at the time of precipitation of the iodide and η is the counting efficiency.

The equation may be rearranged as shown below

$$\frac{A(t)}{e^{-\lambda_{I^{131}}t}} = A^{o}_{I^{131}} + A^{o}_{I^{133}}\left[\frac{e^{-\lambda_{I^{133}}t}}{e^{-\lambda_{I^{131}}t}} + \frac{\lambda_{Xe^{133}}}{\lambda_{Xe^{133}}-\lambda_{I^{133}}}\,\frac{\eta_{Xe^{133}}}{\eta_{I^{133}}}\,\frac{1}{e^{-\lambda_{I^{131}}t}}\left(e^{-\lambda_{I^{133}}t} - e^{-\lambda_{Xe^{133}}t}\right)\right]$$

A straight line of slope $A^{o}_{I^{133}}$ and intercept $A^{o}_{I^{131}}$ should be obtained when $\frac{A(t)}{e^{-\lambda_{I^{131}}t}}$ is plotted against the expression in square brackets.

The initial activity of iodine-132 can then be determined after subtracting calculated contributions for iodine-131 and -133 from the observed activity readings by extrapolating these residual activity values to the time of separation of iodine.

For purposes of calculation the ratio of the independent yield of tellurium-131m to that of tellurium-131 was assumed to be the same as it is for the thermal fission of uranium-235; the latter was found[6] to be 1.8. Using the fractional independent yields given in Table 6.2, 25% of the cumulative yield of iodine-131 was assumed to be formed through 30 hr tellurium-131m, 75% through 24.8 min tellurium-131 and directly as iodine-131.

6.3(b) Iodine-133

The decay chain for mass-133 is set out below.

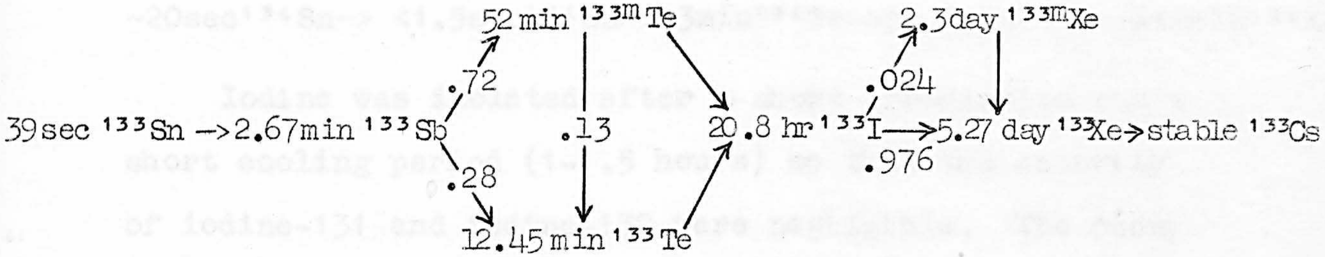
39 sec ¹³³Sn → 2.67 min ¹³³Sb
.72
.28
52 min ¹³³ᵐTe
12.45 min ¹³³Te
.13
20.8 hr ¹³³I
.024
.976
2.3 day ¹³³ᵐXe
5.27 day ¹³³Xe → stable ¹³³Cs

The graphical analyses of the decay curves have been discussed above (see 6.3(a)).

It was shown by Strom et al.[7] that the independent yields of tellurium-133 and -133m were about the same in the thermal fission of uranium-235. This was assumed to be also the case in the 14 MeV neutron induced fission of protactinium-231. It was shown by calculation that the cumulative yield of iodine-133 is not strongly dependent on this ratio. For example, the change in the cumulative yield of xenon-133 was only 1% when it was assumed that all of the independent yield of tellurium-133 belongs to 52 min tellurium-133m.

From the fractional independent yields given in Table 6.2 the apparent independent yield of iodine-133 (this includes the iodine-133 formed independently in fission and through the 12.45 min tellurium-133) and the amount formed through 52 min tellurium-133m were found to be 42% and 58% of its cumulative yield respectively.

6.3(c) Iodine-134

The decay chain for mass-134 is

$$\sim 20\,\mathrm{sec}\,{}^{134}\mathrm{Sn} \rightarrow <1.5\,\mathrm{sec}\,{}^{134}\mathrm{Sb} \rightarrow 43\,\mathrm{min}\,{}^{134}\mathrm{Te} \rightarrow 52.8\,\mathrm{min}\,{}^{134}\mathrm{I} \rightarrow \mathrm{stable}\,{}^{134}\mathrm{Xe}$$

Iodine was isolated after a short irradiation and a short cooling period (1-1.5 hours) so that the activity of iodine-131 and iodine-132 were negligible. The decay curves were then analysed for iodine-134, -135 and -133 ignoring the contributions from xenon-133m and -135m. Because of the difficulties encountered[3] during resolution of the decay data the computed activity for iodine-134 was estimated to be about 10% uncertain. For the same reason the activities obtained for iodine-133 and -135 from measurements primarily intended to give iodine-134 were not used in the cumulative yield calculations for these masses; separate irradiations were carried out.

The fission yield of iodine-134 was calculated assuming that 62% of its cumulative yield formed independently and 38% was produced from its precursors.

6.3(d) Xenon-133

The decay chain for mass-133 has already been discussed (see 6.3(b)).

The separation of xenon was performed about 20 hours after the end of the irradiation. The decay curves showed only the presence of xenon-133 and xenon-135 and they were always easily resolved.

The assumptions made in obtaining the cumulative and independent formation of iodine-133 were those discussed above. The independent yield of xenon-133 was taken to be 3% assuming that xenon-133 had the same independent yield. The amount of xenon-133 formed through xenon-133m was shown to be negligible.

Independent yields measured by Strom et al.[7] were used in calculating the counting efficiencies of the gas counters.

6.3(e) Xenon-135

The decay chain for mass-135 is set out below.

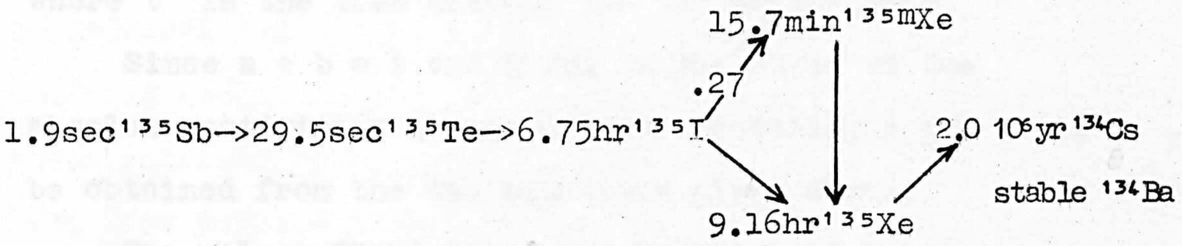

The fraction of cumulative yield of xenon-135 (including xenon-135m) which was formed independently of the precursors was measured for 14.8 MeV neutron induced fission of protactinium-231. For this purpose two xenon extractions were performed from each irradiated sample, the first immediately after the irradiation and the second about 24 hours after the first separation.

The number of xenon-135 (and -135m) atoms recovered from the first extraction is given by

$$N_1 = K.I.Y_{Xe}\left[a\,S_{Xe}e^{-\lambda_{Xe}t'} + b\,\frac{\lambda_I}{\lambda_{Xe}-\lambda_I}\left(S_I\,e^{-\lambda_I t'} - e^{-\lambda_{Xe}t'}\right)\right]$$

K, I, Y and S have already been defined in Chapter 3. a and b are the fractions of the cumulative yield of xenon-135 (and -135m) formed independently and from precursors respectively. t' is the time between the end of the irradiation and the first extraction.

The number of atoms of xenon-135 (and -135m), N_2, recovered from the second extraction is derived only from iodine-135. N_2 is given by

$$N_2 = K.I.Y_{Xe}\, b \frac{\lambda_I}{\lambda_{Xe}-\lambda_I} S_I\, e^{-\lambda_I t'} (e^{-\lambda_I t''} - e^{-\lambda_{Xe} t''})$$

where t" is the time between the two separations.

Since a + b = 1 and N_1/N_2 is the ratio of the absolute activities measured experimentally, a and b can be obtained from the two equations given above.

The values found for a and b were used in the calculation of the cumulative yield of xenon-135. The experiments carried out for cumulative yield measurements were the same as those for xenon-133.

For calibration measurements independent yields were calculated taking C = 0.9 and the number of prompt neutrons emitted with the heavy fragment, ν_H to be 0.8. ν_H was obtained using the empirical formula given by Wahl et al.[8]

$$\nu_H = 0.531\bar{\nu} + 0.062\ (A_H - 143)$$

where $\bar{\nu}$ is the average number of neutrons emitted in fission.

6.4. Results and Discussion

It was shown in Chapter 5 that mass yields for 3 MeV neutron induced fission of protactinium-231 obtained by the recoil method were in good agreement with those measured directly. For xenon measurements, tin was used as catcher material and the foils were melted instead of being subjected to the usual aqueous dissolution as a first step in the separation of xenon from the other fission products. The recoil method was therefore tested using tin as catcher substance. For this purpose cumulative yields of xenon-133 and xenon-135 were measured for fission of uranium-238 induced by 14.8 MeV neutrons using the modified recoil method and the results were compared with those obtained by the more conventional procedure[9]. It is seen from Table 6.3 that the values obtained by the recoil method are in satisfactory agreement with those obtained earlier from a bulk sample of irradiated uranium salt. The ability of the tin to retain xenon was also demonstrated as discussed earlier (see 6.2(b)).

The average number of neutrons emitted in 14.8 MeV neutron induced fission of protactinium-231 was previously[10] estimated to be 4.25. It was assumed that the variation of the number of neutrons emitted per fragment with the initial fragment mass shows the same trend as that observed for a number of other fissioning systems[11]. In support of

Table 6.3

Relative yields for xenon-133 and -135 in 14 MeV neutron induced fission of uranium-238

	Recoil method		Direct method*	
	Y_{133}/Y_{99}	Y_{135}/Y_{99}	Y_{133}/Y_{99}	Y_{135}/Y_{99}
	1.229	1.253		
	0.967	0.982	1.19 ± 0.03	1.26 ± 0.02
	1.149	1.158		
Mean	1.11±0.08	1.13±0.08		

*The mean value for 5 measurements made by Sellars[3].

this it has been found that the form of the distribution of neutrons as a function of mass is the same for fission induced by thermal and fission spectrum neutrons. The distribution is such that $\nu_L + \nu_H \simeq \bar{\nu}$ and at the masses under consideration ν_L is only slightly greater than ν_H. The number of neutrons emitted from heavy fragments (ν_H) was therefore taken to be 2 in the present work for the masses of interest.

The fractional independent yields of the members of the mass-135 chain were calculated using several values for the empirical constant, C (see Chapter 3). Calculated and measured values for a and b (Table 6.4) were in better agreement when C was taken to be 2. It has been suggested by Strom et al.[7] that C is strongly dependent on the mass number of the chain. They obtained 1.10, 0.74 and 0.57 for C for the mass chains 131, 132 and 133 respectively, in the thermal neutron induced fission of uranium-235. Because of the lack of measured independent yield data for protactinium-231, it was not possible to estimate C for masses below 135; C = 2 was therefore used to calculate independent yields for all the other masses. However, the variations in the total chain yields were very small when C was taken to be either 0.9 or 3 (Table 6.5).

The measured cumulative fission yields for xenon-133, -135, iodine-131, -133 and -134, relative to molybdenum-99 are recorded in Tables 6.6 - 6.8. The total and absolute

Table 6.4

Independent yield of xenon-135

Run	t' (hrs)	t" (hrs)	$A_{^{135}Xe}$ at the time of sepn.	Chemical recovery(%)	Counter efficiency(%)	S x 10^5 ^{135}I	S x 10^5 ^{135}Xe	a^*(%)
1	0.95	23.33	1540 619	53.36 54.08	38.5 42.0	5.446	5.501	40.24
2	0.58	24.25	3300 2430	36.87 62.19	38.5 42.0	3.472	3.511	37.81
3	0.83	24.11	1787 591	76.51 62.66	38.5 42.0	5.552	5.616	39.01
							Mean	39.0 ± 0.7

Relative cumulative yield of xenon-135 = 1.80 ± 0.10.

Relative independent yield of xenon-135 = 1.80 x 0.39 = 0.70 ± 0.04.

Normalised independent yield of xenon-135 = 0.70 x 3.21 = 2.25 ± 0.13.

* a is the fraction of the cumulative yield of xenon-135 formed from iodine-135; therefore b = 100-39.0 = 61.0.

Table 6.5

Comparison of the total chain yields calculated using various values for C

Mass	Total chain yield C = 0.9	 C = 2	 C = 3
131	1.04 ± 0.02	1.05 ± 0.02	1.08 ± 0.02
133 (I)	1.70 ± 0.03	1.79 ± 0.03	1.84 ± 0.03
133 (Xe)	2.06 ± 0.07	1.93 ± 0.07	2.00 ± 0.07
134	2.64 ± 0.05	2.86 ± 0.06	2.89 ± 0.06

The number of neutrons emitted from heavy fragments (ν_H) was taken to be 2, in this mass region.

Table 6.6

Cumulative fission yields for xenon-133 and xenon-135

Run	t'	A(t')	A(t')	$A_{^{99}Mo}$	Chemical recovery (%)	Chemical recovery (%)	Counter efficiency(%)	Counter efficiency(%)	Counter efficiency(%)	S x 10^5	S x 10^5	S x 10^5	S x 10^5	S x 10^5	Relative yield	Relative yield
	(hrs)	^{133}Xe	^{135}Xe		Xe	Mo	^{133}Xe	^{135}Xe	^{99}Mo	^{133}I	^{133}Xe	^{135}I	^{135}Xe	^{99}Mo	^{133}Xe	^{135}Xe
1*	19.47	120	1020	117	57.01	58.51	71.2	64.0	29.5	2.934	2.974	2.840	2.876	2.967	2.008	1.949
2	22.65	220	1557	392	34.64	58.51	65.4	60.0	29.5	2.617	2.654	2.525	2.560	2.648	1.801	1.833
3	23.48	312	1634	213	59.63	41.17	66.1	59.6	31.4	3.413	3.461	3.297	3.341	3.452	1.984	1.621
														Mean	1.93 ± 0.07	1.80 ± 0.10

*Measured by Sellars.

Table 6.7

Cumulative fission yields for iodine-131 and iodine-133

Run	t' (hrs)	t" (hrs)	A(t'+t")		$A_{^{99}Mo}$	Chemical recovery (%)		Counter efficiency(%)			S x 10^6				Relative yield	
			^{131}I	^{133}I		I	Mo	^{131}I	^{133}I	^{99}Mo	^{131}I	^{131m}Te	^{133}I	^{99}Mo	^{131}I	^{133}I
1	74.56	0.38	147	258	1412	26.64	67.67	31.9	35.7	32.2	1.270	1.260	1.253	1.266	1.073	1.632
2	70.83	3.80	444	940	1988	79.94	79.87	28.0	35.2	31.5	4.287	4.247	4.206	4.268	1.008	1.635
3	70.28	1.50	333	790	1618	66.31	72.57	29.0	35.5	32.0	7.312	7.248	7.193	7.285	0.989	1.690
4	72.48	2.61	456	946	2343	77.10	97.46	28.2	35.4	30.9	4.237	4.199	4.165	4.220	1.083	1.747
														Mean	1.04±0.02	1.68±0.03

t' is the time between the end of irradiation and the separation of iodine.

t" is the time between the separation and precipitation of iodine.

Table 6.8

Cumulative fission yields for iodine-134

Run	t' (hrs)	t" (hrs)	$A_{^{134}I}(t'+t'')$	$A_{^{99}Mo}$	Chemical recovery (%)		Counter efficiency(%)		S x 10^4			Relative yield
					I	Mo	^{134}I	^{99}Mo	^{134}Te	^{134}I	^{134}Mo	
1	1.5	0.67	8572	266	76.39	60.39	35.3	32.5	4.894	5.112	6.215	1.777
2	1.28	0.68	6514	168	79.27	60.03	35.3	32.5	5.254	5.468	6.407	1.836
3	0.93	0.70	7440	173	73.47	56.91	35.3	32.7	5.697	5.975	7.558	1.899
											Mean	1.84±0.04

Table 6.9

Yield data for 14.8 MeV neutron induced fission of protactinium-231

Mass	Measured yield relative to mass-99	% chain	Total chain yield	Absolute chain yield (%)
131	1.04 ± 0.02	98.8	1.05 ± 0.02	3.37 ± 0.32
133 (I)	1.68 ± 0.03	93.7	1.79 ± 0.03	5.74 ± 0.10
133 (Xe)	1.93 ± 0.07	100	1.93 ± 0.07	6.19 ± 0.22
134	1.84 ± 0.04	64.3	2.86 ± 0.06	9.18 ± 0.19
135	1.80 ± 0.10	84.8	2.12 ± 0.12	6.80 ± 0.38

chain yields are given in Table 6.9. They are also plotted in Fig. 6.3 with the previously[10] measured yields for masses-132 and -143. Absolute yields were obtained using the previously[10] reported value (3.21%) for the absolute yield of molybdenum-99. The measured absolute yield at mass-134 is considered to be less accurate than those at the other masses, because of the uncertainty in the computed activity of iodine-134 and the large correction applied to give the total chain yield. However, it is rather unlikely that the absolute value given in Table 6.9 is in error by more than 15 or 20%. The cumulative yield for mass-132 was re-measured to check the previously reported value[10]. The agreement was found to be satisfactory as it is seen from Table 6.10.

Table 6.10

Comparison of the relative yield of iodine-132 with that measured previously

Y_{132}/Y_{99}

Present work	Previous work*
1.54	
1.37	1.52 ± 0.08
1.50	
Mean 1.47 ± 0.05	

*The mean value for 3 measurements.

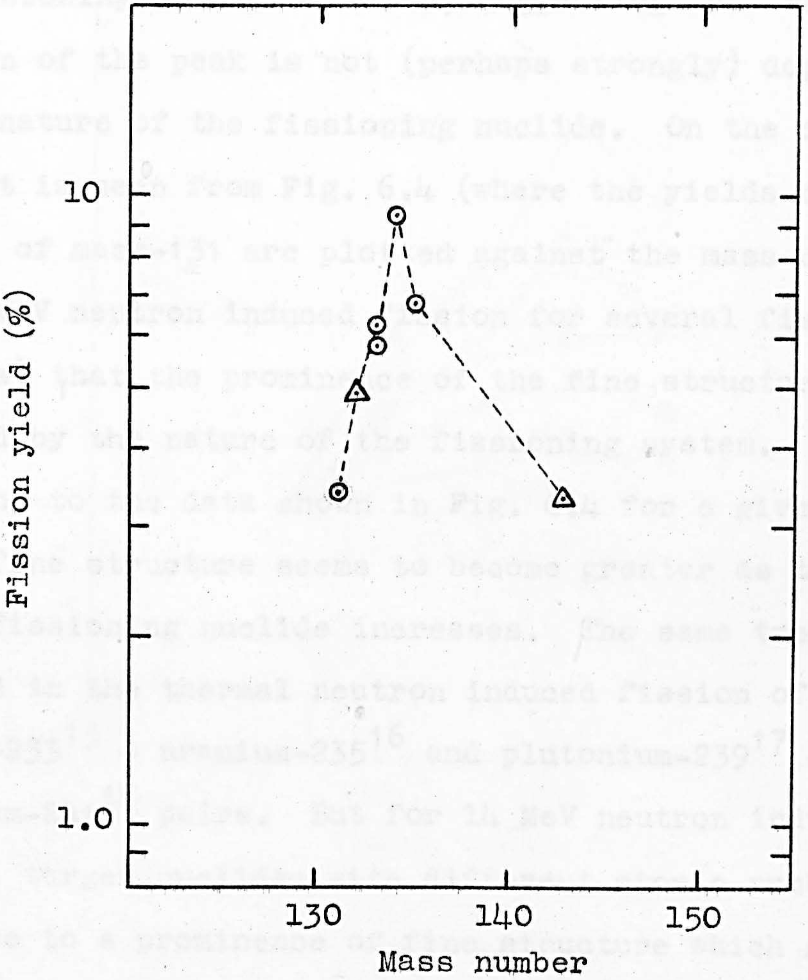

Fig. 6.3. Cumulative yields in the mass region 131-135 from 14.8 MeV neutron induced fission of protactinium-231.

⊙ , this work ∆ , ref. 10.

The results show the presence of a peak at mass-134. At low and moderate neutron energies fine structure appears to be at mass-134 in the mass region 131-135 for the fissioning systems studied, suggesting that the position of the peak is not (perhaps strongly) dependent on the nature of the fissioning nuclide. On the other hand, it is seen from Fig. 6.4 (where the yields relative to that of mass-131 are plotted against the mass number, for 14 MeV neutron induced fission for several fissioning nuclides) that the prominence of the fine structure is affected by the nature of the fissioning system. According to the data shown in Fig. 6.4 for a given atomic number fine structure seems to become greater as the mass of the fissioning nuclide increases. The same trend is observed in the thermal neutron induced fission of uranium-233[15] - uranium-235[16] and plutonium-239[17] - plutonium-241[18] pairs. But for 14 MeV neutron induced fission, target nuclides with different atomic numbers give rise to a prominence of fine structure which seems to increase with decreasing atomic number. Thorium-229[19], uranium-235[16], plutonium-239[17] show the same trend for the thermal neutron induced fission. However, the presence of a more pronounced fine structure in plutonium-241[18] (Z = 94) than in uranium-233[15] (Z = 92) and about the same degree of structure in the uranium-235[16] - plutonium-241[18] and uranium-233[15] - plutonium-239[17] pairs suggest that

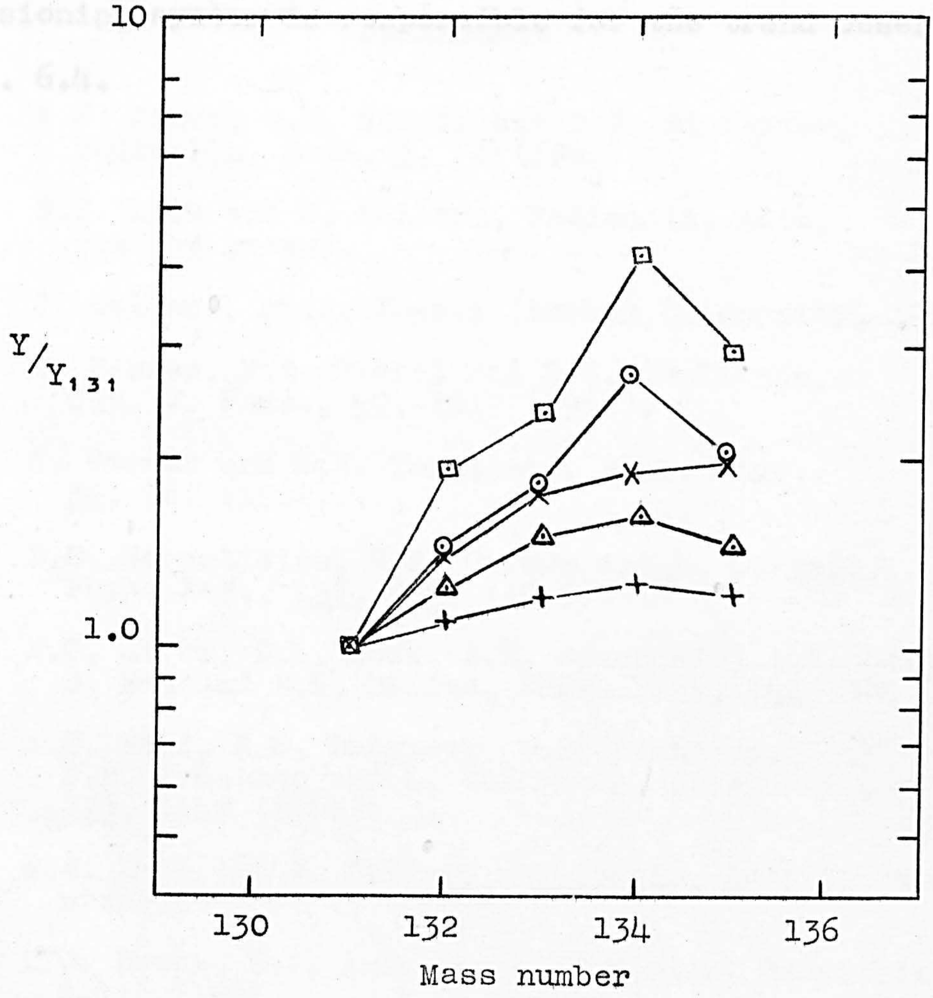

Fig. 6.4. Cumulative yields relative to that of mass-131 in 14 MeV neutron induced fission.

⊡, thorium-232 (ref. 12),
⊙, protactinium-231 (this work),
×, uranium-238 (ref. 9),
△, uranium-238 (ref. 13),
+, uranium-235 (ref. 14).

perhaps a combined effect of mass and atomic number of the fissioning system is responsible for the trend observed in Fig. 6.4.

References

1. R.H. James, G.R. Martin and D.J. Silvester, Radiochim. Acta, 3, 76 (1964).

2. S.J. Lyle and J. Sellars, Radiochim. Acta, (in the press).

3. J. Sellars, Ph.D. Thesis (Durham University, 1967).

4. H. Farrar, H.R. Fickel and R.H. Tomlinson, Can. J. Phys., 40, 1017 (1962).

5. H. Farrar and R.H. Tomlinson, Nucl. Phys., 34, 367 (1962).

6. D.G. Sarantities, G.E. Gordon and D. Coryell, Phys. Rev., 138, B353 (1965).

7. P.O. Strom, D.L. Love, A.E. Greendale, A.A. Delucchi, D. Sam and N.E. Ballau, Phys. Rev., 144, 984 (1966).

8. A.C. Wahl, R.L. Ferguson, D.R. Nethaway, D.E. Troutner and K. Wolfsberg, Phys. Rev., 126, 1112 (1962).

9. S.J. Lyle and J. Sellars, Radiochim. Acta (in the press).

10. M.G. Brown, S.J. Lyle and G.R. Martin, Radiochim. Acta, 6, 16 (1966).

11. J. Terrell, Phys. Rev., 127, 880 (1962).

12. K.M. Broom, Phys. Rev., 133, B874 (1964).

13. D.J. Gorman and R.H. Tomlinson, Can. J. Chem., 46, 1663 (1968).

14. A.C. Wahl, Phys. Rev., 99, 730 (1955).

15. D.R. Bidinosti, D.E. Irish and R.H. Tomlinson, Can. J. Chem., 39, 628 (1961).

16. H. Farrar and R.H. Tomlinson, Nucl. Phys., 34, 367 (1962).

17. H.R. Fickel and R.H. Tomlinson, Can. J. Phys., 37, 916 (1959).

18. H. Farrar, W.B. Clarke, H.G. Thode and R.H. Tomlinson, Can. J. Phys., 42, 2063 (1964).

19. J.W. Harvey, W.B. Clarke, H.G. Thode and R.H. Tomlinson, Can. J. Phys., 44, 1011 (1966).

CHAPTER 7

General Discussion and Further Suggestions

In the course of the study presented in this thesis, experiments were carried out to obtain more information about the fission process. The half-lives of fission products and the decay data for the mass chains have already been studied to a great extent because of their necessity in fission yield measurements. However, there are still some uncertainties in the half-lives of some products. Since tin-129 was one of them, an attempt was made to establish on a firmer basis the half-lives of tin-129 isomers. With a reliable knowledge of the half-lives the work could then be extended with suitable refinement of method to the measurement of the branching and yield ratios of these isomers. The latter may be related to some properties of the compound nucleus[1].

Since the measured quantity is far removed from the primary process, information of mechanistic value obtained from cumulative mass-yield curves is rather limited. However, they may be used to estimate the number of neutrons emitted from each fragment, provided the prompt mass-yield distribution is known and to look for correlations between the nature of the fissioning system and the fission process. The difficulties encountered in measurements of cumulative yields in 3 MeV neutron induced fission of protactinium-231 were due to very high activity of the fissioning nucleus and daughters compared to the activity obtained for individual fission products. Nevertheless, it has been shown that consistent and reproducible relative yields can be obtained leading to a rough estimate for the average number of neutrons emitted per fission and a set of absolute cumulative fission yields. Accurate and detailed data (i.e. neutrons associated with individual fission fragments) in this field can only be got using more advanced techniques than those available at present.

As discussed in Chapter 1, for target nuclides having even numbers of neutrons, a plot of the fission cross-section against neutron energy shows the presence of some steps on the curve. These have been explained as arising from changes in neutron re-emission in competition with fission. According to the data[2] available, such a step is present at a bombarding neutron energy of about 0.85 MeV for protactinium-231. Then the fission cross-section increases very slowly with increasing neutron energy. There is a total lack of published cross-section data in the neutron energy range 3 to 14.8 MeV. The value found in the present work for 14.8 MeV neutron bombardment suggests that the presence of a step in this energy range is rather unlikely. However, if the cross-section of protactinium-231 varies with neutron energy in the same way as that of uranium-238, then it is not unreasonable to expect a small step; this could of course only be proved by doing measurements over a range of neutron energies.

The measured fission cross-section of protactinium-231 was used to estimate the neutron emission probability ($\sigma_{n,n'}$) from the compound nucleus following bombardment by 14.8 MeV neutrons. $\sigma_{n,n'}$ obtained this way is much higher than those for neighbouring heavy nuclides; the same is also true for 3 MeV neutron induced fission. If the ratio of the partial widths for fission and neutron emission from the compound nucleus (Γ_f/Γ_n) calculated by Vandenbosch and Huizenga[3] and symmetric fission yield (Y_s) measured in the present work (see Chapter 5) are used to evaluate Γ_s/Γ_n, then protactinium-231 gives a point far removed from the curve to which data for other fissioning systems may be fitted (see Fig. 5.6). This may be due to a failure of the method to adequately account for the properties of protactinium-231 system, unless the measured symmetric fission yield is in error by a large factor. If the behaviour of protactinium-231 is considered to be an exception for reasons which are not immediately obvious, then the curve given in Fig. 5.6 may be of some value in obtaining information for Γ_s/Γ_n for the other fissioning nuclides. More elaborate expressions[4] can be used for the nuclear level density in the derivation of the expression for Γ_s/Γ_n (see Appendix II). This would, however, mean the introduction of other parameters, (e.g. angular momentum of the excited nucleus and nuclear temperature) adding to the problem of integration and arrangement of the final expression in a form in which it could be tested using experimental data. The introduction of additional parameters if at all possible in the present circumstances, may in any case only tend to obscure the physical significance of the results of tests of the derived expression. Modifications therefore were not attempted. Efforts were however made using the combined data for 3 and 14 MeV neutron induced fission to obtain a value for the nuclear level density parameter; they were unsuccessful because of the approximations and neglect of certain terms made in deriving the expression used to relate Γ_s/Γ_n with the parameter.

A study of the fine structure in the mass-yield curve provides another source of information on the nature of the fission process. Several suggestions have been made to explain the irregularities observed in mass-yield distributions in the fission of various heavy nuclides. According to Wiles[5] there is a structural preference in fission for isotopes with closed shells, so that fine structure may result, at least in part, by the favouring of fragments with 82 neutrons. If this is so, any irregularity in the yield of these species must appear symmetrically in the complementary fragments. The fact that there was a peak at mass complementary to mass-134 in thermal fission of uranium-235[6] supported this hypothesis. Fine structure was also observed at masses complementary to mass-141 in fission of uranium-233[7], uranium-235[8], plutonium-239[9] induced by thermal neutrons.

Farrar and Tomlinson[10] and Terrell[11] proposed that most of the fine structure in the cumulative mass distribution results from the neutron yield changing slowly as a function of mass of the primary fragments. The absence of a peak complementary to that observed at mass-134 in thermal fission of uranium-233[7] and plutonium-239[9] was taken as evidence for this explanation. However, the work done by Thomas and Vandenbosch[12] suggests that the fine structure in the mass distribution before and after neutron emission has the same origin; this was confirmed by the more recent work of Andritsopoulos[13].

Since the yield measurements made in the present work to establish the fine structure for fission of protactinium-231 induced by 14.8 MeV neutrons were confined only to the mass region 131-135, it is difficult to show that the present data support any of the suggestions made above. Yield measurements on the light mass peak could provide us useful information for a discussion of the origin of the fine structure.

In Chapter 6 an attempt was made to find a correlation between fine structure and charge and mass of the fissioning nuclide. Because of the very limited available data this could not be achieved with any certainty. To draw any firm conclusion requires a knowledge of experimentally determined independent yields, the number of neutrons emitted from each fragment and measurements on a larger range of fissile nuclides (especially with higher atomic and mass number than that of uranium). It is doubtful whether all these experiments are technically feasible at present for fissioning systems leading to satisfactory tests of the ideas.

References

1. J.R. Huizenga and R. Vandenbosch, Phys. Rev., 120, 1305 (1960).

2. D.J. Hughes and R.B. Schwartz, Report, BNL-325 (1958).

3. R. Vandenbosch and J.R. Huizenga, Proceedings of the Second United Nations International Conference on the Peaceful Uses of Atomic Energy, 15, P/688 (1958).

4. D. Bodansky, Ann. Rev. Nucl. Sci., 12, 79 (1962).

5. D.R. Wiles, B.W. Smith, R. Horsley and H.G. Thode, Can. J. Phys., 31, 419 (1953).

6. L.E. Glendenin, E.P. Steinberg, M.G. Inghram and D.C. Hess, Phys. Rev., 84, 860 (1951).

7. D.R. Bidinosti, D.E.Irish and R.H. Tomlinson, Can. J. Chem., 39, 628 (1961).

8. H. Farrar, H.R. Fickel and R.H. Tomlinson, Can. J. Phys., 40, 1017 (1962).

9. H.R. Fickel and R.H. Tomlinson, Can. J. Phys., 37, 916 (1959).

10. H. Farrar and R.H. Tomlinson, Can. J. Phys., 40, 943 (1962).

11. J. Terrell, Phys. Rev., 127, 880 (1962).

12. T.D. Thomas and R. Vandenbosch, Phys. Rev., 133, 976 (1964).

13. G. Andritsopoulos, Nucl. Phys., 94, 537 (1967).

Appendix I

Chemical Procedures

All carrier solutions used contained 5 mg ml^{-1} of the element of interest.

1. Bromine

Carrier Solution

Potassium bromide was dried and an accurately weighed amount of it was dissolved in water.

Separation Procedure

Separation and purification of bromine was performed by using the method of Glendenin[1] as modified by Ramaniah[2].

1. The catcher foils were dissolved in the minimum amount of concentrated sodium hydroxide and refluxed for about 30 minutes in the presence of a reducing agent. The solution was cooled in ice and cautiously acidified with diluted nitric acid without allowing the temperature to rise. Bromide was oxidised to bromine by adding a few drops of saturated ceric sulphate solution and the element extracted into carbon tetrachloride.

2. The carbon tetrachloride extract was transferred to another separatory funnel and bromine back extracted into water to which a few drops of a saturated solution of sulphur dioxide had been added. 2 ml of iodide

(~ 5 mg ml^{-1}) carrier were added to the acidified aqueous phase and iodide oxidised with 0.1 M sodium nitrite and extracted into carbon tetrachloride. The extraction was repeated once more.

3. The bromide was oxidised to bromine with permanganate, extracted into carbon tetrachloride and back-extracted into water containing a little saturated sulphur dioxide. The aqueous phase was boiled to expel sulphur dioxide and bromide was then precipitated as silver bromide.

2. Strontium

Carrier Solution

Strontium nitrate was dissolved in water and standardised by precipitation as strontium carbonate.

Separation Procedure

Strontium was separated by the procedure recommended by Sunderman[3].

1. An acid solution of the catcher foils was made alkaline with strong sodium hydroxide solution and a little solid sodium carbonate added to complete the precipitation of strontium as carbonate. This precipitate was dissolved in the minimum volume of dilute nitric acid, the solution cooled in ice and strontium reprecipitated by the addition of 20 ml of fuming nitric acid.

2. The strontium nitrate was dissolved in the minimum amount of water and reprecipitated by adding 15 ml of fuming nitric acid to the cooled solution. This precipitate was dissolved in water, 1 ml of iron carrier added and ferric hydroxide precipitated with 6 M ammonium hydroxide.

3. 2 ml of barium carrier were added to the supernate. The solution was neutralised with 6 M nitric acid and buffered by the addition of 1 ml of 6 M acetic acid and 2 ml of 6 M ammonium acetate. Barium chromate was precipitated by the addition of 1 ml of 1.5 M sodium chromate and heating to boiling. The precipitate was discarded, more barium carrier added and barium chromate again precipitated.

4. 2 ml of concentrated ammonia were added to the supernate and strontium carbonate was precipitated by the addition of saturated sodium carbonate solution. The precipitate was washed with water and ethanol.

3. Zirconium

Carrier Solution

Zirconium carrier was prepared by dissolving zirconyl nitrate in 5 M nitric acid and the solution was standardised gravimetrically by the precipitation of zirconium tetramandelate[4].

Separation Procedure

The separation procedure used was essentially that of Hahn and Skomieczmy[5], but it was modified for this protactinium work by including an extraction of protactinium from a concentrated hydrochloric acid solution with di-isobutyl ketone to reduce the contamination.

1. A solution prepared from the catcher foils was made alkaline with sodium hydroxide and zirconium hydroxide precipitated. The precipitate was dissolved in 5 M hydrochloric acid and 10 ml of a 15% solution of mandelic acid added. The solution was heated for about 20 minutes at 80-90°C for complete precipitation of zirconium tetramandelate. The precipitate was transferred to a polythene centrifuge tube and dissolved by the addition of 1 ml of 20 M hydrofluoric acid.

2. 0.5 ml of lanthanum carrier (containing 10 mg ml^{-1} of lanthanum) were added, and the precipitate of lanthanum fluoride centrifuged down. The lanthanum fluoride precipitation step was repeated.

3. 1 ml of barium solution (20 mg ml^{-1}) was added to the solution from step 2 and the precipitate which formed was slurried with 2 ml of water, 2 ml of saturated boric acid and 2 ml of concentrated nitric acid to effect its solution. The zirconium was then re-

precipitated by the addition of 1 ml of barium solution and 1 ml of hydrofluoric acid.

4. The dissolution and precipitation were repeated as in step 3.

5. The precipitate was dissolved in 2 ml of water, 2 ml of saturated boric acid and 2 ml of 6 M hydrochloric acid and zirconium hydroxide precipitated by the addition of 5 M sodium hydroxide.

6. The hydroxide precipitate was washed with water, dissolved in concentrated hydrochloric acid with the addition of the minimum of water and transferred to a separatory funnel with more acid. An equal volume of di-isobutyl ketone (previously equilibrated with concentrated hydrochloric acid) was added, the funnel was shaken for 5 minutes and the organic phase was discarded; a fresh portion of di-isobutyl ketone was added and the extraction was repeated.

7. The aqueous phase was heated to expel the remaining di-isobutyl ketone and zirconium precipitated by the addition of 5 M sodium hydroxide.

8. The zirconium hydroxide was washed with water and dissolved using 3 ml of concentrated hydrochloric acid and 3 ml of water. The solution was transferred to a glass tube, heated on the water bath and 10 ml of 15% mandelic acid solution added; heating was continued for

20 minutes to complete the precipitation of zirconium tetramandelate. The precipitate was mounted on a filter disc and washed successively with a 5% solution of mandelic acid in 2% hydrochloric acid and ethanol.

4. Molybdenum

Carrier Solution

Ammonium molybdate was dissolved in water with the addition of dilute hydrochloric acid and sodium bromate, and standardised by precipitation of molybdenum 8-hydroxyquinolate by the method described by Vogel[6].

Separation Procedure

The separation procedure was based on the extraction method given by Maeck et al.[7]. The precipitation method[8] was used to separate the molybdenum in the work described in Chapter 4 and where the catcher material was tin.

Extraction Method

1. To 2-4 M acid solution prepared from the catcher foils and containing 10 mg of molybdenum carrier, 30 ml of ethyl acetate and 5 ml of α-benzoin oxime (4% in 95% ethyl alcohol) were added. The α-benzoin oxime complex of molybdenum was extracted into ethyl acetate by shaking for about 2 minutes.

2. The organic phase was washed with 1 M hydrochloric acid and the aqueous phase was discarded. Molybdenum was back-extracted into 15 ml of 4 N ammonium hydroxide. The aqueous phase was transferred to another separatory funnel and acidified by the addition of 10 ml of 10 M hydrochloric acid.

3. Extraction and back-extraction of molybdenum were repeated.

4. 1 ml of iron carrier was added to the aqueous solution and ferric hydroxide was precipitated.

5. The supernate was made just acid to methyl red with 5 N sulphuric acid, 5 ml of 2 M ammonium acetate was added and the solution heated to 90°C. Molybdenum was precipitated by the addition of a slight excess of a 3% solution of 8-hydroxyquinoline; heating was continued until the precipitate coagulated. It was mounted, washed with hot water and ethanol.

Precipitation Method

1. An acid solution of the catcher foils was adjusted to 1-2 M in acid and 5 ml of 4% alcoholic solution of α-benzoinoxime was added. Precipitation was complete on standing for about 10 minutes. The precipitate was centrifuged, washed with water and dissolved in 3 ml of fuming nitric acid. It was then diluted to 25 ml, excess acidity was removed by the addition of 1 to 2 ml

of concentrated ammonia and molybdenum was precipitated by the addition of 5 ml of α-benzoinoxime solution.

2. The dissolution and precipitation of molybdenum were repeated after which the final precipitate was dissolved in 3 ml of fuming nitric acid and boiled with 3 ml of 60% perchloric acid. After cooling the solution was diluted to 10 ml with water and 1 ml of iron carrier added; ferric hydroxide was precipitated by the addition of concentrated ammonia.

3. As in step 5 of the extraction method.

5. Ruthenium

Carrier Solution

Ruthenium trichloride was dissolved in 1 M hydrochloric acid to give a solution of about 5 mg ml^{-1} and this solution was used as standard in the colorimetric[9] determination of the amount of ruthenium in fission product sources.

Separation Procedure[10]

1. To a weakly acid solution prepared from the catcher foils a few drops of saturated cerium(IV)sulphate were added to ensure isotopic exchange and ruthenium was precipitated by passing hydrogen sulphide into the solution.

2. The sulphide precipitate was transferred to a distillation apparatus by using 5 N sulphuric acid, 1g of sodium bismuthate was added and ruthenium tetroxide was separated by distillation in a stream of nitrogen. The product was collected in 10 ml of ice-cold, freshly prepared 12 M sodium hydroxide. Distillation was continued until 1 to 2 ml of liquid had passed over. The ruthenate solution was scavenged by the addition of 1 ml of iron carrier.

3. The supernate was diluted to 25 ml and made just acid. 1 ml of freshly prepared 6 M sodium hydroxide and 5 ml of ethanol were added and ruthenium dioxide precipitated by boiling. The precipitate was slurried with about 10 ml of water and boiled after the addition of 1 ml of 6 M sodium hydroxide. It was then filtered, washed with hot water and ethanol.

6. Silver

Carrier Solution

Dry silver nitrate was weighed and dissolved in water.

Separation Procedure

The method given by Sunderman[11] was used for the separation of silver with some modifications.

1. Silver chloride was precipitated by the addition of hydrochloric acid to a nitric acid solution of catcher foils or by the dilution of a hydrochloric acid solution. The precipitate was dissolved in 2 ml of concentrated ammonia, diluted to 10 ml and scavenged with 1 ml of iron carrier.

2. 5 ml of a 40% solution of EDTA in ammonia were added to the solution and silver was precipitated with 1 ml of a 2.5% ammoniacal solution of benzotriazole and left for 5 minutes at room temperature.

3. The precipitate was dissolved in 1 ml of concentrated nitric acid and the solution diluted to 20 ml. Silver chloride was precipitated by the addition of 1 ml of 1 M hydrochloric acid. It was warmed to coagulate the precipitate.

4. Steps 1 and 2 were repeated.

5. The precipitate was dissolved in 1 ml of concentrated nitric acid. After dilution the solution was made just alkaline with 6 M sodium hydroxide and 3 drops added in excess to complete the precipitation of silver oxide. The precipitate was dissolved in 4 drops of concentrated sulphuric acid and the solution was evaporated to dryness.

6. The residue was dissolved in 20 ml of distilled water and 1 ml of 2 M iodic acid was added to precipitate silver iodate.

7. Silver iodate was dissolved in 4 drops of concentrated ammonia and iodate re-precipitated by the addition of 3 drops of concentrated sulphuric acid and diluting the solution to 10 ml with water. The precipitate was washed with water and ethanol.

7. Antimony

Carrier Solution

Antimony trichloride was dissolved in 3 M hydrochloric acid and the solution standardised by precipitating antimony as the n-propyl gallate[12].

Separation Procedure

The method given by Pappas[13] was used with some modifications for the separation of antimony.

1. An acid solution of the catcher foils was boiled with bromine to ensure isotopic exchange and antimony(III)sulphide was precipitated by passing hydrogen sulphide into a hot solution 1 to 2 M in acid. The precipitate was dissolved in 2 ml of 0.5 M potassium hydroxide and the solution was scavenged twice with ferric hydroxide. Antimony(III)sulphide was recovered by acidifying the solution.

2. The precipitate was dissolved in 5 ml of concentrated hydrochloric acid and hydrogen sulphide was removed by evaporation. The solution was diluted until 3 M in acid, a few drops of tellurium carrier were added

and tellurium metal was precipitated from the hot solution with the aid of hydrazine and sulphur dioxide.

3. The solution was boiled to expel sulphur dioxide and antimony was re-precipitated by hydrogen sulphide.

4. The precipitate was dissolved in 10 ml of 8 M hydrochloric acid. After boiling off hydrogen sulphide the solution was transferred to a separatory funnel and antimony was extracted into a mixture of 5 ml of benzene, 5 ml of isoproyl ether and a few drops of bromine. Extraction was complete when the organic phase remained brown. The organic phase was washed with 8 M hydrochloric acid.

5. Antimony was back-extracted into 10 ml of 8 M hydrochloric acid containing a little hydrazine hydrochloride. Back-extraction was complete when the organic phase was colourless.

6.* Antimony was precipitated as antimony(III)-sulphide from the aqueous solution by ammonium thiocyanate[14].

---

*The final precipitation of antimony described in the work contained in Chapter 4 was performed with hydrogen sulphide.

8. Cerium

Carrier Solution

Cerium(III) nitrate was dissolved in water and the solution standardised[15] by precipitating cerous oxalate and igniting it to cerium dioxide at 800°C.

Separation Procedure

A modified form of the method given by Hicks and Nervik[16] was used for the separation and purification of cerium.

1. Catcher foils were dissolved in the smallest amount of concentrated hydrochloric acid in the presence of cerium(III) and zirconium carriers and diluted until about 2 M in acid. The solution was boiled with 6-8 drops of saturated sodium bromate followed by 5 ml of 6% hydroxylamine hydrochloride. Cerium and zirconium were precipitated by the addition of concentrated sodium hydroxide solution.

2. The precipitate was dissolved in dilute hydrochloric acid and cerium was precipitated with hydrofluoric acid. The cerium(III)fluoride was washed with water.

3. The cerium fluoride was taken into a solution consisting of 3 ml concentrated nitric acid and 3 ml of saturated boric acid. The solution was made 4 M in nitric acid and digested with a few drops of 1 M potassium nitrite to ensure that all cerium was in the cerium(III) state.

4. The solution was transferred to a separatory funnel with 10 ml of 4 M nitric acid and extracted twice (5 minutes shaking each time) with 20 ml of 0.1 M HDEHP in carbon tetrachloride. Organic phases were discarded and the aqueous phase was washed with 10 ml of carbon tetrachloride. Cerium(III) was precipitated with ammonia and the hydroxide washed with water.

5. The precipitate was dissolved in 2 ml of concentrated nitric acid and 4 ml of 1 M potassium bromate warming to ensure that cerium was present as cerium(IV). 10 ml of 4 M nitric acid were added and cerium was extracted by shaking for 5 minutes with 10 ml of 0.3 M HDEHP in petroleum ether. The organic phase was washed three times with 10 ml of 4 M nitric acid and once with 10 ml of 0.5 M nitric acid.

6. Cerium was back-extracted by shaking with 10 ml of 5 M hydrochloric acid containing sulphur dioxide until the organic phase was colourless. The aqueous phase was filtered and cerium was precipitated with ammonia.

7. The precipitate was dissolved in diluted hydrochloric acid and diluted to 20 ml with water. Cerium(III)oxalate was precipitated by the addition of 10 ml of saturated oxalic acid and the mixture was warmed for 10 minutes. The precipitate was filtered and washed with ethanol and ether. Cerium contents of the precipitates were determined afterwards by titrating with EDTA[17].

9. Praseodymium

Carrier Solution

Praseodymium oxide was dissolved in the minimum of hydrochloric acid and standardised by titration with EDTA using xylenol orange as indicator[17].

Separation Procedure[15]

Separation of praseodymium was carried out in two stages: (a) separation of the rare earths as a group from other fission products, and (b) ion-exchange separation of praseodymium from the purified rare earths.

(a) Separation of Rare Earths

1. Catcher foils were dissolved in concentrated hydrochloric acid in the presence of praseodymium, cerium(III) and zirconium carriers. Rare earths were precipitated by the addition of concentrated sodium hydroxide.

2. The precipitate was dissolved in dilute hydrochloric acid and rare earth fluorides were precipitated by digesting with 2 ml of hydrofluoric acid for a few minutes.

3. The precipitate, previously centrifuged and washed with water, was dissolved in 3 ml of concentrated nitric acid and 3 ml of saturated boric acid, diluted to 15 ml and the fluoride precipitation was repeated.

4. The precipitate was again dissolved in nitric acid, boric acid mixture and the rare earths precipitated with ammonia.

5. The precipitate was dissolved in 4 ml of concentrated hydrochloric acid and the solution was passed through an anion-exchange column (10 cm x 6 mm) containing De-Acidite FF, previously equilibrated with concentrated hydrochloric acid. The centrifuge tube was rinsed with 3 ml of concentrated hydrochloric acid and the wash solution was passed through the column. The column was finally washed with 2 ml of concentrated hydrochloric acid. All of the eluant and wash solutions were collected.

6. The solution from step 5 was made alkaline with ammonia and rare earth hydroxides were precipitated.

7. The precipitate was dissolved in 5 ml of concentrated nitric acid. 3 ml of saturated potassium bromate solution was added and the solution warmed. Cerium(IV) was extracted twice with 10 ml of 0.3 M HDEHP in petroleum ether. The aqueous phase was washed with petroleum ether.

8. Rare earth hydroxides were re-precipitated from the aqueous phase. The precipitate was dissolved in 1 ml of concentrated nitric acid, 1 ml of saturated potassium bromate was added. The solution was warmed and then cooled in ice, diluted to 15 ml and

cerium(IV) was precipitated with 20 ml of 0.35 M iodic acid. One drop of cerium(IV) was added to help the scavenging action. The precipitate was centrifuged and discarded.

9. Rare earths were precipitated as hydroxide and washed. The precipitate was dissolved in 1 ml of concentrated hydrochloric acid and diluted to 10 ml. 1 ml of resin was added, digested for 10 minutes and the resin was put on to the top of the ion exchange column which was previously heated to 90°C.

(b) Ion-exchange Separation of Praseodymium from other Rare Earths

A gradient elution method was used to separate praseodymium from the other rare earths.

Resin

Bio-Rad resin AG 50W-X8 capacity 5.1 meq/dry resin, wet mesh (U.S. Std) range 230-400, moisture content 50% was used. It was washed with 6 M ammonium thiocyanate until the red ferric thiocyanate colour was no longer observed in the effluent. It was then washed with distilled water, 6 M hydrochloric acid and with sufficient distilled water to free it from chloride. Finally, it was converted into the ammonium form with 1 M ammonium lactate solution of pH 3.2 and stored under distilled water until loaded into the column.

Eluant

Two solutions of 1 M lactic acid, one at pH 3.2 and the other at 7.0 were used in the elution. The solution of high pH was allowed to drip into the low pH solution at a rate which will give the desired increase in pH per unit time. Before using the acid for the preparation of solutions it was refluxed for 3 hours in 0.1 M hydrochloric acid to ensure the hydrolysis of any anhydride present in the acid. pH's of the solution were adjusted to 3.2 and 7.0 with concentrated ammonia.

Apparatus

A schematic diagram of the apparatus used is shown in Fig. 1. The ion exchange column was 60 cm long and 7 mm in internal diameter; it was surrounded by a glass tube 7 cm in internal diameter serving as a water jacket for uniformly heating the column. An electrothermal heating tape was wound round the outer jacket tube, the temperature of which was controlled by means of a simmerstat within ± 3°C.

The eluting system consisted of two 500 ml flasks fitted one above the other. The lower flask contained the solution of lower pH and the upper one that having the higher pH. To attain the required flow rate of eluant, a positive pressure controlled with a pressure regulator, was applied to the flasks. The eluting solution was pre-heated

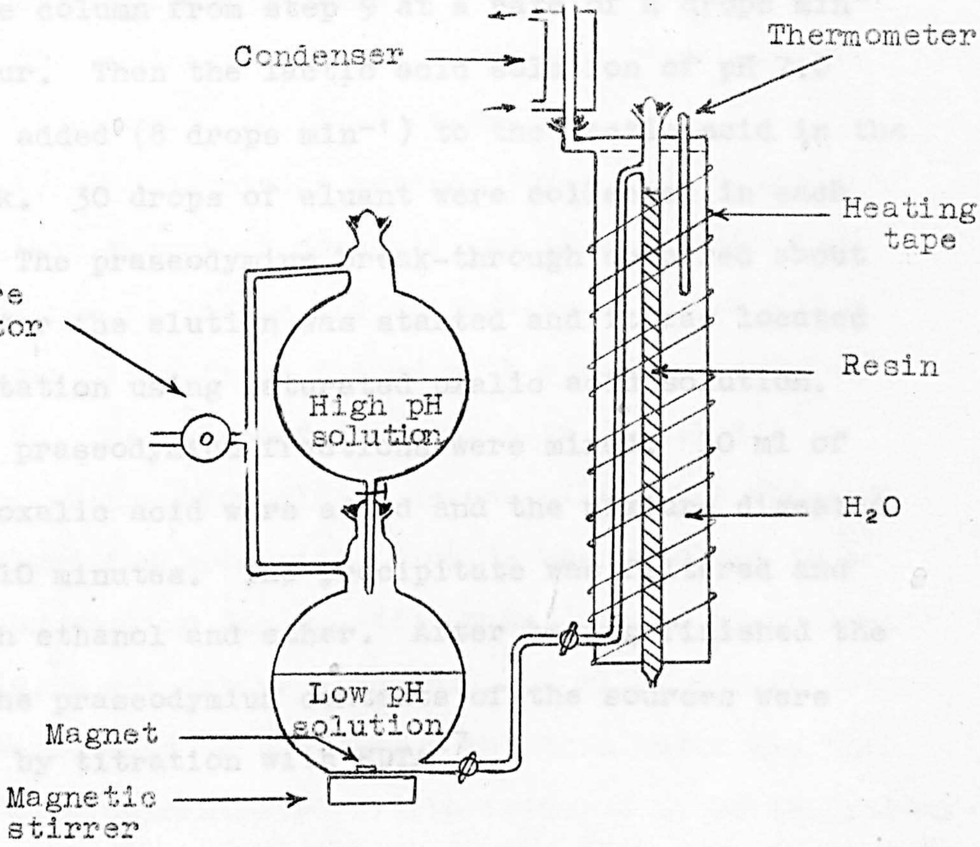
Condenser
Thermometer
Heating tape
Pressure regulator
Resin
High pH solution
H_2O
Low pH solution
Magnet
Magnetic stirrer

Fig. 1. Ion-exchange column apparatus.

by passing it through a glass tube of 2 mm internal diameter fitted inside the reservoir.

Elution Procedure

Lactic acid solution* of pH 3.2 was passed through the column from step 9 at a rate of 4 drops min^{-1} for one hour. Then the lactic acid solution of pH 7.0 was slowly added (8 drops min^{-1}) to the lactic acid in the lower flask. 30 drops of eluant were collected in each fraction. The praseodymium break-through occurred about 7 hours after the elution was started and it was located by precipitation using saturated oxalic acid solution. The middle praseodymium fractions were mixed. 10 ml of saturated oxalic acid were added and the mixture digested for about 10 minutes. The precipitate was filtered and washed with ethanol and ether. After having finished the counting the praseodymium contents of the sources were determined by titration with EDTA[17].

*Elution was started with 100 ml of lactic acid solution of pH 3.2.

10. Iodine

Carrier Solution

Iodine carrier was prepared by dissolving a weighed amount of dried potassium iodide in water.

Separation Procedure

The separation method which was based on that described by Meinke[18] is given below.

1. The aluminium catcher foils were dissolved in the minimum amount of concentrated hydrochloric acid in the presence of iodine and molybdenum carriers and a reducing agent in a flask fitted with a reflux condenser.

2. The solution was made alkaline by the addition of sodium hydroxide. Excess alkali was added to dissolve aluminium hydroxide. Iodide was oxidised to periodate by boiling the solution with 2 ml of hypochlorite solution (2.5% w/v active chlorine). 5 ml of carbon tetrachloride were added to the cooled solution which was then acidified with concentrated nitric acid. 2 ml of 1M hydroxylamine hydrochloride were then added and the iodine was extracted into carbon tetrachloride.

The time of extraction was taken as the time of separation of iodine isotopes from their precursors.

3. The carbon tetrachloride layer was shaken with 5 ml of water containing sulphur dioxide until both phases were colourless.

4. 1 ml of 6M nitric acid and a few drops of 1M sodium nitrite were added to the aqueous phase and iodine was extracted into 5 ml of carbon tetrachloride.

5. Steps 3 and 4 were repeated and iodine was extracted as iodide into 5 ml of water containing sulphur dioxide.

6. The aqueous solution was boiled to remove excess sulphur dioxide and iodide was precipitated by the addition of palladium(II) chloride solution. The precipitate was filtered, washed with water and methanol and dried at 120°C.

The time of precipitation was taken as the zero time for the growth of xenon daughters from iodine precursors.

References

1. L.E. Glendenin, R.R. Edwards and H. Gest, 'Radiochemical Studies: The Fission Products', N.N.E.S., Div. IV, Vol. 9, p. 1451 (1951).

2. M.V. Ramaniah, Ph.D. Thesis (Washington University, 1956).

3. D.N. Sunderman, Report AECU-3159 (1956).

4. R. Belcher, A. Sykes and J.C. Tatlow, Anal. Chim. Acta, 10(1), 34 (1954).

5. R.B. Hahn and R.F. Skomieczmy, Nucleonics, 14(2), 56 (1956).

6. A.I. Vogel, Quantitative Inorganic Analysis, p.508, (Longmans, Green and Co., London, 1961).

7. W.J. Maeck, M.E. Kussy and J.E. Rein, Anal. Chem., 33(2), 237 (1961).

8. E.M. Scadden, Nucleonics, 14(2), 59 (1956).

9. F.D. Snell, C.T. Snell and C.A. Snell, Colorimetric Methods of Analysis, Vol. IIA, P.451, (D. Van Nostrand Company, Inc, 1959).

10. R.P. Larsen, L.E. Ross and G. Kesser, ANL-5810 (1957).

11. D.N. Sunderman, Report AECU-3159 (1956).

12. A.D. Wilson and D.T. Lewis, The Analyst, 88, 585 (1963).

13. A.C. Pappas, Report AECU-2806 (1953).

14. J. Morandat and C. Duval, Anal. Chim. Acta, 4, 498 (1950).

15. P.C. Stevenson and W.E. Nervik, The Radiochemistry of the Rare Earths, Scandium, Yttrium and Actinium', NAS-NS 3020 (1961).

16. H.G. Hicks and W.E. Nervik, Report UCRL-14258 (1965).

17. Md. M. Rahman, Ph.D. Thesis (Durham University, 1965).

18. W.W. Meinke, Report AECD-2738 (1949).

APPENDIX II

Derivation of the Ratio of the Partial Width for Symmetric Fission to that for Neutron Re-emission (Γ_s/Γ_n)

The energy release in symmetric division of a nucleus (Z_o, A_o) can be obtained as a function of Z_o and A_o using the semi-empirical mass formula (S.E.M.F.). Taking thorium-230 as datum[1] and ignoring the effect of closed shells, the following expression is found for the energy available for symmetric fission, in addition to the initial excitation energy of the compound nucleus.

$$[a_s(1-2^{\frac{1}{3}})A_o^{\frac{2}{3}} - a_c(1-2^{-\frac{2}{3}})Z_o^2/A_o^{\frac{1}{3}} + 22.6] \text{ MeV} \quad (1)$$

where a_s and a_c are the coefficients of the 'surface' and 'Coulomb' terms in the S.E.M.F. The 22.6 is a correction term which comes from a comparison of the energy released calculated using the S.E.M.F., with that obtained from the atomic mass excesses given by Everling et al.[2] Taking the values[3] -13.1 MeV and -0.585 MeV for a_s and a_c respectively the total available energy for neutron induced fission is found to be

$$[0.217\, Z_o^2/A_o^{\frac{1}{3}} - 3.41\, A_o^{\frac{2}{3}} + 22.6 + E_n + B_n] \text{ MeV} \quad (2)$$

where E_n is the incident neutron energy and B_n is the binding energy of neutron.

It has been shown by Terrell[4] that the average total kinetic energy of the two fragments is given by the relation,

$$E_K = 0.121\ Z_o{}^2/A_o{}^{\frac{1}{3}}\ \text{MeV}$$

which is obtained from a plot of $\bar{E}_K$ against $Z_o{}^2/A_o{}^{\frac{1}{3}}$ for a range of fissioning nuclides. The difference between this and the total energy gives the average excitation energy, T, to be shared between the two fragments,

$$T = [0.096\ Z_o{}^2/A_o{}^{\frac{1}{3}} - 3.41\ A_o{}^{\frac{2}{3}} + 22.6 + E_n + B_n]\ \text{MeV} \tag{3}$$

From the statistical model of the nucleus[5] the ratio of the partial widths for symmetric fission and neutron re-emission is obtained as

$$\frac{\Gamma_s}{\Gamma_n} = K \frac{\int_0^T \varrho_1(E).\varrho_2(T-E)}{\int_0^{E_n} E\varrho_r(E_n-E)dE} \tag{4}$$

where (E) is the level density of the appropriate nucleus with excitation energy E and K is an energy dependent factor; but it has been shown[6] that this dependence is unimportant compared to that of the remaining terms.

In the absence of shell effects, the level density of a nucleus is expressed by

$$\varrho(E) = C\ e^{2\sqrt{aE}}$$

where C and a are functions of the mass number.

Using this expression for level density in eq. (4)

$$\frac{\Gamma_s}{\Gamma_n} \; \alpha \; \frac{\int_0^T e^{2\sqrt{a_f E} + 2\sqrt{a_f(T-E)}} dE}{\int_0^{E_n} E \; e^{2\sqrt{a_r(E_n-E)}} dE} \qquad (5)$$

is obtained for the ratio of partial widths.

The numerator cannot be integrated exactly. The values of the integrand fall away rapidly from a maximum value with changing E so that the integral is determined essentially by integration in the neighbourhood of the maximum of the integrand (at E = T/2). The integration is given below in detail.

$$I_1 = \int_0^T e^{2\sqrt{a_f E} + 2\sqrt{a_f(T-E)}} dE$$

Putting

$$f(E) = 2\sqrt{a_f E} + 2\sqrt{a_f(T-E)}$$

$$= 2\sqrt{a_f}(\sqrt{E} + \sqrt{T-E})$$

$$f'(E) = 2\sqrt{a_f}\left(\frac{\frac{1}{2}}{\sqrt{E}} - \frac{\frac{1}{2}}{\sqrt{T-E}}\right)$$

$$f'(E) = 0, \text{ when } E = \frac{T}{2},$$

$$f''(E) = \sqrt{a_f}\;\left(\frac{-\frac{1}{2}}{E^{\frac{3}{2}}} - \frac{\frac{1}{2}}{(T-E)^{\frac{3}{2}}}\right)$$

Taylor's expansion gives

$$f(E) \simeq f(T/2) + (E-T/2)f'(T/2) + \frac{(E-T/2)^2}{2!} f''(T/2) + \ldots\ldots$$

$$\simeq 4\sqrt{a_f}\sqrt{\frac{T}{2}} + \frac{(E-T/2)^2}{2} \sqrt{a_f}\left(\left(-\tfrac{1}{2}\right)\left(\frac{2}{T}\right)^{\frac{3}{2}} - \tfrac{1}{2}\left(\frac{2}{T}\right)^{\frac{3}{2}}\right) + \ldots\ldots$$

$$= 4\sqrt{a_f}\sqrt{\frac{T}{2}} - \frac{(E-T/2)^2}{2} \sqrt{a_f}\left(\frac{2}{T}\right)^{\frac{3}{2}}$$

$$I_1 = \int_0^T e^{4\sqrt{\frac{a_fT}{2}}}\, e^{-\frac{\sqrt{a_f}}{2}(E-T/2)^2(2/T)^{\frac{3}{2}}}\, dE$$

$$= e^{4\sqrt{\frac{a_fT}{2}}} \int_{-\frac{T}{2}}^{\frac{T}{2}} e^{-\frac{\sqrt{a_f}}{2}E^2(2/T)^{\frac{3}{2}}}\, dE,$$

putting $a^2 = \frac{\sqrt{a_f}}{2}\left(\frac{2}{T}\right)^{\frac{3}{2}}$

$$I_1 = e^{\sqrt{8a_fT}} \int_{\infty}^{\infty} e^{-a^2E^2}\, dE \,, \quad \int_{-\infty}^{\infty} e^{-a^2E^2}\, dE = \frac{\sqrt{\pi}}{a}$$

$$I_1 = \frac{\sqrt{\pi}}{\frac{a_f^{\frac{1}{4}}}{2^{\frac{1}{2}}}\left(\frac{2}{T}\right)^{\frac{3}{4}}}\; e^{\sqrt{8a_fT}} \qquad (6)$$

The integration of the denominator which can easily be solved using the reduction formula, gives

$$I_2 = \frac{1}{2a_r}\left(E_n - \frac{3}{2a_r}\right) + \frac{1}{2a_r}\, e^{2\sqrt{a_rE_n}}\left(2E_n - \frac{3}{\sqrt{a_r}}\sqrt{E_n} + \frac{3}{2a_r}\right) \qquad (7)$$

Since the first term in the above expression is very small compared with the second, it can be neglected. The ratio of the partial widths is then

$$\frac{\Gamma_s}{\Gamma_n} = K' \frac{e^{\sqrt{8a_fT}}}{e^{2\sqrt{a_rE_n}}} \qquad (8)$$

or

$$\ln \frac{\Gamma_s}{\Gamma_n} = \ln K' + (8a_fT)^{\frac{1}{2}} - 2(a_rE_n)^{\frac{1}{2}} \qquad (9)$$

K' depends on T and E_n, but its variation was neglected in comparison with that of the exponential terms.

References

1. S.J. Lyle, G.R. Martin and J.E. Whitley, Radiochim. Acta, 3, 80 (1964).
2. F. Everling, L.A. König, J.H.E. Mattauch and A.H. Wapstra, Nucl. Phys., 18, 529 (1960).
3. G. Friedlander, J.W. Kennedy and J.M. Miller, 'Nuclear and Radiochemistry', John Wiley and Sons Inc., 1964 .
4. J. Terrell, quoted by R.B. Leachman, Proceedings of the Second United Nations International Conference on the Peaceful Uses of Atomic Energy, 15, P/2467 (1958).
5. J.M. Blatt and V.F. Weiskopf, 'Theoretical Nuclear Physics', John Wiley and Sons, Inc., New York, 1952.
6. P. Fong, Phys. Rev., 102, 434 (1956).

KENT LIBRARY UNIVERSITY